



저작자표시-비영리-변경금지 2.0 대한민국

이용자는 아래의 조건을 따르는 경우에 한하여 자유롭게

- 이 저작물을 복제, 배포, 전송, 전시, 공연 및 방송할 수 있습니다.

다음과 같은 조건을 따라야 합니다:



저작자표시. 귀하는 원저작자를 표시하여야 합니다.



비영리. 귀하는 이 저작물을 영리 목적으로 이용할 수 없습니다.



변경금지. 귀하는 이 저작물을 개작, 변형 또는 가공할 수 없습니다.

- 귀하는, 이 저작물의 재이용이나 배포의 경우, 이 저작물에 적용된 이용허락조건을 명확하게 나타내어야 합니다.
- 저작권자로부터 별도의 허가를 받으면 이러한 조건들은 적용되지 않습니다.

저작권법에 따른 이용자의 권리는 위의 내용에 의하여 영향을 받지 않습니다.

이것은 [이용허락규약\(Legal Code\)](#)을 이해하기 쉽게 요약한 것입니다.

[Disclaimer](#)

Ph.D Thesis
박사 학위논문

The role of hippocampal mossy cells in antidepressant actions

Seo-Jin Oh (오 서 진 吳 瑞 珍)

Department of
Brain and Cognitive sciences

DGIST

2020

Ph.D Thesis
박사 학위논문

The role of hippocampal mossy cells in antidepressant actions

Seo-Jin Oh (오 서 진 吳 瑞 珍)

Department of
Brain and Cognitive sciences

DGIST

2020

The role of hippocampal mossy cells in antidepressant actions

Advisor: Professor Yong-Seok Oh
Co-advisor: Professor Sang Ryong Kim

by

Seo-Jin Oh
Department of Brain & Cognitive sciences
DGIST

A thesis submitted to the faculty of DGIST in partial fulfillment of the requirements for the degree of Doctor of Philosophy in the Department of Brain and cognitive science. The study was conducted in accordance with Code of Research Ethics¹

11. 18. 2019

Approved by

Professor Yong-Seok Oh
(Advisor)

Professor Sang Ryong Kim
(Co-Advisor)

(signature)

(signature)

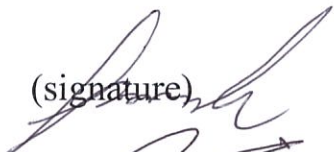
¹ Declaration of Ethical Conduct in Research: I, as a graduate student of DGIST, hereby declare that I have not committed any acts that may damage the credibility of my research. These include, but are not limited to: falsification, thesis written by someone else, distortion of research findings or plagiarism. I affirm that my thesis contains honest conclusions based on my own careful research under the guidance of my thesis advisor.


The Role of Hippocampal Mossy Cells in Antidepressant Actions

Seo-Jin Oh

Accepted in partial fulfillment of the requirements for the degree of Doctor of Philosophy.

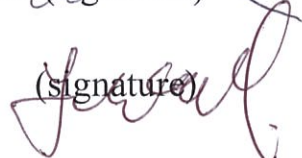
11. 18. 2019

Head of Committee Prof. Ja Wook Koo (signature) 

Committee Member Prof. Sang Ryong Kim (signature) 

Committee Member Prof. Hyosang Lee (signature) 

Committee Member Prof. Han Kyung Choe (signature) 

Committee Member Prof. Yong-Seok Oh (signature) 

Ph.D/BS
201425006

오 서 진. Seo-Jin Oh. The role of hippocampal mossy cell in depression and antidepressant responses. Department of Brain and Cognitive Sciences. 2020. 104p. Advisors Prof. Yong-Seok Oh, Co-Advisors Prof. Sang Ryong Kim

ABSTRACT

Most antidepressants, including selective serotonin reuptake inhibitors (SSRIs), initiate their drug actions by rapid elevation of serotonin, but they take several weeks to achieve therapeutic onset. This therapeutic delay suggests slow adaptive changes in multiple neuronal subtypes and their neural circuits over prolonged periods of drug treatment. Mossy cells are excitatory neurons in the dentate hilus that regulate dentate gyrus activity and function. Here I show that neuronal activity of hippocampal mossy cells is enhanced by chronic, but not acute, SSRI administration. Behavioral and neurogenic effects of chronic treatment with the SSRI, fluoxetine, are abolished by mossy cell-specific knockout of *p11* or *Smarca3* or by an inhibition of the p11/AnxA2/SMARCA3 heterohexamer, an SSRI-inducible protein complex. Furthermore, simple chemogenetic activation of mossy cells using Gq-DREADD is sufficient to elevate the proliferation and survival of the neural stem cells. Conversely, acute chemogenetic inhibition of mossy cells using Gi-DREADD impairs behavioral and neurogenic responses to chronic administration of SSRI. In addition, modulations of mossy cell

activity are influence to excitation-inhibition balance in dentate gyrus. The present data establish that mossy cells play a crucial role in mediating the effects of chronic antidepressant medication. These results indicate that compounds that target mossy cell activity would be attractive candidates for the development of newer antidepressant medications.

Keywords: Hippocampus, Mossy cells, antidepressant, p11/AnxA2/Smad3 complex.

List of contents

Abstract	i
List of contents	iii
List of figures	vii
List of tables	ix

Chapter 1. Background	1
1. Major depressive disorder	1
1.1 MDD in the hippocampus	1
2. Antidepressive therapeutics	4
Chapter 2. The role of hippocampal mossy cells in antidepressant actions.	7
1. Introduction	7
1.1 Molecular mechanism of SSRI actions	7
1.2 Mossy cells in the hippocampus	10
1.3 p11, An SSRI-inducible molecule	13
2. Materials and methods	15
2.1 Materials	15
2.1.1 Antibodies	15
2.1.2 Virus strains	15
2.1.3 Recombinant DNAs	16
2.1.4 Chemicals	16
2.1.5 Experimental models	17
2.2 Methods	18
2.2.1 Animal breeding	18
2.2.2 Drug treatment	18
2.2.3 Plasmid constructions	19
2.2.4 Immunoprecipitation of p11/AnxA2/SMARCA3 complex	19
2.2.5 Stereotaxic surgery	20
2.2.6 Behavioral assessments	21
2.2.6.1 Elevated plus maze (EPM)	21
2.2.6.2 Open field test (OF)	22
2.2.6.3 Light and dark box test (LD box)	22

2.2.6.4 Novelty suppressed feeding test (NSF)	22
2.2.6.5 Tail suspension test (TST)	23
2.2.7 Chronic unpredictable mild Stress paradigm	23
2.2.8 Immunohistochemistry	25
2.2.9 BrdU labeling and neurogenesis assay	26
2.2.10 Electrophysiological recordings of mossy cells	27
2.2.10.1 Fluorescence labeling of mossy cells	27
2.2.10.2 Slice preparation	27
2.2.10.3 Electrophysiology	28
2.2.11. Data analysis and statistics	29
3. Results	30
3.1. The role of p11/AnxA2/SMARCA3 complex in hippocampal mossy cells in antidepressant responses	30
3.1.1 Effects of genetic deletion of <i>p11</i> or <i>Smarca3</i> in hippocampal mossy cells on behavioral responses to chronic SSRI administration	30
3.1.2 Effects of mossy cell-specific inhibition of the p11/AnxA2/SMARCA3 complex on neurogenic and behavioral responses to chronic antidepressant treatment	38
3.1.3. Effects of cell type-specific inhibition of the p11/AnxA2/SMARCA3 complex on neuronal activity of mossy cells	50
3.2. The role of hippocampal mossy cells in antidepressant responses	59
3.2.1 Effects of selective stimulation of dentate mossy cells on adult neurogenesis in the hippocampus	59
3.2.2 Effects of selective inhibition of dentate mossy cells on antidepressant actions in the hippocampus	67
3.3. Effects of modulation of mossy cells on micro-circuits in the dentate gyrus	78
4. Discussion	82
Reference	95
Summary in Korean	103

List of figures

Figure 1. Abnormality in the hippocampus under the major depressive disorders	3
Figure 2. Monoamine hypothesis of depression	6
Figure 3. Delayed therapeutic effects of SSRIs	9
Figure 4. Characteristics of hippocampal mossy cells	12
Figure 5. Chronic unpredictable mild stress paradigm	24
Figure 6. Mossy cell-specific Cre-driver line : D2-Cre	33
Figure 7. Mossy cell-specific knockout of <i>p11</i> gene abolishes behavioral responses to chronic SSRI treatment	34
Figure 8. Mossy cell-specific knockout of <i>Smarca3</i> gene abolishes behavioral responses to chronic SSRI treatment	35
Figure 9. Mossy cell-specific Cre driver line ; MC-Cre	36
Figure 10. Mossy cell-specific knockout of <i>Smarca3</i> gene using MC-Cre mice abolishes behavioral responses to chronic SSRI treatment	37
Figure 11. Development of viral construct for mossy cell specific disruption of the p11/AnxA2/SMARCA3 complex	43
Figure 12. Mossy cell specific expression of control AcGFP1 or PASIP-AcGFP1 construct along the rostro-caudal axis of the hippocampus	44
Figure 13. Effects of mossy cell specific disruption of p11/AnxA2/SMARCA3 complex on proliferation of new-born cells in response to chronic SSRI treatment	46
Figure 14. Effects of mossy cell specific disruption of p11/AnxA2/SMARCA3 complex on differentiation of new-born cells in response to chronic SSRI treatment	47
Figure 15. Effects of mossy cell specific disruption of the p11/AnxA2/SMARCA3 complex on basal locomotion or anxiety-related behaviors	48
Figure 16. Effect of mossy cell specific disruption of the p11/AnxA2/SMARCA3 complex on behavioral responses to chronic SSRI treatment	49

Figure 17. Neuronal activity of mossy cells is enhanced by chronic SSRI treatment, but not by acute treatment.	54
Figure 18. Effect of chronic unpredictable stress or antidepressant administration on expression of c-Fos a neuronal activity marker in the mossy cells.....	55
Figure 19. Neuronal activity of mossy cells is silenced by mossy cell specific deletion of <i>p11</i> or <i>Smarca3</i> gene	56
Figure 20. Neuronal activity of mossy cells is silenced by mossy cell specific disruption of p11/AnxA2/SMARCA3 complex	57
Figure 21. Effects of p11/AnxA2/SMARCA3 complex inhibition on c-Fos expression in mossy cells	58
Figure 22. Mossy cell-specific expression of control or Gq-DREADD construct along the rostro-caudal axis of the hippocampus	61
Figure 23. Mossy cell specific expression of Gq-DREADD construct stimulate the mossy cell activity by CNO administration	62
Figure 24. Effects of chemogenetic stimulation of mossy cells on proliferation of new-born cells	63
Figure 25. Effects of chemogenetic stimulation of mossy cells on differentiation of new-born cells.....	64
Figure 26. Effect of chemogenetic stimulation of mossy cells on the basal locomotion or anxiety-related behaviors	65
Figure 27. Effects of chemogenetic stimulation of mossy cells on depression-related behaviors	66
Figure 28. Mossy cell specific expression of control or Gi-DREADD construct along the rostro-caudal axis of the hippocampus	70
Figure 29. Mossy cell specific expression of Gi-DREADD construct silence the mossy cell activity by CNO administration	71
Figure 30. Effects of chemogenetic silencing of mossy cells on proliferation of new-born cells in response to chronic SSRI administration	72

Figure 31. Effects of chemogenetic silencing of mossy cells on differentiation of new-born cells in response to chronic SSRI administration	73
Figure 32. Mossy cell-specific expression of control or tethered toxin construct along the rostro-caudal axis of the hippocampus	74
Figure 33. Effects of t-toxin induced silencing of mossy cells on neurogenic responses to chronic SSRI administration	75
Figure 34. Effects of chemogenetic silencing of mossy cells on the basal locomotion or anxiety-related behavior	76
Figure 35. Effects of chemogenetic silencing of mossy cells on the depression-related behaviors in response to chronic SSRI treatment	77
Figure 36. Effects of mossy cell suppression on dentate granule cell activity	80
Figure 37. Effects of mossy cell specific disruption of the p11/AnxA2/SMARCA3 complex on PV-positive basket cells in dentate gyrus	81
Figure 38. Graphical summary	94

List of tables

Table 1. Antibody list	15
Table 2. Viral vector list	16
Table 3. Recombinant DNA list	16
Table 4. Chemical list	16
Table 5. Transgenic mice list	17

Chapter 1. Background

1. Major depressive disorder

Major depressive disorder (MDD) is a common and serious medical illness, which characterized by lasting at least two weeks of low mood that is present across most situation and constitute one of the leading causes of disability worldwide [1]. MDD was affected to more than 300 million people around the world, regardless of culture, age, gender, religion, race or economic status [2]. Its symptoms are various including depressed mood, diminished interest and impaired cognitive function. MDD is caused by a combination of genetic, biological, environmental, and psychological factors. In addition, MDD has many risk factors that can also appear as a complication of other disease including diabetes, heart disease and stroke and frequently co-occurs with other psychiatric disorders [3, 4]. However, the mechanisms underlying the pathogenesis of MDD is still unclear.

1.1 MDD in the hippocampus

Although numerous factors can cause the MDD, the chronic stress is the most common cause of occurrence [5]. The most well-described effects of stress on MDD have been

supported by abnormalities in the hypothalamic pituitary adrenal (HPA) axis in patients with MDD, and this may impact the release of glucocorticoids [6]. In particular, stress-related circuitry in the HPA axis is deeply involved with the hippocampus [7], which regulate the production of cortisol and has been a therapeutic target for treatment of MDD. In human neuroimaging studies, one of the limbic systems, hippocampus, was reduced in depressed patients [8]. In addition, rodent models of depression show shrinkage of hippocampal volume, reduced neurogenesis in the subgranular zone and atrophy of CA3 pyramidal neurons [9-11] (Figure 1). These abnormalities are occurred by abnormal plastic changes in the hippocampus, which induced by chronic stress. In addition, synaptic protein, growth factors and neuromodulators are abnormally regulated in animal depression model. However, the causes of these dysregulation of plasticity changes and the factors that involved in these changes is not well understood.

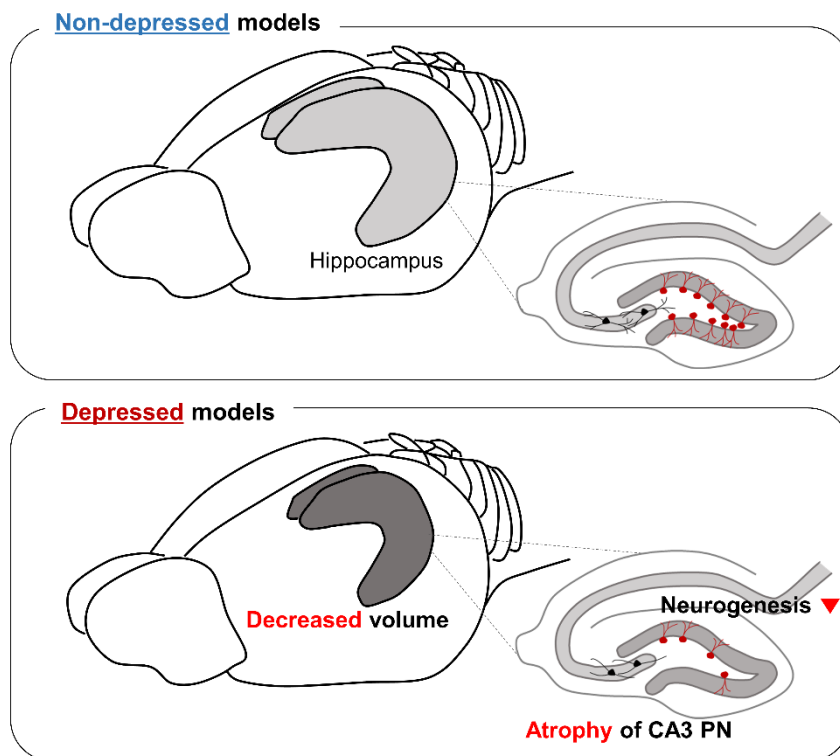


Figure 1. Abnormality in the hippocampus under the major depressive disorders.

The hippocampus has been therapeutic target of mood-related disorder. There are several evidences about the pathological association between hippocampal dysregulation and MDD. Firstly, the hippocampi of the depressed patients are about 20% smaller than those of healthy people. Secondly, adult hippocampal neurogenesis is decreased in the depressed patients compare to the control group. Lastly, repeated exposure to severe stress result in the atrophy of CA3 pyramidal neuron. Abbreviation: PN, pyramidal neurons.

2. Antidepressive therapeutics

One popular theory of depression, the Monoamine hypothesis, is that depression is the result of monoamine deficiency, especially serotonin [12] (Figure 2). This hypothesis was first discovered when the hypertensive drug reserpine, a monoamine antagonist, which was used to treat high blood pressure, induced MDD in 15 percent of treated patients in the 1950s [13]. Another piece of evidence is that low levels of 5-HT metabolites were found in patients with severe MDD [5]. These findings implied that abnormally down-regulated monoamine levels in the brain could cause depression. This insight led to the development of the first class of antidepressants, monoamine oxidase inhibitors (MAOIs), which stop the breakdown of monoamines including serotonin, dopamine, and norepinephrine in the brain. Since then, several monoamine-based pharmacological drugs including tricyclic antidepressants (TCAs), serotonin-norepinephrine reuptake inhibitors (SNRIs), and selective serotonin reuptake inhibitors (SSRIs) have been developed and approved for the treatment of MDD. However, there is a time delay of several weeks to show therapeutic effects of antidepressants, and the remission rate among treated patients is 67%, in other words, about one-third of patients are still depressed. Recently, glutamatergic dysfunctions have been found in MDD patients

[14, 15] and glutamate receptor blocker as a fast-acting antidepressant, ketamine, are approved for MDD treatment in a few countries. However, it also has critical side-effects that is drug abuse problem and high level of relapse rate. Therefore, currently available antidepressant has limitations for remission of depression. From these perspectives, several investigators are eager to figure out accurate mechanisms of existing antidepressant actions to develop new strategies for depression treatment and find new therapeutic target of depression. However, the mechanisms mediating antidepressant actions are still unclear yet.

In this study, I performed genetic, molecular biological, histological, pharmacological, and behavioral experiment to examine the role of hippocampal mossy cells in antidepressant actions.

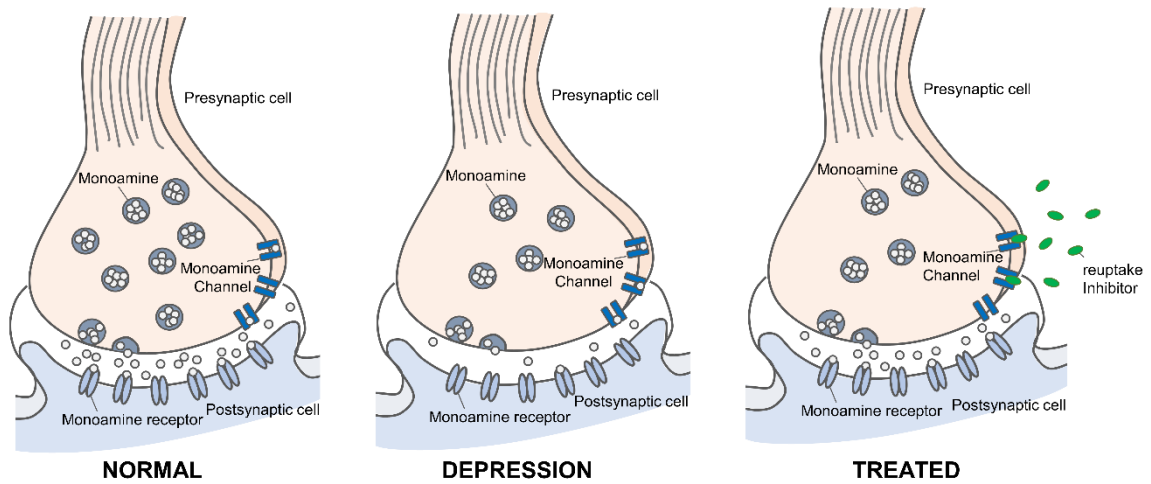


Figure 2. Monoamine hypothesis of depression.

Monoamine hypothesis has been accepted as the most common hypothesis for the pathophysiological theory of MDD. Monoamine level including serotonin, norepinephrine and dopamine in the synaptic cleft was decreased in the depressed patients. Thus, recent antidepressants block the reuptake of monoamine at the presynaptic membrane and it causes increasing its concentration at the postsynaptic nerve terminal membrane.

Chapter 2. The role of hippocampal mossy cells in antidepressant actions.

1. INTRODUCTION

Major depressive disorder (MDD) is the most prevalent mental illness, of which lifetime prevalence is estimated to be as high as 16.2% in the United States. This disease encompasses various symptoms, including anhedonia, depressed mood, increased stress sensitivity, helplessness, apathy, shift towards negative emotions (sadness, emotional numbness, irritability and anxiety) and cognitive deficits [16, 17].

1.1 Molecular mechanism of SSRI actions

Selective serotonin reuptake inhibitors (SSRIs) are the most widely used class of antidepressants [18]. Antidepressant drugs are generally beneficial for depressed patients, but SSRIs generally take several weeks to show therapeutic effects, despite their immediate effect on serotonin neurotransmission [18, 19]. This therapeutic delay suggests the existence of slow adaptive changes in neural circuits over a long-lasting period of drug treatment, possibly involving changes in gene expression and protein translation [20-22]. In addition, although significant progress has been made in treating depression by SSRIs, only a little more than half of severely depressed patients has been found to respond to this class of drugs [23]. Our

knowledge of the molecular mechanisms underlying therapeutic responses to long-term treatment with SSRIs, as well as the side effects of the drugs, have yet to be established at the level of neuronal cell types (Figure 3).

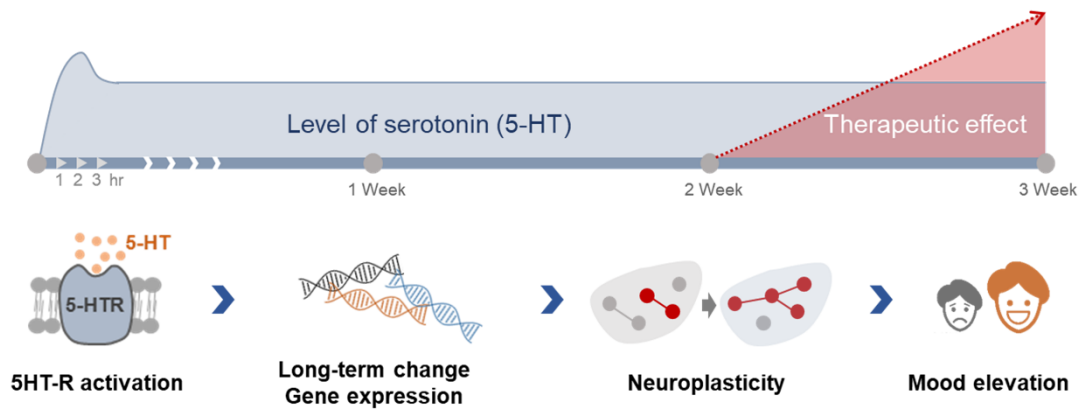


Figure 3. Delayed therapeutic effect of SSRIs.

Selective serotonin reuptake inhibitor (SSRI) rapidly increases the serotonin levels within an hour. However, the onset of therapeutic effect usually takes at least 3 to 4 weeks. It means that, therapeutic responses to antidepressant treatment is not ascribed to only short-lived chemical changes, but substantial, long-lasting neuroplastic changes in the brain.

1.2 Mossy cells in the hippocampus

Mossy cells reside in the hilus of the dentate gyrus and make synaptic connections with various types of cells, such as granule cells and basket cells [24-27]. Moreover, they are positioned to integrate numerous inputs mainly from multiple granule cells, CA3c pyramidal cells, as well as from the local GABAergic interneurons including basket cells and HIPP (Hilar perforant path-associated) cells and then to propagate a signal over the longitudinal axis of the hippocampus [27-29] (Figure 4).

Of particular interest, recent studies have shown that mossy cells are highly enriched in selective subsets of monoamine receptors, proving mossy cells to be immediate regulatory targets of monoaminergic inputs to the hippocampus [25, 30, 31]. They also highly express type II glucocorticoid receptors which sense the stress hormone, cortisol [32]. Mossy cells fire frequently in multiple place fields in various environments, in contrast to granule cells which fire sparsely [33-35]. The neuronal activity of mossy cells within the dentate gyrus circuitry is crucial for the proper function of the hippocampus [36]. Indeed, degeneration of mossy cells results in the dysregulation of granule cell excitability, which leads to abnormal

behaviors such as elevated anxiety, and impaired pattern separation [37]. Despite the potential implication of the mossy cells in the affective disorders, as well as in the actions of monoaminergic drugs, a detailed analysis of the role of mossy cells in antidepressant responses has not yet been carried out.

Chronic antidepressant administration is believed to reverse depressive symptoms through neuronal plasticity. Plasticity occurs at several levels, ranging from gene expression and protein translation to neurogenesis and adjustment of synaptic transmission and thereafter modulation of the structure and function of the neuronal circuits and networks associated with mood regulation.

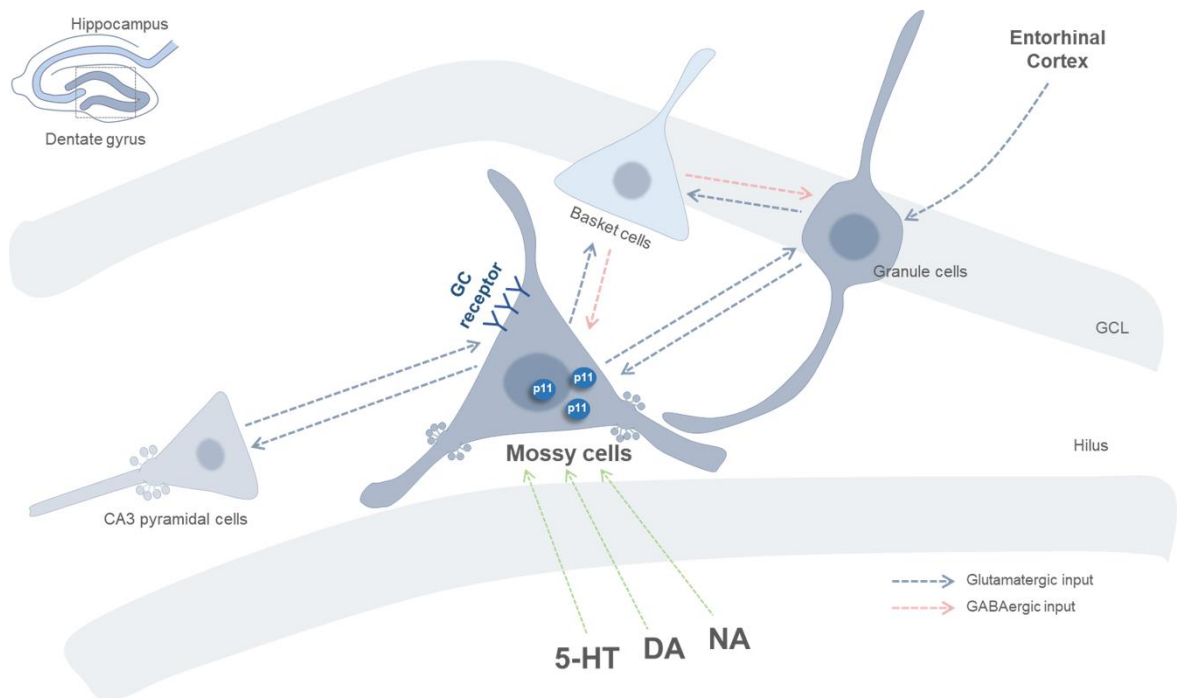


Figure 4. Characteristics of hippocampal mossy cells.

Mossy cells localize in the hilus of dentate gyrus and make synaptic connections with various types of cell population such as granule cells and basket cells. And they have proximal dendrite with numerous large spine called thorny excrescences which give an advantage to receive the excitatory synaptic input from granule cells. In addition, mossy cells are highly enriched in selective subsets of monoamine receptors, type II glucocorticoid receptors and antidepressive molecule, p11. Abbreviation: GC receptor, glucocorticoid receptor; GCL, granule cell layer; 5-HT, serotonin; DA, dopamine; NA, norepinephrine.

1.3 p11, an SSRI-inducible molecule

p11 (S100A10) is a key factor involved in regulating affective state and in determining responses to antidepressants [38, 39]. It is down-regulated in depressed humans and rodents and is induced by chronic but not by acute administration of antidepressants in rodents [38, 40, 41]. Global abolition of p11 in mice produces a depressive state [38]. Removal of p11 from specific classes of p11-enriched neurons produces a variety of depressive effects, depending on the subtype of p11-containing neurons that is targeted [40, 42-50].

p11 was initially identified within a heterotetrameric complex where it forms with Annexin A2 (AnxA2) [51], and this complex form of p11 and AnxA2 can be induced in the hippocampal dentate gyrus by chronic treatment with an SSRI. Previous studies identified SMARCA3 as a binding partner of the p11/AnxA2 complex and both p11 and SMARCA3 are crucial for behavioral and neurogenic responses to chronic antidepressant administration [46]. Chronic SSRI administration increased the level of the heterohexameric complex of p11/AnxA2/SMARCA3 in the hippocampus [46]. In addition, p11 and SMARCA3 are highly

enriched in hilar mossy cells and basket cells in the hippocampal dentate gyrus [46]. However, a cell type-specific role of the p11/AnxA2/SMARCA3 heterohexameric complex in antidepressant action has not yet been explored. Here I examine the role of mossy cells in mediating the actions of the antidepressant, fluoxetine. Results from this study have suggested that the heterohexameric complex of p11/AnxA2/SMARCA3 regulates the activity of mossy cells, which is required for behavioral and neurogenic responses to chronic antidepressant medication.

2. MATERIALS AND METHODS

2.1 Materials

2.1.1 Antibodies

Table 1. Antibody list

REAGENT	SOURCE	IDENTIFIER
Antibodies		
Mouse monoclonal anti-p11	BD bioscience	-
Goat polyclonal anti-p11	R&D systems	AF2377
Goat polyclonal anti-SMARCA3	NOVUS	NB 100-1041
Rabbit polyclonal anti-SMARCA3	Thermo Scientific	PA3-16554
Mouse monoclonal anti-AnxA2	Santa Cruz	sc-28385
Goat polyclonal anti-GFP	Santa Cruz	sc-5385
Goat polyclonal anti-Doublecortin	Santa Cruz	sc-8066
Rat monoclonal anti-BrdU	Abcam	ab6326
Mouse monoclonal anti-calretinin	SWANT	6B3
Rabbit polyclonal anti-parvalbumin	SWANT	PV27
Rabbit monoclonal anti-c-Fos	cell-signaling	2250
Rabbit polyclonal anti-Neuropeptide Y	phoenix pharmaceutical	8711
Rabbit polyclonal anti-GluR2/3	Millipore	AB1506
Donkey polyclonal anti-Goat Alexa Fluor 488	Invitrogen	A11055
Chicken polyclonal anti-Rat Alexa Fluor 488	Invitrogen	A21470
Goat polyclonal anti-Rat Alexa Fluor 568	Invitrogen	A11077
Donkey polyclonal anti-Mouse Alexa Fluor 488	Invitrogen	A21202
Donkey polyclonal anti-Mouse Alexa Fluor 568	Invitrogen	A10037
Donkey polyclonal anti-Rabbit Alexa Fluor 488	Invitrogen	A21206
Donkey polyclonal anti-Rabbit Alexa Fluor 568	Invitrogen	A10042

2.1.2 Virus strains

Table 2. Viral vector list

RESOURCE	SOURCE	IDENTIFIER
Virus Strains		
AAV2-EF1a.DIO.AcGFP1-myc-hGH	This paper	N/A
AAV2-EF1a-DIO-AcGFP1-myc-C-AHNAK1-hGH	This paper	N/A
AAV2-EF1a-DIO-N-AHNAK1-AcGFP1-C3xNLS-hGH	This paper	N/A
AAV8-hSyn-DIO-hM4Di-DREADD	UNC Vector Core	N/A
AAV8-hSyn-DIO-mTomato	UNC Vector Core	N/A

2.1.3 Recombinant DNAs

Table 3. Recombinant DNA list

RESOURCE	SOURCE	IDENTIFIER
Recombinant DNA		
pAAV-EF1a-DIO-AcGFP1-myc-C-AHNAK1-hGH	This paper	N/A
pAAV-EF1a-DIO-N-AHNAK1-AcGFP1-C3xNLS-hGH	This paper	N/A
pAAV-EF1a.DIO.AcGFP1-myc-hGH	This paper	N/A

2.1.4 Chemicals

Table 4. Chemical list

REAGENT	SOURCE	IDENTIFIER
Chemicals		
Clozapine-N-oxide (CNO)	Sigma-Aldrich	C0832
Fluoxetine hydrochloride	Spectrum	F1200
5-bromo-2-deoxyuridine	Sigma-Aldrich	B5002

2.1.5 Experimental models

Table 5. Transgenic mice list

RESOURCE	SOURCE	IDENTIFIER
Experimental Models: Mice Strains		
Crlcl-Cre	Nakajawa Lab. Jinde S et al., 2012	JAX #023014
Drd2R-Cre	Genesat	Clone #ER44
p11(f/f) / Drd2R Cre	Greengard lab	N/A
HLTF(f/f) / Drd2R Cre	This paper	N/A
HLTF(f/f) / Crlcl Cre	This paper	N/A
tdTomato Reporter	Allen Brain Atlas	JAX #007908

2.2 Methods

2.2.1 Animal breeding

I produced the progeny for each line using *in vitro* fertilization (IVF) and embryo transfer (ET) techniques, to produce a number of age-matched animals sufficient for the behavioral tests and other animal experiments. I carried out all of the animal experiments using age (10-15 weeks) and gender (male)-matched littermates. The *BAC-[Drd2]-Cre* Tg mice (GENSAT, Clone #ER44) and MC-Cre (*[Calcr1]-Cre*, JAX stock #023014) [37] were bred against C57BL/6mice (Taconics) to obtain hemizygotes. *p11* floxed mice and *Smarca3* floxed mice were generated by introducing flanked loxP sites as described in our previous studies [46, 50]. All animal were kept in a 12 hour light/dark cycle at room temperature (RT; $22 \pm 1^\circ\text{C}$) and provided with standard diet and water *ad libitum*. Male mice were used for all experiments. Care was taken to minimize the number of animals.

2.2.2 Drug treatments

For chronic drug administration, mice were housed 2-5 per cage. Fluoxetine hydrochloride (Spectrum Chemicals, USA) was administrated by a daily intraperitoneal injection ($10 \text{ mg kg}^{-1}\text{day}^{-1}$) for up to 3 weeks and was dissolved in dimethylsulfoxide (50%) and then

diluted in saline. Control group was administrated daily with vehicle solution (0.9 % saline) without the drug. For experiments in Gi-DREADD and Gq-DREADD mice, clozapine-N-oxide (CNO) (Sigma-Aldrich, USA) was dissolved directly in 0.9 % saline solution. The dose of CNO was 0.3 mg/kg and was injected intraperitoneally using a volume of 100 μ l/10 g body weight 2 hours before each behavioral test.

2.2.3 Plasmid constructions

PASIP (p11/AnxA2/SMARCA3 complex Inhibitory Peptide) sequence is derived from p11/AnxA2 complex binding region of AHNAK1 (aa 5654-5671) [46]. I designed a series of PASIP constructs: Control AcGFP1 (pAAV-Efl α -DIO-AcGFP1-myc.hGH), PASIP-AcGFP1c (pAAV-Efl α -DIO-PASIP-AcGFP1-myc.hGH) and nucleus targeted PASIP-AcGFP1-NLS (pAAV-Efl α -DIO-PASIP-AcGFP1-myc-C3xNLS.hGH) [52-54]. Coding sequence of PASIP constructs was prepared using standard gene synthesis method (GENEWIZ, USA) and subcloned into pAAV-Efl α -DIO-EYFP vector (Addgene, #29056) at the two restriction enzyme cleavage sites (NheI, AscI) (Table 3).

2.2.4 Immunoprecipitation of p11/AnxA2/SMARCA3 complex

HEK293 cells (CRL-1573, ATCC) were transfected with CMV-Cre plasmid. 24 hours post transfection the cells were infected with AAV stocks expressing either Control AcGFP1 or PASIP-AcGFP1 constructs. Immunoprecipitation was performed with α -SMARCA3 antibody (rabbit polyclonal antibody, made with peptide immunization) [46]. Immunoblotting was performed with a standard protocol using the following antibodies α -p11 (mouse monoclonal, 1:1000, BD bioscience), α -p11 (goat polyclonal, 1:200, R&D systems), α -SMARCA3 (goat polyclonal, 1:200, NOVUS), α -AnxA2 (mouse monoclonal, Santa Cruz Biotech.), α -GFP (Goat polyclonal, Santa Cruz Biotech.) (Table 1).

2.2.5 Stereotaxic surgery

Stereotaxic injection of AAV was carried out on an Angle Two™ stereotaxic frame for mice (Leica, Buffalo Grove, IL, USA). Mice were anesthetized by intraperitoneal injection of avertin (250 mg/kg) prior to stereotaxic injection of AAV constructs. Cre-dependent AAVs were stereotaxically injected bilaterally into dorsal and ventral regions of the dentate hilus (coordinates for Dorsal: AP -2.1, ML \pm 1.4, DV -1.95, Ventral: AP -3.3, ML \pm 2.7, DV -3.6) using 10 μ l Hamilton syringes (33 gauge needle; Reno, NV, USA) (Table 2). Flow rate (0.2 μ l/min) was controlled with a nanopump controller (WPI, US). After viral injection, the

needle was left for 5 min, and the incision was closed. Mice were placed back in the home cage for recovery. All animals were allowed at least 2 weeks of rest before the next experimental stage. Any mice with abnormal locomotor activity after stereotaxic surgery were excluded from analysis.

2.2.6 Behavior assessments

For all behavior tests, mice were brought to the testing room for 1 hour before testing, and all of the tests were conducted during the light cycle by experimenters blind to treatment- and genotype information. Experimental groups were randomly assigned during all of the tests.

2.2.6.1 Elevated plus maze (EPM)

The elevated plus maze used plus-shape and was elevated 50 cm from the floor with two open arms and two enclosed arms (30 cm long and 5 cm wide). Mice were placed in the center of the maze and allowed to freely move into the four arms of the maze for 10 min. The mice were videotaped, and the amounts of time spent in the open and closed arms were recorded and measured using Ethovision™ software (Noldus, USA)[55].

2.2.6.2 Open field test (OF)

Mice were placed in the center of the open field area (40 × 40 × 40 cm, Plexiglas chamber). Mice were allowed to move freely in the open field for 1 hour. An automated Superflex™ software (Accuscan Instruments, Columbus, OH, USA) was used to measure the duration in the center and periphery. The measures were automatized using two rows of infrared photocells placed 20 and 50 mm above the floor, spaced 31 mm apart. Photocell beam interruptions were recorded using Superflex™ software [46].

2.2.6.3 Light and dark box test (LD box)

Mice were placed in the open field area (40 × 40 × 40 cm). The black box was inserted into the open field. Mice were placed into the light compartments at the beginning of the session and allowed to move freely between compartments for 10 min. An automated Superflex™ software was used to measure the time spent in each compartment and first latency to enter the dark compartment [46].

2.2.6.4 Novelty suppressed feeding test (NSF)

The novelty-suppressed feeding test was carried out during a 15 min period as described with minor modification [56]. 24 hours prior to behavioral testing, all food was removed from the home cage. At the end of this time, a single 1.8cm square shaped food pellet was placed on a white filter paper positioned in the center of the test box. The mouse was placed in a corner of the open field and a stopwatch was immediately started. The latency to the first bite was recorded. Immediately after this test, mice were placed in their home cage and the amount of food intake were measured for 10 min.

2.2.6.5 Tail suspension test (TST)

Mice were suspended by their tails for 6 min. The test session was videotaped and their immobility was scored by using automated TST analysis software from Clever system (Reston, VA, USA). The immobility time during the last 4 min (excluding the initial 2 min) was calculated [57].

2.2.7 Chronic unpredictable mild stress (CUMS) paradigm

Mice were exposed to various kinds of stressors in random order over three weeks [58]. Control group was handled daily for 30 s in the housing room for the same period. Specific details of the CUMS paradigm were as follows: Restraint stress (2hrs), Over-crowding (24

hrs), Tail pinch (10 min or 1 hr), No bedding (12 ~ 24 hrs), Tilted cage (12 ~ 24 hrs), Restrainer tilting (2 hrs), Wet bedding (12 ~ 24 hrs), Single housing (12 ~ 24 hrs), Food and water deprivation (24 hrs), Cold swimming (6 min), Over hanging (30 min), Overnight illumination, Restrainer rotating (30 min) (Figure 5).

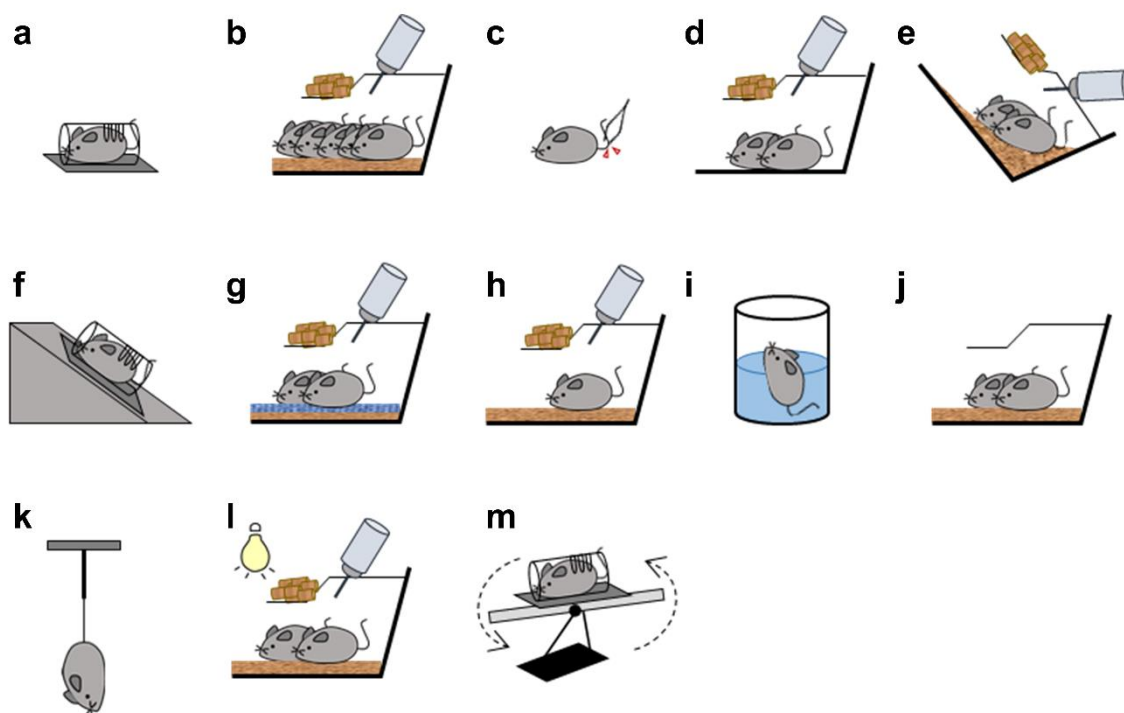


Figure 5. Chronic unpredictable mild stress paradigm.

(a) Restraint stress (b) Over-crowding (c) Tail pinch (d) No bedding (e) Tilted cage (f) Restrainer tilting (g) Wet bedding (h) Single housing (i) Cold swimming (j) Food and water deprivation (k) over hanging (l) Overnight illumination (m) Restrainer rotating.

2.2.8 Immunohistochemistry

Immunostaining was carried out using the standard free-floating method. Sections were washed three times with PBS for 10 min each time and pre-incubated in 2% normal donkey serum, 0.2% bovine serum albumin and 0.3% Triton-X100 for 1 hour. After the blocking step, sections were incubated with the primary antibody diluted in the blocking buffer overnight at 4°C. The following primary antibodies were used: α -doublecortin (goat polyclonal, 1:200, Santa Cruz Biotech.), α -calretinin (mouse monoclonal, 1:500, SWANT), α -parvalbumin (rabbit polyclonal, 1:1000, SWANT), α -neuropeptide Y (rabbit polyclonal, 1:1000, Phoenix pharmaceutical), α -GluR2/3 (rabbit polyclonal, 1:100, Millipore), α -c-Fos (rabbit polyclonal, 1:250, Cell signaling), α -p11 (goat polyclonal, 1:100, R&D systems), α -SMARCA3 (rabbit polyclonal, 1:500, Thermo Scientific) (Table 1). After 24 hours incubation, sections were washed three times with PBS containing 0.2% Triton-X100 (PBS-T) for 10 min each time, and incubated with AlexaTM-fluor-conjugated secondary antibody (1:400, Life technologies, USA) for 3 hours at RT. Sections were washed again in PBS-T, three times for 10 min each at RT and cover-slipped with ProlongTM Gold, anti-fading mounting medium (Life technologies, USA).

2.2.9 BrdU labeling and neurogenesis assay

The mice were administrated BrdU solution (200 mg/kg) intraperitoneally for 3 hours prior to sacrifice. After transcardial perfusion, brain was post-fixed with 4% PFA overnight and a cryostat (CM3050S, Leica) was used to collect coronal sections of 40- μ m-thickness along the rostro-caudal axis of hippocampus. Sections were processed using a free-floating procedure. Every sixth section throughout the hippocampus was processed for BrdU immunohistochemistry. Sections were pre-incubated for 30 min at 45°C in 1 M HCl to denature DNA and the acid neutralized by rinsing sections three times with 0.1 M PBS [59]. The immunohistochemistry was done using α -BrdU (rat polyclonal, 1:200, Abcam, Cambridge, MA, USA) and AlexaTM-fluor-conjugated secondary antibody (1:400, Life technologies, USA). An experimenter blinded to the slide code counted all BrdU-labeled cells in the granule cell layer (GCL) and the subgranular zone (SGZ) of the dentate gyrus (DG) in the total 12 sections from the individual mouse. The total number of BrdU-labeled cells per section was determined and multiplied by 6 to obtain the total number of cells per dentate gyrus.

2.2.10 Electrophysiological recordings of mossy cells

2.2.10.1 Fluorescence labeling of mossy cells

To label and visualize mossy cells in hippocampal slices, recombinant AAV vector (AAV2.EF1 α .DIO.AcGFP1-myc) was bilaterally injected into the dentate hilus of ventral hippocampus in MC-Cre ([*Calcr*]-Cre) Tg mice. AcGFP1 was selectively expressed in the mossy cells. During electrophysiological recordings, mossy cells were further confirmed by their morphology, membrane capacitance and electrophysiological properties.

2.2.10.2 Slice preparation

Male mice between 8-15 weeks of age were euthanized with CO₂. Brains were then removed and placed in an ice-cold N-Methyl-D-glucamine (NMDG)-containing cutting solution (in mM: 93 NMDG, 2.5 KCl, 1.2 NaH₂PO₄, 30 NaHCO₃, 25 glucose, 20 HEPES, 5 sodium ascorbate, 3 sodium pyruvate, 2 thiourea, 0.5 CaCl₂, 10 MgSO₄. pH 7.4, 295-305 mOsm). Brain slices (400 μ m thickness) containing the ventral hippocampus were prepared by using a VT1000 S Vibratome (Leica Microsystems Inc., Buffalo Grove, IL, USA). After cutting, slices were allowed to recover in the cutting solution for 15 min at 37°C and then transferred to the recording solution at room temperature for at least 1 hour before recording.

2.2.10.3 Electrophysiology

Electrophysiological recordings were performed as described previously [60]. During recording, brain slices were placed in a perfusion chamber attached to the fixed stage of an upright microscope BX51WI (Olympus, Tokyo, Japan) and submerged in continuously flowing oxygenated recording solution containing the following (in mM): 125 NaCl, 25 NaHCO₃, 25 glucose, 2.5 KCl, 1.25 NaH₂PO₄, 2 CaCl₂, and 1 MgCl₂, pH 7.4, 295-305 mOsm. Neurons were visualized with a 40× water immersion lens and illuminated with near infrared (IR) light. Electrophysiological recordings were performed with a Multiclamp 700B/Digidata1440A system (Molecular Devices, Sunnyvale, CA, USA). Patch electrodes were filled with the internal solution (in mM: 126 K-gluconate, 10 KCl, 10 HEPES, 10 phosphocreatine, 4 ATP, and 0.3 GTP, pH 7.3, 290 mOsmol). Whole-cell patch-clamp recordings were used to record the spontaneous action potentials of mossy cells in the hippocampal slices. All recordings were done at 37°C. In the chemogenetic experiments, action potentials of mossy cells were recorded for 5 minutes as baseline. CNO (1 μM) was then perfused on brain slices to examine the effects of Gi-DREADD. Data were analyzed by pClamp10 software (Molecular

Devices) and GraphPad Prism 6 (GraphPad Software, La Jolla, CA, USA).

2.2.11 Data analysis and statistics

All data were presented as means \pm SEM. Statistical analysis was conducted using GraphPad Prism Version 7.0a. Two group comparisons were done by two-tailed, unpaired or paired Student's t test. Multiple group comparisons were assessed using a one-way or two-way ANOVA, followed by appropriate post hoc test. Significance thresholds were as follows:

* $p < 0.05$, ** $p < 0.01$, *** $p < 0.001$.

3. RESULTS

3.1 Effects of modulation of p11/AnxA2/SMARCA3 complex in mossy cells in antidepressant responses to chronic SSRI administration.

3.1.1 Effects of genetic deletion of *p11* or *Smarca3* in hippocampal mossy cells on behavioral responses to chronic SSRI administration.

Previous studies identified SMARCA3 as a binding partner of the p11/AnxA2 complex and, using constitutive *Smarca3* KO mice, demonstrated its crucial role for neurogenic and behavioral responses to chronic antidepressant administration. Those studies also showed that p11 and SMARCA3 were highly enriched in hippocampal mossy cells [46]. However, a possible mossy cell-specific involvement of the p11/AnxA2/SMARCA3 complex in antidepressant actions was not studied. Therefore, I generated mossy cell-specific deletion of *p11* or *Smarca3* conditional KO mice to identify the cell type-specific role of the ternary complex. To investigate the possibility of a mossy cell-specific role of *p11* and/or *Smarca3* in the actions of antidepressants, I used a transgenic Cre driver line to target hippocampal mossy cells. According to previous reports, dopamine D2 receptor gene expression is limited to mossy cells in the dentate gyrus [61, 62]. I validated dopamine D2 receptor promoter driven Cre recombinase expression in a mossy cell-specific manner in the dentate gyrus

by crossing a D2-Cre (*[Drd2]-Cre*) driver mouse line with a tdTomato reporter line (Figures 6a - 6c). Then, I crossed them with a *p11* or *Smarca3* floxed conditional line to achieve specific deletion of *p11* or *Smarca3* in mossy cells (Figures 7a and 7b, Figures 8a and 8b). After chronic administration of SSRI to a *p11* or *Smarca3* conditional KO (cKO) line, I carried out the novelty suppressed feeding test to investigate depression-like states. I found that the latency to approach food pellet was reduced in the control mice (*p11*^(f/f) and *Smarca3*^(f/f)), but not in *p11* cKO (*p11*^{(f/f);D2-Cre}) or *Smarca3* cKO (*Smarca3*^{(f/f);D2-Cre}) mice (Figure 7c and 8c), but that their home cage feeding level was unaffected (Figures 7d and 8d). I further validated the effect of genetic deletion of *Smarca3* in the mossy cells using another type of mossy cells-specific Cre mouse line, MC-Cre (*[Calcr1]-Cre*) (Figures 9a - 9c). This MC-Cre line was very specific in the hippocampus, but exhibited wide activity in both hilar mossy cells of dentate gyrus and some pyramidal cells of the CA3 region [37]. I deleted the *Smarca3* gene by crossing MC-Cre mice with *Smarca3* floxed conditional mice (*Smarca3*^(f/f)) (Figure 10a) and conducted the novelty suppressed feeding test (NSF) and the tail-suspension test (TST) after chronic administration of SSRI. I found that the latency to feed in the NSF and the immobility in the TST were reduced in the control mice by fluoxetine treatment (*Smarca3*^(f/f)), but not in

Smarca3 cKO (*Smarca3*^{(f/f);MC-Cre}) (Figures 10b - 10d), without any significant change in locomotor activity (Figure 10e).

All of these data indicate that selective deletion of *p11* or *Smarca3* in dentate mossy cells affects the antidepressant responses. These results suggest that *p11* and *Smarca3* in mossy cells are involved in mediating the behavioral responses to chronic antidepressant treatment.

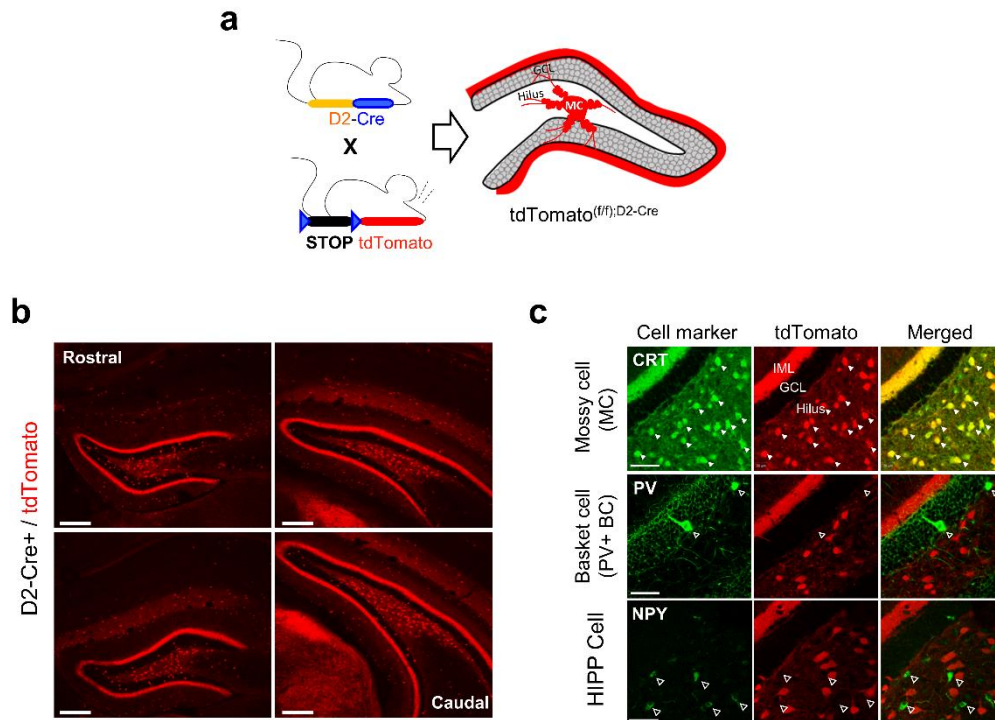


Figure 6. Mossy cell-specific Cre-driver line : D2-Cre

(a) Schematic design to confirm mossy cell-specific Cre recombination in the hippocampus of D2-Cre transgenic mice. (b) Representative images showing longitudinal fluorescent of tdTomato along the rostral-caudal axis of the hippocampus of D2-Cre/tdTomato mice. Scale bar, 100 μ m. (c) Co-localization of Cre-dependent reporter (tdTomato, red) with CRT, a mossy cell marker (green, filled arrowheads), but not in neither PV+ basket cells nor NPY+HIPP cells (green, open arrowheads). Scale bar, 25 μ m. Abbreviations: GCL, granule cell layer; IML, inner molecular layer, CRT, calretinin; PV, parvalbumin; NPY, neuropeptide Y; HIPP, Hilar perforant path-associated.

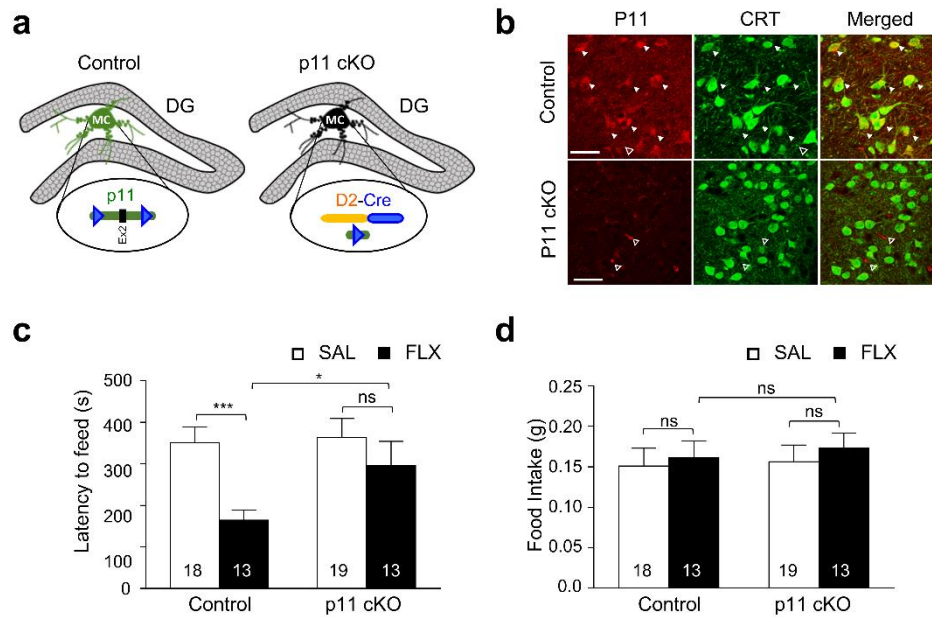


Figure 7. Mossy cell-specific knockout of *p11* gene abolishes behavioral responses to chronic SSRI treatment.

(a) Schematic illustration of genetic deletion of *p11* gene in mossy cells using a D2-Cre line. (b) Cell type-specific knockout of *p11* gene in the dentate hilus. Representative co-labeling images showing the co-localization between *p11* (red) and a mossy cell marker calretinin (CRT)(green) in control mice, but not in *p11* cKO mice. Solid arrowheads indicate representative doubly labeled cells and open arrowheads show cells labeled only with *p11*, but without CRT. Scale bar, 50 μ m. (c) Novelty suppressed feeding (NSF) test. Bar graphs showing latency to food pellet. Control and *p11* cKO group have genotype of *p11*^(*fl/fl*) without Cre, and *p11*^(*fl/fl*) with D2-Cre, respectively. Two-way ANOVA, [genotype x drug interaction $F(1,54)=5.031$; $P=0.0290$, genotype factor $F(1,54)=7.435$; $P=0.0086$, drug factor $F(1,54)=6.728$; $P=0.0122$], followed by the Turkey's post hoc test. (d) Assessment of the hunger level in control and *p11* cKO group using home cage feeding test right after NSF test of the same set of animals. Data are represented as means \pm SEM. Pair-wise comparison by post hoc test; * $p < 0.5$, *** $p < 0.001$, ns, nonsignificant. Abbreviations: DG, dentate gyrus; MC, mossy cells; SAL, saline; FLX, fluoxetine.

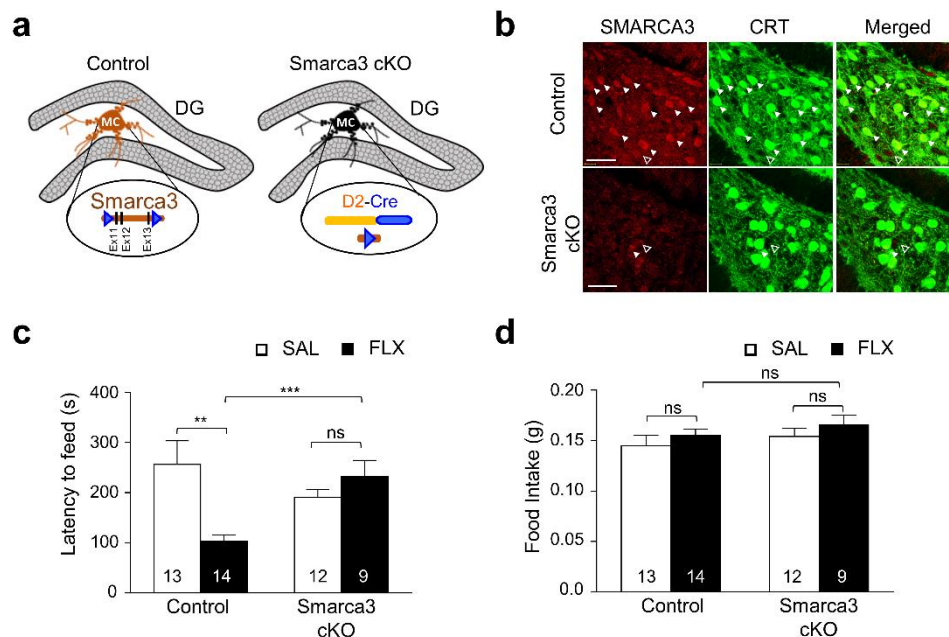


Figure 8. Mossy cell-specific knockout of *Smarca3* gene abolishes behavioral responses to chronic SSRI treatment.

(a) Schematic illustration of genetic deletion of *Smarca3* gene in mossy cells using a D2-Cre line. (b) Cell type-specific knockout of *Smarca3* gene in the dentate hilus. Representative co-labeling images showing the co-localization of SMARCA3 (red) and CRT (green) in the control mice, but not in p11 cKO mice. Solid arrowheads indicate representative doubly labeled cells and open arrowheads show cells labeled only with SMARCA3, but without CRT. Scale bar, 50 μm . (c) NSF tests. Control and *Smarca3* cKO group have genotype of *Smarca3*^(f/f) without Cre, and *Smarca3*^(f/f) with D2-Cre, respectively. Two-way ANOVA, [genotype x drug interaction $F(1,44)=9.111$; $P=0.0042$, genotype factor $F(1,44)=0.9715$; $P=0.3297$, drug factor $F(1,44)=3.094$; $P=0.0855$], followed by the Turkey's post hoc test. (d) Assessment of the hunger level in control and *Smarca3* cKO group. Data are represented as means \pm SEM. Pair-wise comparison by post hoc test; ** $p < 0.01$, *** $p < 0.001$, ns, non-significant. Abbreviations: DG, dentate gyrus; MC, mossy cells; SAL, saline; FLX, fluoxetine.

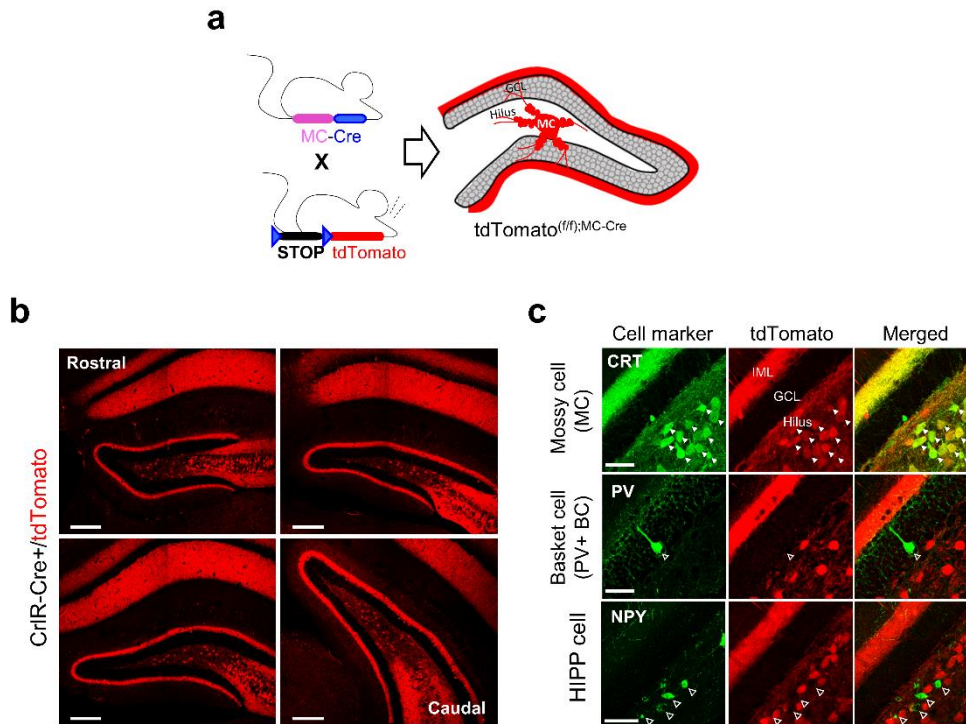


Figure 9. Mossy cell-specific Cre-driver line : MC-Cre

(a) Schematic design to confirm mossy cell-specific Cre recombination in the hippocampus of MC-Cre transgenic mice. (b) Representative images showing longitudinal fluorescent of tdTomato along the rostro-caudal axis of the hippocampus of MC-Cre/tdTomato mice. Scale bar, 100 μ m. (c) Co-localization of Cre-dependent reporter (tdTomato, red) with CRT, a mossy cell marker (green, filled arrowheads), but not in neither PV+ basket cells nor NPY+HIPP cells (green, open arrowheads). Scale bar, 25 μ m. Abbreviations: GCL, granule cell layer; IML, inner molecular layer, CRT, calretinin; PV, parvalbumin; NPY, neuropeptide Y; HIPP, Hilar perforant path-associated.

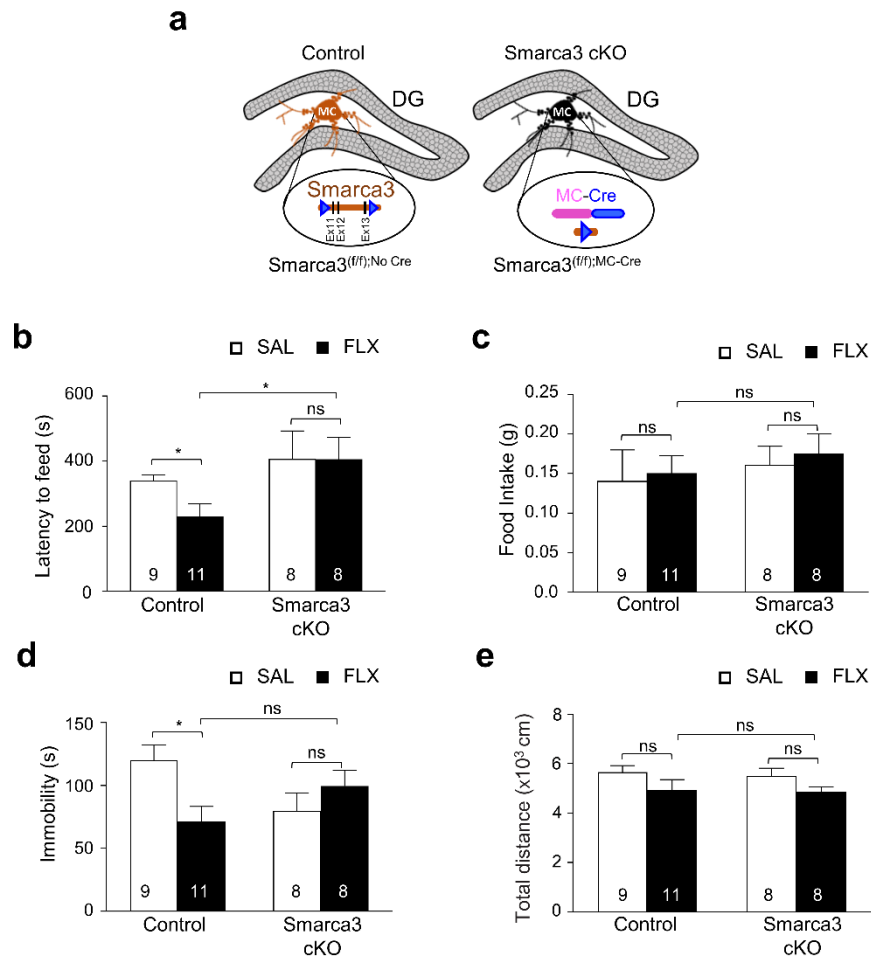


Figure 10. Mossy cell-specific knockout of *Smarca3* gene using MC-Cre mice abolishes behavioral responses to chronic SSRI treatment.

(a) Schematic illustration of genetic deletion of *Smarca3* gene in mossy cells using MC-Cre line. (b) The NSF test. Control and *Smarca3* cKO group have genotype of *Smarca3*^(ff/ff) without Cre, and *Smarca3*^(ff/ff) with MC-Cre, respectively. Two-way ANOVA, [genotype x drug interaction $F(1,31)=4.334$; $P=0.0489$, genotype factor $F(1,31)=4.404$; $P=0.00441$, drug factor $F(1,31)=2.77$; $P=0.3238$], followed by the Turkey's post hoc test. (c) The hunger level was assessed by home cage feeding test with the same set of animals. (d) Depressive-like behavioral testing in the tail suspension test [TST]. (e) Basal locomotor activity of control and *Smarca3* cKO mice in the open field test [OFT]. Data are represented as means \pm SEM. Pair-wise comparison by post hoc test; * $p < 0.5$, ns, non-significant.

3.1.2 Effect of mossy cell-specific inhibition of the p11/AnxA2/SMARCA3 complex on neurogenic and behavioral responses to chronic antidepressant treatment.

Although I evaluated the effects of genetic deletion of *p11* or *Smarca3* gene in mossy cells on antidepressant responses using cell type-specific KO mice, these transgenic approaches could not rule out the possibility that these behavioral changes are due to developmental defects or off-target deletion of *p11* or *Smarca3* gene in those cKO mice. Thus, I further examined the neurogenic and behavioral effects of mossy cell-specific inhibition of the p11/AnxA2/SMARCA3 complex in adult mice. To this end, I developed recombinant constructs to inhibit the assembly of the p11/AnxA2/SMARCA3 complex. Our previous study showed that the p11/AnxA2 heterotetramer formed a stable heterohexameric complex with either SMARCA3 or AHNAK1, using very similar recognition principles. The short peptide derived from the binding region of SMARCA3 or AHNAK1 makes a stable complex with the p11/AnxA2 heterotetramer by occupying the hydrophobic binding pocket created on the surface of the P11/AnxA2 heterotetrameric complex [46]. Based on information about the co-crystallization structure of the ternary complex, I designed a recombinant inhibitor of the p11/AnxA2/SMARCA3 complex (**P11/AnxA2/SMARCA3 complex Inhibitory Peptide-**

AcGFP1 fusion construct (**PASIP-AcGFP1**) along with an inert control (**control AcGFP1**) (Figure 11a). I assumed that this recombinant inhibitor protein competes with endogenous SMARCA3 on the binding pocket and thus blocks the functional assembly of the active ternary complex, the p11/AnxA2/SMARCA3 heterohexamer (Figure 11b). By conducting an *in vitro* co-immunoprecipitation assay, I confirmed that the recombinant PASIP-AcGFP1 construct was able to successfully block the assembly of the P11/AnxA2/SMARCA3 complex (Figure 11c). I further generated Cre-dependent AAVs to deliver those PASIP-AcGFP1 constructs into the hippocampal mossy cells. Cre-dependent AAVs were injected locally into hilus regions of MC-Cre transgenic mice (Figure 11d and 11e). Because MC-Cre mice were known to display Cre-recombination in both dentate mossy cells and a minor pyramidal subpopulation in the CA3c region [37], I delivered recombinant AAV solution in the middle of the hilus region to avoid the unnecessary diffusion of viral particles. My histological analysis confirmed that AcGFP1 signal was found exclusively in the hilus and the inner molecular layer (IML) where somas and axonal fibers of mossy cells localize, respectively, but not in the CA3 region where pyramidal cells localize (Figure 12b - 12c), ensuring the hippocampal subregion specificity. In addition, I confirmed that AcGFP1-fusion proteins (control AcGFP1,

PASIP-AcGFP1) were specifically expressed in mossy cells, but not in other GABAergic interneurons, including PV+ basket cells and NPY+ HIPP cells (Figure 12d and 12e), ensuring the cell type specificity in the dentate gyrus.

After preventing formation of the p11/AnxA2/SMARCA3 complex with mossy cell-specific expression of the PASIP-AcGFP1 construct, I examined the neurogenic and behavioral outcome of chronic administration of SSRI (Figure 12a). It is well established that adult neurogenesis in the dentate gyrus is induced in response to chronic antidepressant treatment [63-65]. In control and PASIP-AcGFP1 mice, I assessed chronic fluoxetine-induced proliferation activity of neural progenitors. A significant increase in BrdU+ proliferating cells was observed in the subgranular zone (SGZ) of control AcGFP1 mice after chronic fluoxetine treatment, which was abolished in the SGZ of PASIP-AcGFP1 mice ($p=0.73$) (Figures 13a - 13d). In addition, I analyzed the expression level of doublecortin (DCX), which represent a snapshot of newborn postmitotic cells undergoing neuronal differentiation and maturation [66]. Chronic fluoxetine administration increased the DCX immunofluorescence signal in the SGZ of control AcGFP1 mice, but the effect of fluoxetine was attenuated in the SGZ of

PASIP-AcGFP1 mice (Figures 14a - 14d). I found that the inhibitory effect of PASIP-AcGFP1 expression on fluoxetine-induced neurogenic activities was observed consistently along the rostro-caudal axis of the dentate gyrus (Figures 13d and 14d).

I next investigated the possible functional significance of the p11/AnxA2/SMARCA3 complex in mossy cells for basal locomotor activity, anxiety-related behaviors and SSRI-induced behavioral changes. Control AcGFP1 and PASIP-AcGFP1 mice did not display a difference in basal locomotor activity when monitored using the open field [OF] test (Figure 15a). In addition, inhibition of the p11/AnxA2/SMARCA3 complex failed to show a consistent effect on multiple anxiety-related behaviors. Control AcGFP1 and PASIP-AcGFP1 mice showed a difference in the light/dark box [LDB] test ($p = 0.0064$) (Figure 15c), but not in the other two anxiety-related behaviors (thigmotaxis test ($p = 0.74$), Figure 10b; the elevated plus maze test [EPM] ($p = 0.587$), Figure 15d). In addition, they did not display any baseline difference in depression-like behavioral tests (tail suspension test [TST], Figure 16c; novelty-suppressed feeding [NSF] test, Figure 16a). However, the latency to feed was decreased after chronic fluoxetine administration in control AcGFP1 mice, but not in PASIP-AcGFP1 mice (Figure 16a). Neither fluoxetine treatment nor inhibition of the

p11/AnxA2/SMARCA3 complex caused any significant effect on home cage feeding (Figure 16b), suggesting that this behavioral change was unlikely due to different hunger levels between comparison groups. The antidepressant-induced behavioral change observed in the NSF test was also observed in the tail suspension test [TST] (Figure 16c). Taken together, these data indicate that the p11/AnxA2/SMARCA3 complex in mossy cells may play a crucial role in behavioral changes after chronic treatment with SSRIs.

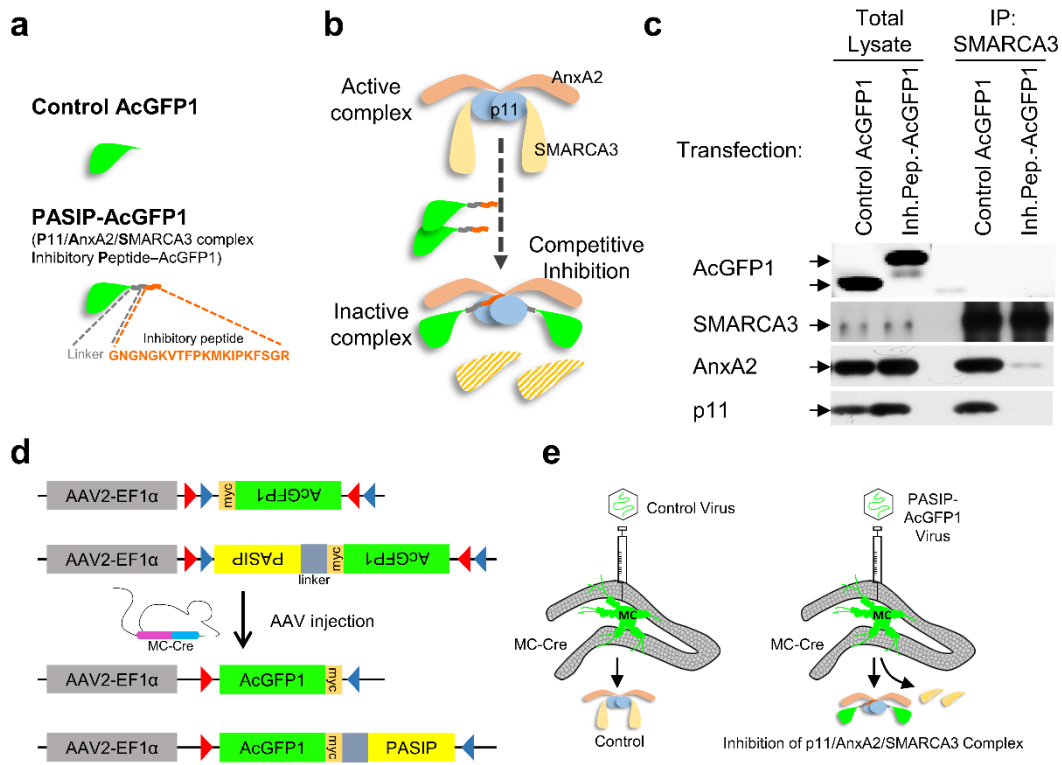


Figure 11. Development of viral construct for Mossy cell-specific disruption of the p11/AnxA2/SMARCA3 complex.

(a) Molecular design for the p11/AnxA2/SMARCA3 complex-Inhibitory Peptide (PASIP)-AcGFP1 fusion protein (PASIP-AcGFP1). (b) Schematic illustration of how the recombinant inhibitor (PASIP-AcGFP1) blocks the functional assembly of the p11/AnxA2/SMARCA3 heterohexameric complex. Upon dissociation from the complex, SMARCA3 becomes inactive. (c) *In vitro* pull-down assay demonstrates that PASIP-AcGFP1 disrupts the p11/AnxA2/SMARCA3 complex. SMARCA3 was immunoprecipitated from HEK 293 cells that were transfected with either control AcGFP1 or PASIP-AcGFP1 construct. The immune complexes were subjected to immunoblot analysis using AcGFP1-, SMARCA3-, AnxA2- and p11 antibodies. (d) Schematic illustration of the double-floxed Cre-dependent AAV vectors expressing control AcGFP1 or PASIP-AcGFP1 under control of EF-1 α promoter. (e) Recombinant AAVs, expressing either control AcGFP1 or the PASIP-AcGFP1, were stereotaxically injected into the dentate gyrus of MC-Cre transgenic mice.

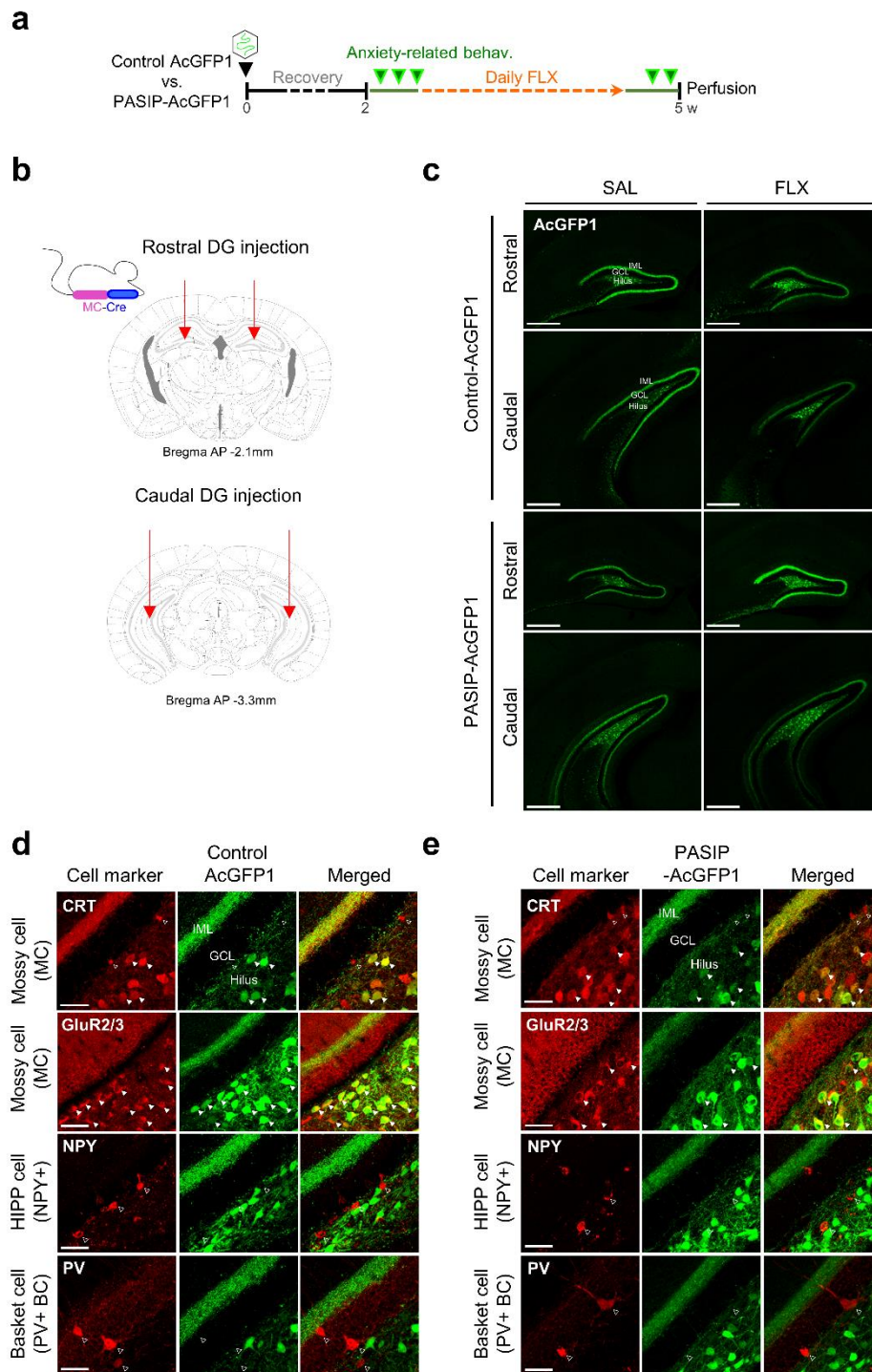


Figure 12. Mossy cell-specific expression of control AcGFP1 or PASIP-AcGFP1 construct along the rostro-caudal axis of the hippocampus.

(a) Experimental design. Control AcGFP1- or PASIP-AcGFP1-injected mice were administered saline (SAL) or fluoxetine (FLX) for 3 weeks. After behavioral testing, all the animals were labeled with BrdU for the last 3

hours prior to perfusion. (b) Schematic illustration for stereotaxic injection of Cre-dependent AAVs expressing either control AcGFP1 or PASIP-AcGFP1 along the rostral-caudal axis of the hippocampus. Stereotaxic coordinates for either rostral or caudal injection of AAV (Rostral : AP -2.1 mm, ML \pm 1.4 mm, DV -1.95 mm. Caudal : AP -3.3 mm, ML \pm 2.7 mm, DV -3.6 mm). (d and e) Mossy cell-specific expression of control AcGFP1 or PASIP-AcGFP1 construct. Hippocampal sections from the AAV-injected animals were immunostained with CRT (Calretinin; mossy cell maker), GluR2/3 (glutamate receptor subunit GluR2/3; mossy cell marker), PV (parvalbumin; PV+basket cell marker), NPY (neuropeptide Y; HIPP cell marker). Representative co-labeling images for the cell type-specific expression of control AcGFP1 or PASIP-AcGFP1 in mossy cells (filled arrowheads), but in neither PV+basket cells nor NPY+HIPP cells (open arrowheads). Solid arrowheads indicate representative double labeled cells, and open arrowheads show cells labeled only with markers. Abbreviations: DG, dentate gyrus; GCL, granule cell layer; IML, innermolecular layer; NPY, neuropeptide Y; HIPP, Hilar perforant path-associated; GluR2/3, glutamate receptor 2/3; PV, parvalbumin; MC, mossy cell. Scale bar, 50 μ m.

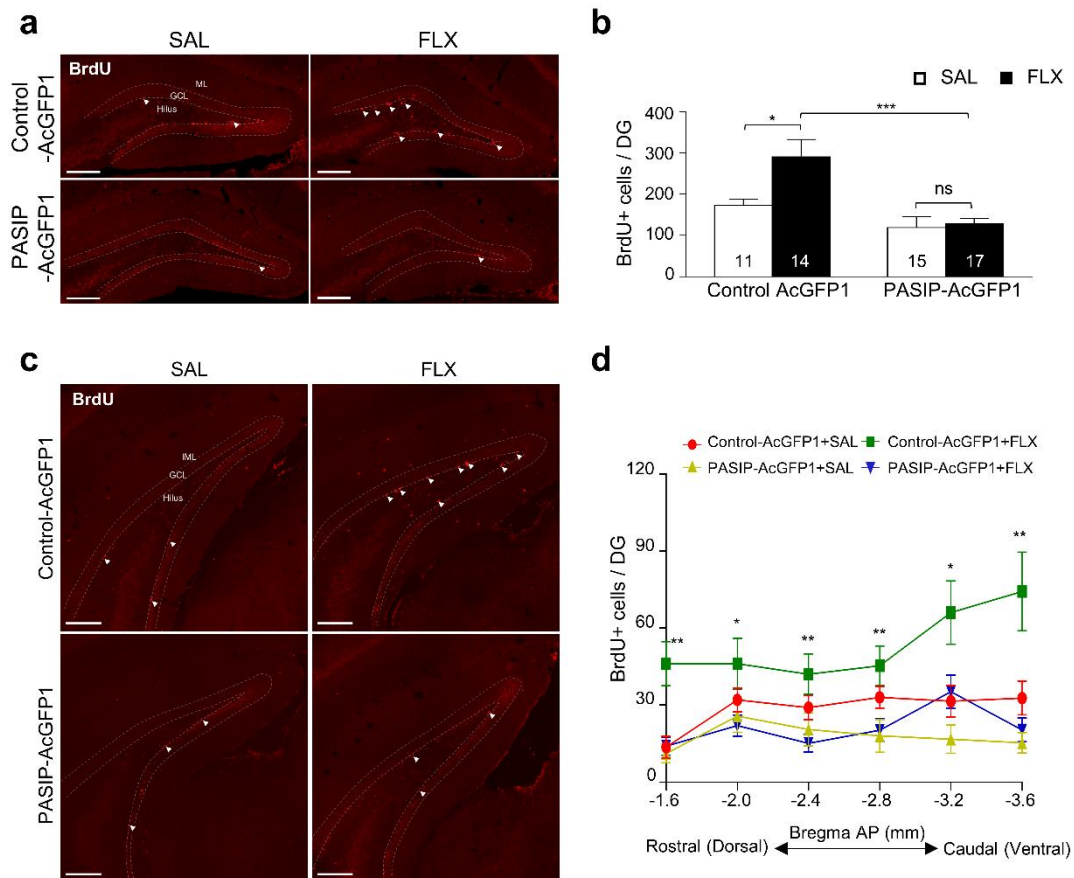


Figure 13. Effects of mossy cell specific disruption of p11/Anx2/SMARCA3 complex on proliferation of new-born cells in response to chronic SSRI treatment.

(a) Representative images with α -BrdU immunostaining results. BrdU+cells in the subgranular zone (SGZ) are as indicated in each image (solid arrowheads). Scale bars, 100 μ m. (b) Quantification of BrdU-positive cells in the SGZ. Two-way ANOVA, [AAV x drug interaction $F(1,51)=4.129$; $P=0.0498$, AAV factor $F(1,51)=18.54$; $P<0.0001$, drug factor $F(1,51)=8.65$; $P=0.0049$], followed by the Turkey's post hoc test. (c) Representative images with BrdU-positive cells in the caudal dentate gyrus from control AcGFP1 and PASIP-AcGFP1 mice. (d) Quantification of BrdU-positive cells along the rostro-caudal axis of the hippocampus. Data are represented as means \pm SEM. Pair-wise comparison by post hoc test; * $p < 0.5$, ** $p < 0.01$, *** $p < 0.001$, ns, nonsignificant. Abbreviations: GCL, granule cell layer; IML, inner molecular layer; DG, dentate gyrus.

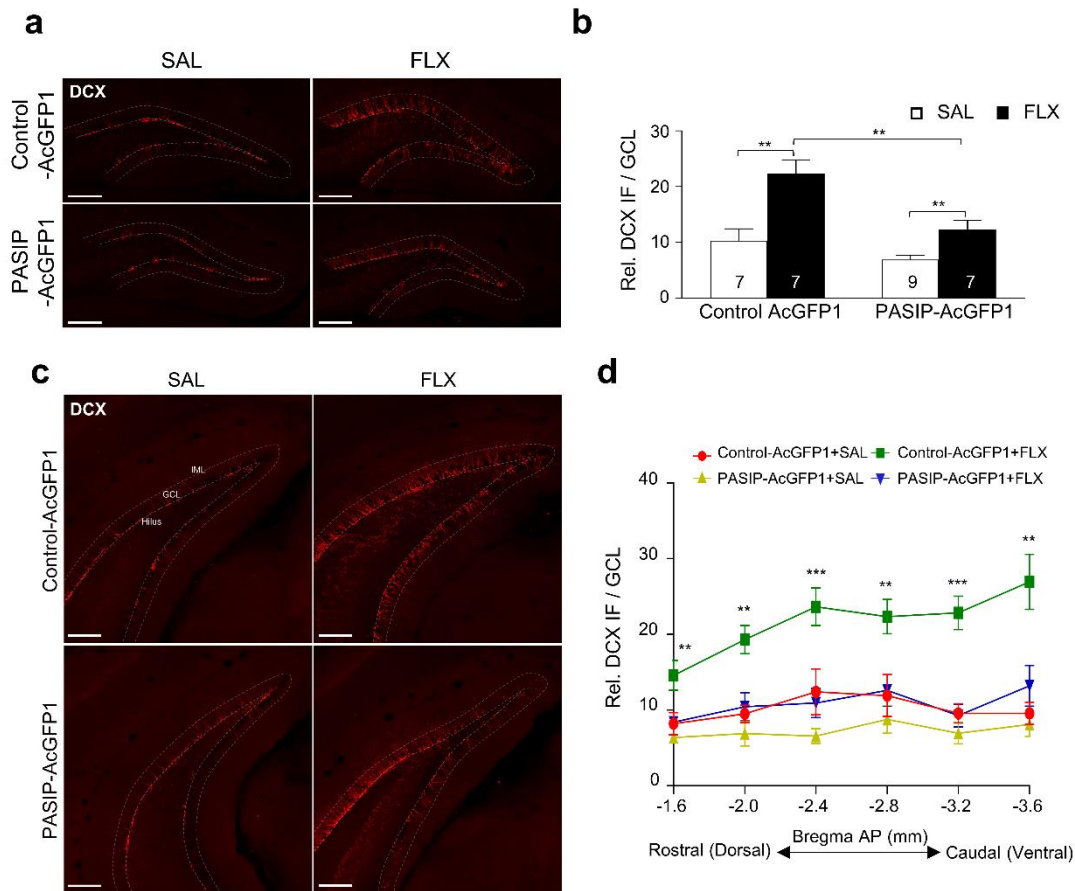


Figure 14. Effects of mossy cell specific disruption of p11/Anx2/SMARCA3 complex on differentiation of new-born cells in response to chronic SSRI treatment.

(a) Representative images of DCX-positive cells in control-AcGFP and PASIP-AcGFP1 mice. (b) Quantitation of DCX-positive cells in the SGZ and the GCL. Two-way ANOVA, [AAV x drug interaction $F(1,25)=6.364$; $P=0.0184$, AAV factor $F(1,25)=18.54$; $P<0.0001$, drug factor $F(1,25)=8.65$; $P=0.0049$], followed by the Turkey's post hoc test. (c) Representative images of DCX-immunostaining results in the caudal dentate gyrus from control AcGFP1 and PASIP-AcGFP1 mice. (d) Quantitation of DCX-immunofluorescence along the rostro-caudal axis of the hippocampus. Data are represented as means \pm SEM. Pair-wise comparison by post hoc test; ** $p < 0.01$, *** $p < 0.001$. Abbreviations: Rel. DCX IF, relative doublecortin immunofluorescence; GCL, Granule cell layer; IML, innermolecular layer; SAL, saline; FLX, Fluoxetine.

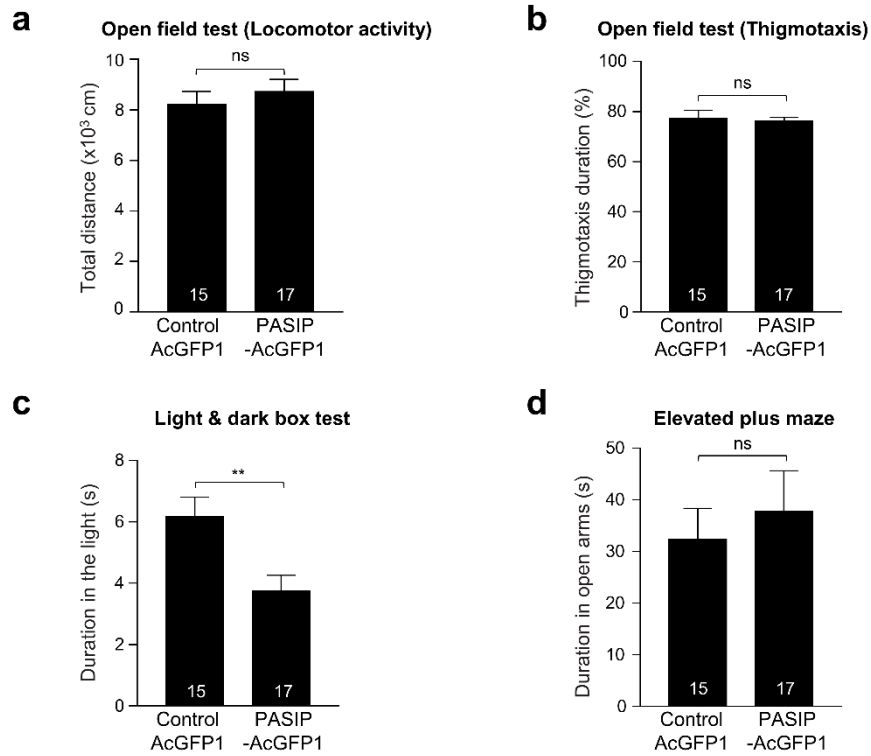


Figure 15. Effects of mossy cell-specific disruption of the p11/AnxA2/SMARCA3 complex on basal locomotion or anxiety-related behaviors.

(a) Basal locomotor activity of control AcGFP1 and PASIP-AcGFP1 mice in the open field [OF] test. (b) Thigmotaxis of control AcGFP1 and PASIP-AcGFP1 mice in the open field [OF] test. (c) Light & Dark Box [LDB] test. (d) Elevated plus maze [EPM] test. Data are represented as means \pm SEM. Paired Student's t-test. **p<0.01, ns; non-significant.

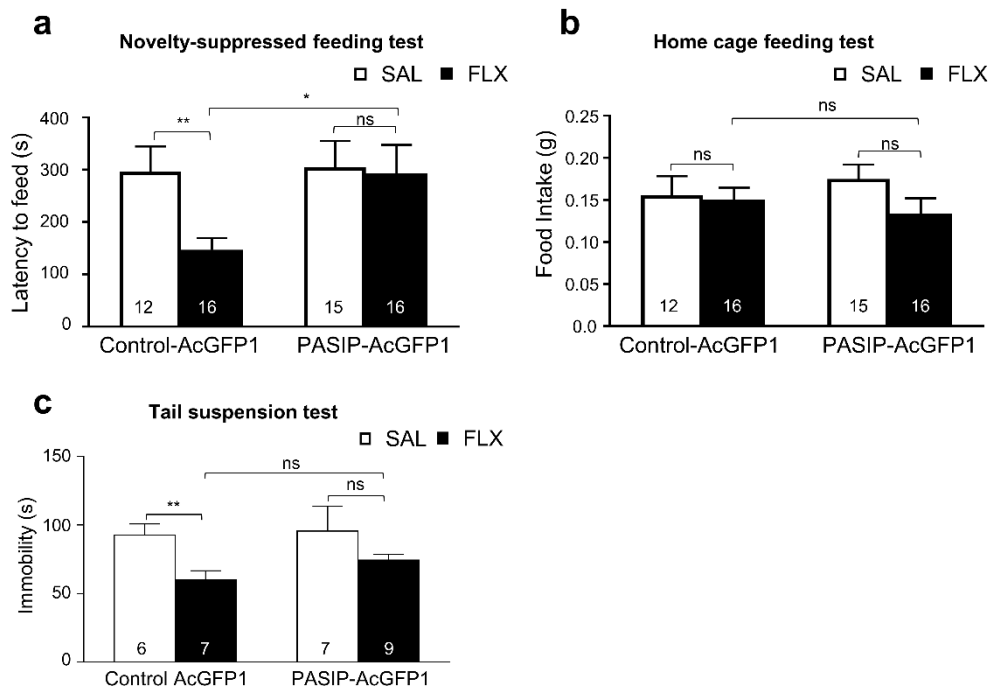


Figure 16. Effects of mossy cell-specific disruption of the p11/AnxA2/SMARCA3 complex on behavioral response to chronic SSRI treatment.

(a) Novelty suppressed feeding test (NSF). Two-way ANOVA, [AAV x drug interaction $F(1,54)=4.09$; $P=0.0481$, AAV factor $F(1,54)=4.084$; $P=0.0327$, drug factor $F(1,54)=4.584$; $P=0.0368$], followed by the Turkey's post hoc test. (b) Home cage feeding levels. (c) Tail suspension test [TST]. Data are represented as means \pm SEM. Pair-wise comparison by post hoc test; * $p < 0.05$, ** $p < 0.01$, ns, non-significant.

3.1.3 Effects of cell type-specific inhibition of the p11/AnxA2/SMARCA3 complex on neuronal activity of mossy cells.

I first examined the effects of chronic antidepressant administration on neuronal activity of mossy cells. Mossy cells are spontaneous firing neurons in the hilus, whose activity modulates neuronal circuitry and function of the dentate gyrus [67]. To identify mossy cells for electrophysiological recordings, I labeled mossy cells with a fluorescence protein, AcGFP1, by injecting Cre-dependent AcGFP1 AAVs into mossy cell-specific Cre (MC-Cre) mice (Figure 17a). AcGFP1 was shown to be restrictively expressed in mossy cells in the dentate gyrus (Figure 17b). Mossy cells were further confirmed by their morphology, tonic firing pattern and membrane capacity (50-100 pF). Electrophysiological recordings showed that chronic fluoxetine treatment significantly enhanced the spontaneous firing rate of mossy cells (Figures 17c and 17d), but acute treatment of the drug had no effect on mossy cell activity (Figures 17e and 17f).

Previous studies have shown that acute restraint stress decreases c-fos immunoreactivity in hilar mossy cells of the hippocampus [68]. I further investigated whether neuronal

activity of mossy cells was altered by chronic stress exposure and the following antidepressant administration. After using the chronic unpredictable mild stress (CUMS) paradigm, which is a rodent model of chronic stress-induced depression [69] (Figure 18a), I counted the active mossy cells in the hilus by immunostaining c-Fos, a neural activation marker [68, 70]. c-Fos immunoreactivity in mossy cells was significantly reduced by chronic exposure to unpredictable stress (Figures 18b and 18c). In contrast, chronic fluoxetine administration to the stressed animals resulted in a remarkable increase in c-Fos immunoreactivity in mossy cells (Figures 18d, 18e and 18f), which was consistent with my electrophysiological recording shown above (Figures 17c and 17d). These results revealed that the neuronal activity of mossy cells was suppressed by chronic stress, and the effect was reversible by chronic fluoxetine administration.

I next examined the regulation by p11 and SMARCA3 of mossy cell activity. I found that the spontaneous firing rate of mossy cells was greatly reduced in *p11* cKO mice (Figures 19a and 19b) and *Smarca3* cKO mice (Figures 19c and 19d) compared to control mice. These data suggested that p11 and SMARCA3 played a role in regulating neuronal activities of

mossy cells.

I further investigated the effects of inhibition of the p11/AnxA2/SMARCA3 complex on neuronal activity of mossy cells. Previous studies have shown that the p11/AnxA2/SMARCA3 complex is induced in the mossy cells by chronic fluoxetine administration and is further targeted to the nuclear matrix to regulate gene transcription [71, 72]. Thus, I additionally generated a PASIP-AcGFP1-NLS construct that was specifically targeted to the nucleus of mossy cells due to triple nuclear localization signals (3×NLS) fused at the C-terminus (Figure 20a). I generated a series of Cre-dependent viral vectors, including control AcGFP1, PASIP-AcGFP1, and PASIP-AcGFP1-NLS (Figure 20a). By co-transfection into cultured HEK 293 cells or stereo-injection into the dentate gyrus of mossy cell-specific Cre (MC-Cre) transgenic mice, I verified the nuclear-specific expression of the PASIP-AcGFP1-NLS construct (Figure 20b) and also the cell-type specific expression of the PASIP-AcGFP1 constructs in the dentate mossy cells (Figure 20b). Of note, the firing rate of mossy cells was significantly decreased by PASIP-AcGFP1 or PASIP-AcGFP1-NLS expression compared to control AcGFP1 expression (Figures 20c and 20d). I further observed that c-Fos immune-reactivity was markedly reduced by PASIP-AcGFP1 expression in mossy cells, but

not by control AcGFP1 expression (Figures 21a – 21c), verifying a significant role of the p11/AnxA2/SMARCA3 complex in the regulation of mossy cell excitability.

Collectively, these results show that the neural activity of mossy cells is decreased during chronic stress-induced depression and this decrease is reversed by chronic antidepressant administration, possibly through the p11/AnxA2/SMARCA3, an inducible protein complex.

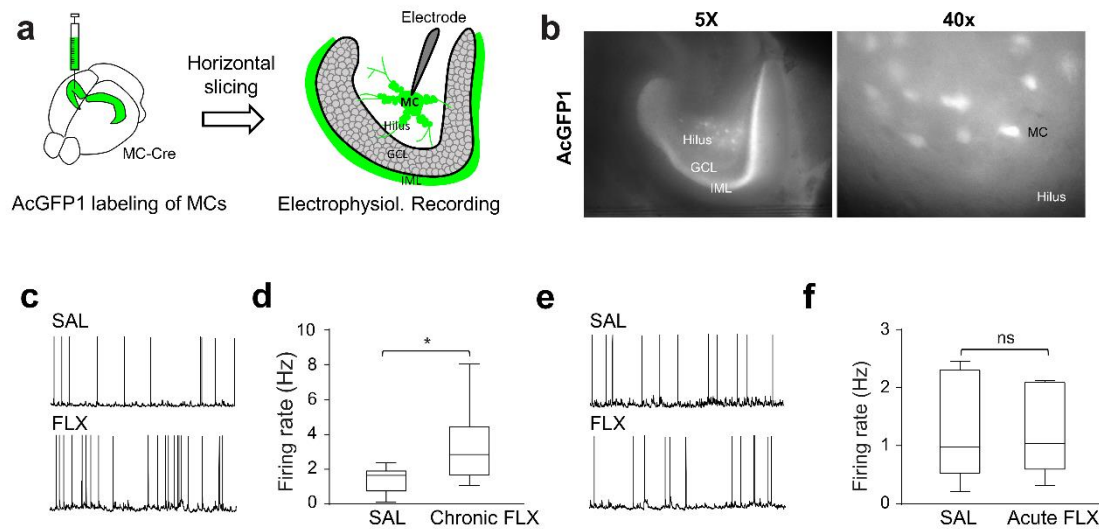


Figure 17. Neuronal activity of mossy cells is enhanced by chronic SSRI treatment, but not by acute treatment.

(a) Schematic of AcGFP1 AAV injection into the hippocampus of MC-Cre mice. Ventral hippocampal slices were used for electrophysiological recordings. (b) Representative fluorescence images of AcGFP1-labeled mossy cells in a hippocampal section of the AAV-injected mice. Magnifications: 5 \times or 40 \times objective lens. (c and d) Representative traces (c) and Whisker box plot (d) showing the spontaneous firing rate of mossy cells by chronic FLX administration on 8-week-old mice (oral administration, 18 days, n = 9 cells / 3 mice per group). Scale bar: 1 s, 50 mV. Two-tailed, unpaired T-test; P=0.044. (e and f) Representative traces (e) and Whisker box plot (f) showing the spontaneous firing rate of mossy cells from 8-week-old mice injected with a single dose of saline or fluoxetine (10 mg/kg). n = 9 cells / 3 mice per group. Scale bar: 1 s, 50 mV. Two-tailed, unpaired T-test; P=0.9401. Data are represented as means \pm SEM. Paired Student's t-test, *p<0.05, ns, non-significant. Abbreviations: GCL, granule cell layer; IML, inner molecular layer; MC, mossy cell; SAL, saline; FLX, fluoxetine.

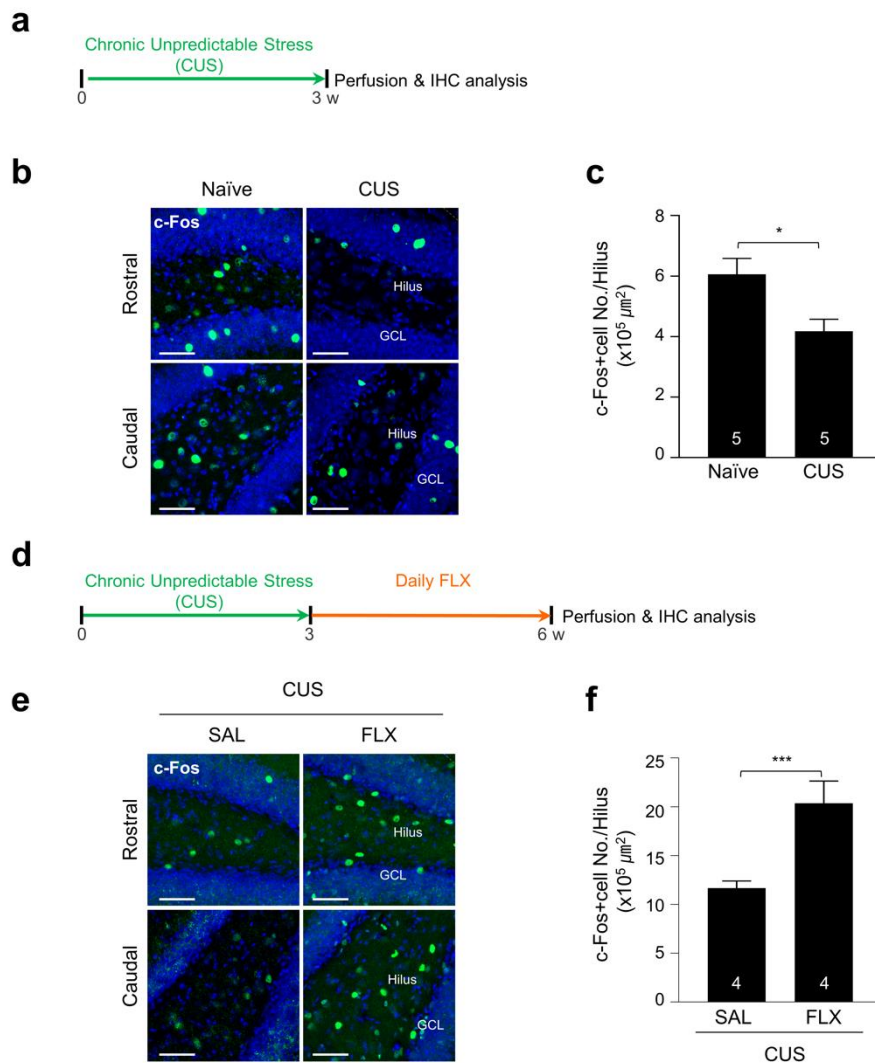


Figure 18. Effect of chronic unpredictable stress or antidepressant administration on expression of c-Fos a neuronal activity marker in the mossy cells.

(a) Schematic of experimental design. Wild-type mice were subjected to chronic unpredictable stress (CUS) paradigm. (b) Representative images of c-Fos positive cells (Green) with counter staining (Blue, DraQ5) in the naïve or the stressed mice. Scale bar, 50 μm . (c) Quantitative graph of c-Fos positive cell number in the hilus region of the Naïve or the stressed mice. (d) Schematic of experimental design. Wild-type mice were subjected to chronic unpredictable stress (CUS) paradigm which was followed by daily administration of saline (SAL) or fluoxetine (FLX) for last 3 weeks. (e) Representative images of c-Fos positive cells (Green) with counter staining (Blue, DraQ5) in the stressed mice treated with either saline (SAL) or fluoxetine (FLX). Scale bar, 50 μm . (f) Quantitative graph of c-Fos positive cell number in the dentate hilus region of the stressed mice with or without fluoxetine treatment. Data are represented as means \pm SEM. Paired Student's t-test, * $p < 0.05$, *** $p < 0.001$.

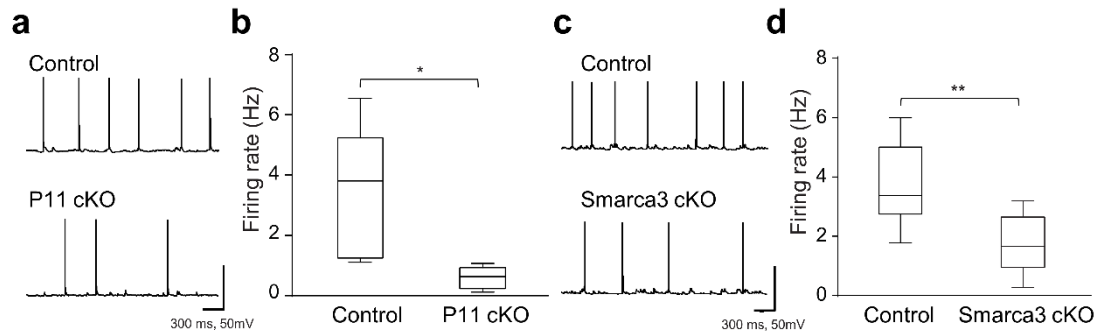


Figure 19. Neuronal activity of mossy cells is silenced by mossy cell-specific deletion of *p11* or *Smarca3* gene.

(a and b) Reduced neuronal activity of mossy cells in *p11* cKO mice. Mossy cells were labeled by injecting Cre-dependent AcGFP1 AAV into *p11* wild-type (+/+, MC-Cre)(Control) and *p11* conditional KO (*p11*^{(f/f);MC-Cre}) (*p11* cKO). Representative traces (a) and Whisker box plot (b) showing the spontaneous firing rate of mossy cells in the dentate gyrus of control and *p11* cKO mice at 16 weeks of age. n = 10 cells / 3 mice for control; n = 6 cells / 3 mice for *p11* cKO. Scale bar: 300 ms, 50 mV. Two-tailed, unpaired T-test; P=0.0255. (c and d) Reduced electrophysiological activity of mossy cells in *Smarca3* cKO mice. Mossy cells were labeled by injecting the Cre-dependent AcGFP1 AAV into *Smarca3* wild-type (+/+, MC-Cre) (Control) and *Smarca3* conditional KO (*Smarca3*^{(f/f);MC-Cre}) (*Smarca3* cKO). Representative traces (a) and Whisker box plot (b) showing the spontaneous firing rate of mossy cells in the dentate gyrus of control and *Smarca3* cKO mice at 16 weeks of age. n = 9 cells / 3 mice per group. Scale bar: 300 ms, 50 mV. Two-tailed, unpaired T-test; P=0.0073. Data are represented as means ± SEM. Paired Student's t-test, *p<0.05, **p<0.01.

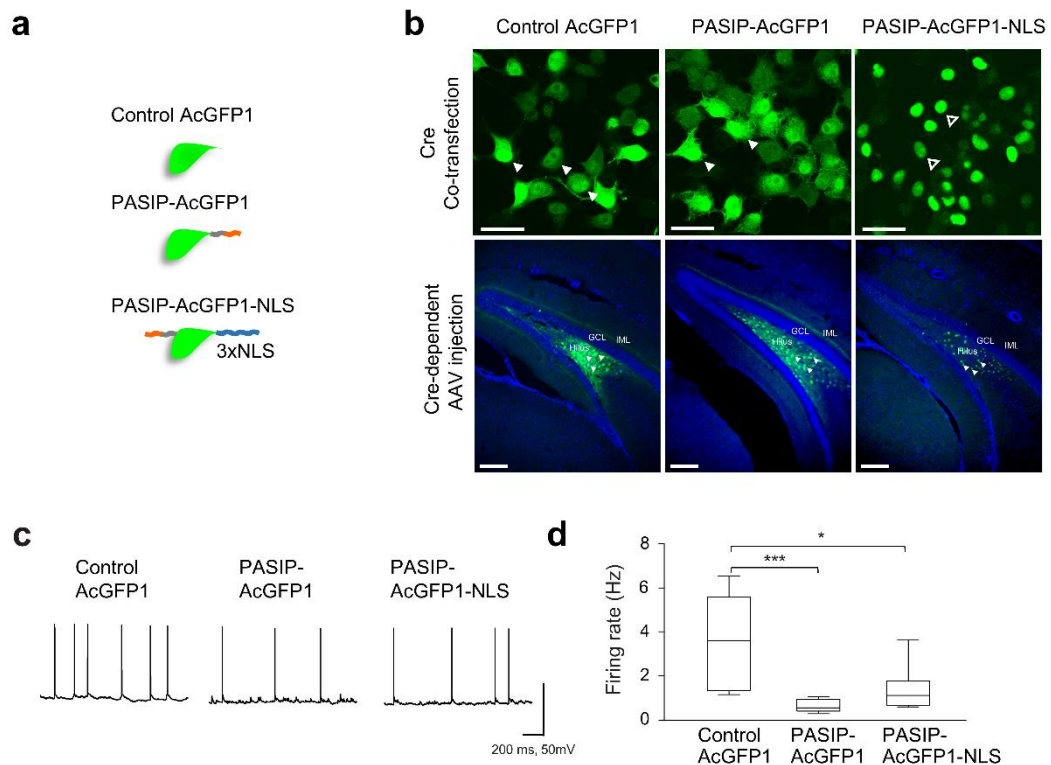


Figure 20. Neuronal activity of mossy cells is silenced by mossy cell-specific disruption of p11/AnxA2/SMARCA3 complex.

(a) Schematic design for a series of PASIP-fusion constructs, including control AcGFP1, whole cell inhibitor construct (PASIP-AcGFP1) and nucleus-targeted inhibitor construct (PASIP-AcGFP1-NLS). (b) Immunofluorescence images showing subcellular localization of each AcGFP1 construct in HEK 293 cells where each recombinant AAV was co-transfected with Cre-expressing vectors. Differently from control AcGFP1, and PASIP-AcGFP1 (solid arrowheads), PASIP-AcGFP1-NLS show the nuclear localization in the co-transfected cells (open arrowheads). Scale bar, 100 μ m (Upper) and mossy cell-specific expression in the dentate gyrus of AAV-injected mice. AcGFP1-positive MC was indicated (filled arrowheads). Scale bar, 100 μ m. (bottom) (c and d) Disrupted p11/AnxA2/SMARCA3 complex reduces firing rate of mossy cells. Representative traces (c) and Whisker box plot (d) showing the spontaneous firing rate of mossy cells expressing each construct: control AcGFP1 (n = 12 cells / 4 mice), PASIP-AcGFP1 (n = 8 cells / 3 mice), PASIP-AcGFP1-NLS (n = 8 cells / 3 mice) in 16-week-old mice. Scale bar: 200 ms, 50 mV. One-way ANOVA [F(2,21)=10.08; P=0.0009], followed by Bonferroni's multiple comparison test. Pair-wise comparison; * P < 0.01, *** p < 0.001. Abbreviations: GCL, granule cell layer; IML, inner molecular layer; NLS, nuclear localization signal.

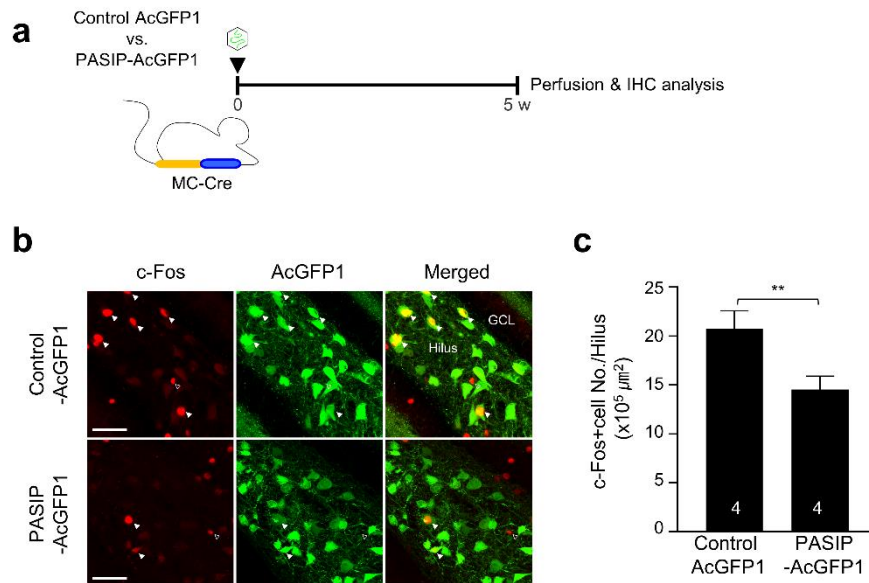


Figure 21. Effect of p11/AnxA2/SMARCA3 complex inhibition on c-Fos expression in the mossy cells.

(a) Preparation of the control AcGFP1- or PASIP-AcGFP1-injected mice. (b) Representative images of c-fos immunostaining of the dentate gyrus section from the control AcGFP1 or PASIP-AcGFP1 mice. Solid arrowheads indicate representative double labeling of AcGFP1 (green) and c-Fos (red). Open arrowheads show cells labeled only with c-Fos expression, but without detectable AcGFP1 expression. Scale bar, 50 μm . (c) Quantitation of c-fos positive cell number in the hilus region of the dentate gyrus. Data are represented as means \pm SEM. Paired Student's t-test, ** $p < 0.01$, *** $p < 0.001$, ns; non-significant.

3.2 Effects of modulation of mossy cells activity in antidepressant responses to chronic SSRI administration.

3.2.1 Effects of selective stimulation of dentate mossy cells on adult neurogenesis in the hippocampus.

Next I examined whether acute chemogenetic stimulation of mossy cells using the Gq-DREADD system was able to mimic the chronic effects of fluoxetine. To modulate the dentate mossy cells, I delivered viral vectors expressing control mCherry (Control) or hM3D-Gq-mCherry (Gq-DREADD), into hilus regions of MC-Cre transgenic mice (Figure 22a - 22c). By using immunostaining with c-Fos, I verified that mossy cells were stimulated by clozapine-N-oxide (CNO) administration in Gq-DREADD mice, when compared to control mice (Figure 23a – 23e).

I assessed adult neurogenesis activities using BrdU-labeling of neural progenitor cells and doublecortin (DCX)-immunolabeling of post-mitotic immature neurons, in the presence or the absence of CNO/Gq-DREADD activation. Interestingly, Gq-DREADD stimulation of mossy cells significantly increased the number of BrdU⁺ proliferating cells and DCX immunostaining intensity in the SGZ of the dentate gyrus compared to control mice (Figures 24a - 24b and 25a - 25b). Mossy cell-dependent regulation of neurogenesis activities was

consistent throughout the rostro-caudal axis of the dentate gyrus. (Figures 24c - 24d and 25c - 25d). Next, I investigated the effects of direct stimulation of mossy cells on basal locomotion, anxiety, and depression-related behaviors (Figures 26a - 26d and 27a - 27c). Chemogenetic-stimulation of mossy cells alone increased the duration in the open arms of the EPM test (Figure 26d), but failed to induce significant differences in other types of anxiety-related behaviors (Figures 26a - 26c). Furthermore, acute stimulation of mossy cells with CNO injection did not result in any significant change in the depression-like behaviors including the NSF test, and the TST (Figures 27a – 27c). Collectively, these results suggest that acute stimulation of mossy cells is sufficient to trigger adult neurogenesis, but that is unlikely sufficient to achieve full improvement in anxiety and depressive-like behaviors.

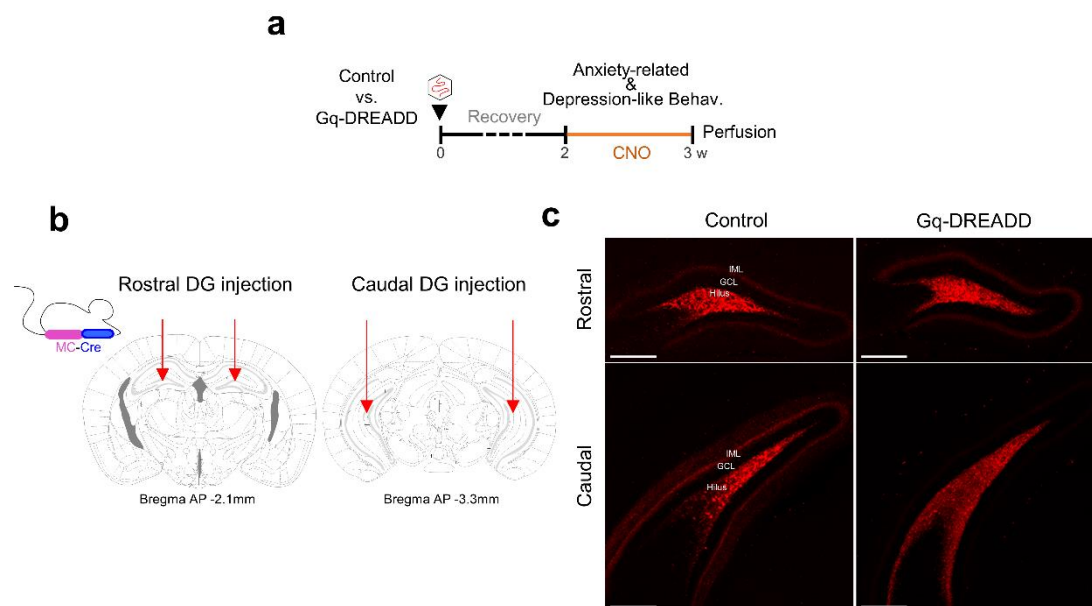


Figure 22. Mossy cell-specific expression of the control or Gq-DREADD construct along the rostro-caudal axis of the hippocampus.

(a) Schematic of experimental design. Control and Gq-DREADD mice were tested for anxiety-related or depression-like behaviors with CNO injection. One day after the last behavioral testing, all mice were labeled with BrdU for 3 hours and then sacrificed with transcardinal perfusion. (b) Schematic illustration for stereotaxic injection of Cre-dependent AAVs expressing either control or Gq-DREADD along the rostro-caudal axis of the hippocampus. Stereotaxic coordinate for either rostral or caudal injection of AAV (Rostral: AP - 2.1 mm, ML \pm 1.4 mm, DV -1.95 mm. Caudal: AP -3.3 mm, ML \pm 2.7 mm, DV -3.6 mm). (c) Representative images showing longitudinal expression of control or Gq-DREADD along the rostro-caudal axis of the hippocampus of MC-Cre mice. Scale bar, 100 μ m. Abbreviations: DG, Dentate gyrus; GCL, Granule cell layer; IML, innermolecular layer.

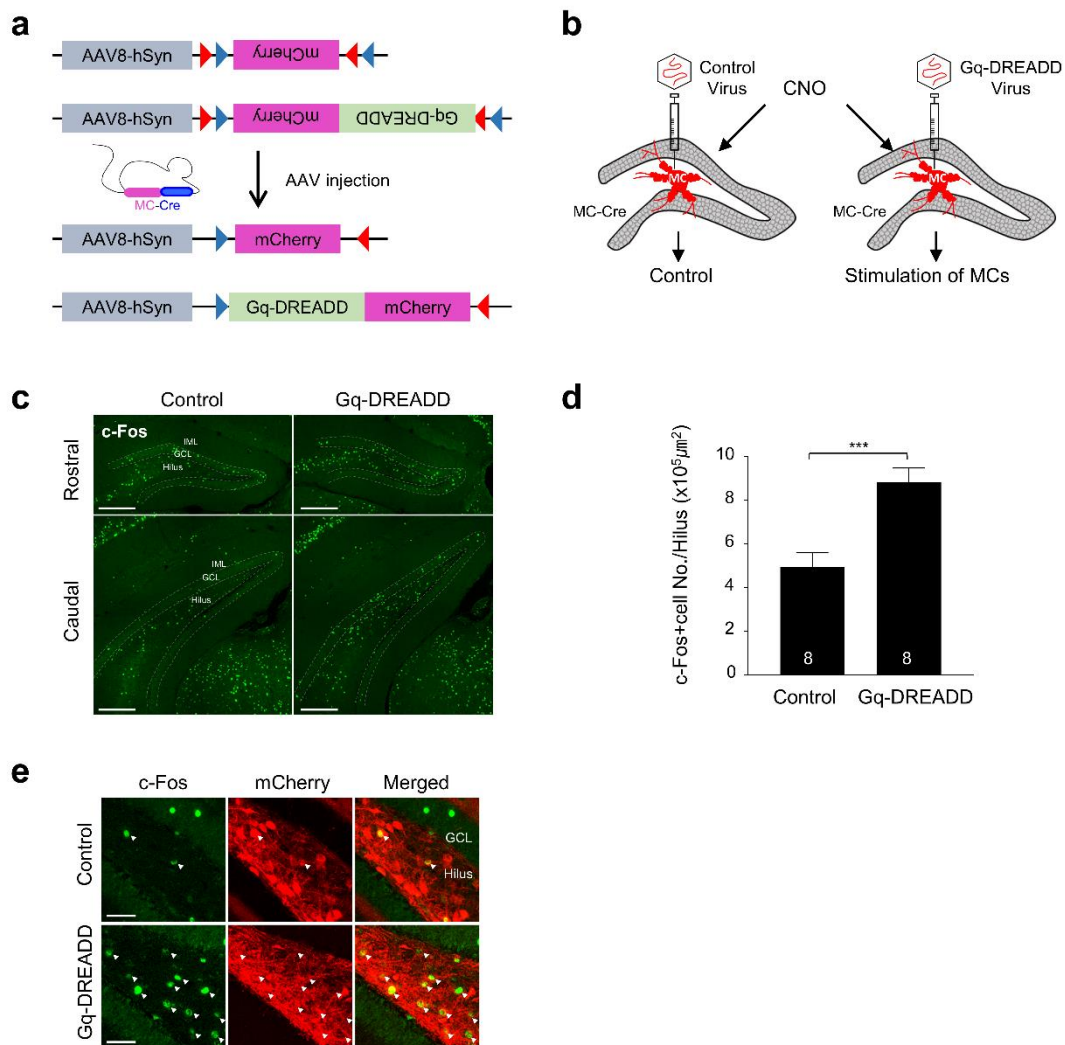


Figure 23. Mossy cell-specific expression of Gq-DREADD construct stimulates the mossy cell activity by CNO administration.

(a) Schematic illustration of the double-floxed Cre-dependent AAV vector expressing control and Gq-DREADD constructs under control of human Synapsin I (hSyn) promoter. (b) Schematic illustration of chemogenetic stimulation of mossy cells with Gq-DREADD system. (c) Representative images of c-Fos positive cells in the control or Gq-DREADD mice. Scale bar, 100 μm . (d) Quantification of c-Fos positive cell number in the hippocampal hilus region of control or Gq-DREADD mice. (e) Representative images of c-Fos positive cells (Green) in the dentate hilus of the control or Gq-DREADD mice, 2 hours after CNO injection. Scale bar, 50 μm . Data are represented as means \pm SEM. Paired Student's t-test, *** $p < 0.001$, Abbreviations: DG, Dentate gyrus; GCL, Granule cell layer; IML, innermolecular layer.

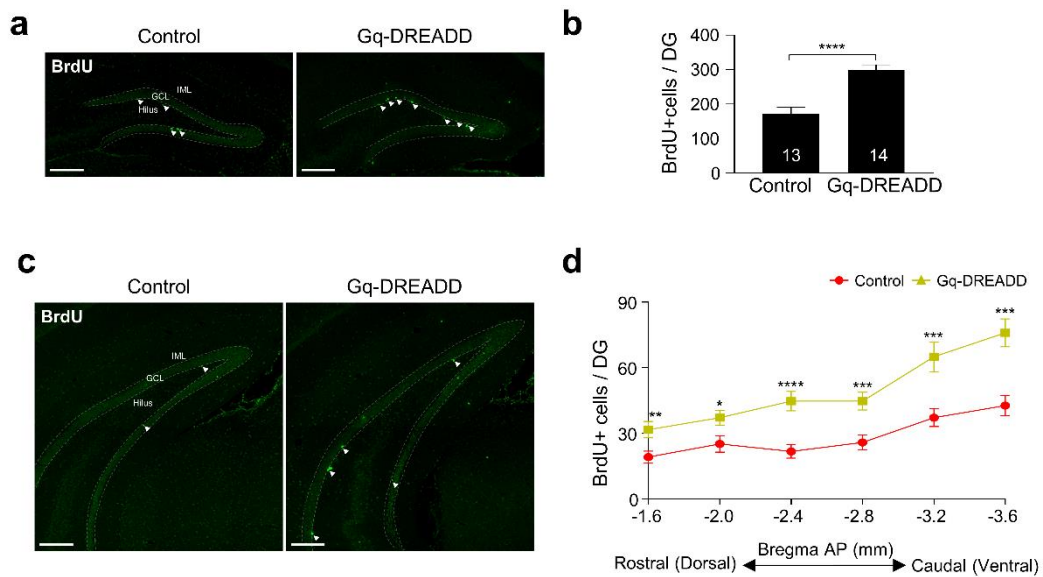


Figure 24. Effects of chemogenetic stimulation of mossy cells on proliferation or newborn cells.

(a) Representative images of BrdU immunostaining in the dorsal hippocampal sections from the control or Gq-DREADD mice. (b) Quantitation of BrdU-positive cells in the SGZ. Two-tailed, unpaired T-test; $P < 0.0001$. (c) Representative images of BrdU-immunostaining results in the caudal subregion of the hippocampus from the control or Gq-DREADD mice. Scale bar, $100 \mu\text{m}$. (d) Quantification of BrdU-positive cells along the dorso-ventral axis of the hippocampus. Data are represented as means \pm SEM. Student's t-test, * $p < 0.05$, ** $p < 0.01$, *** $p < 0.001$, **** $p < 0.0001$. Abbreviations: SGZ, subgranular zone; GCL, granule cell layer; IML, inner molecular layer.

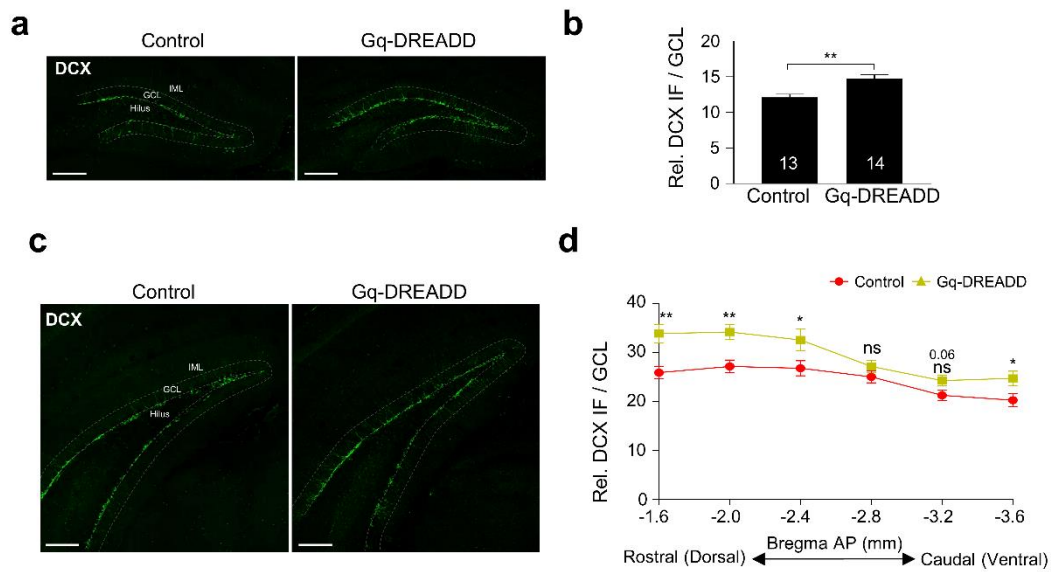


Figure 25. Effects of chemogenetic stimulation of mossy cells on differentiation of new-born cells.

(a) Representative images of DCX-immunostaining in the dorsal hippocampal sections from the control and Gq-DREADD mice. (b) Quantitation of relative intensity of DCX immunofluorescence in the SGZ and the GCL of the dentate gyrus. Two-tailed, unpaired T-test; $P=0.0021$. (c) Representative images of doublecortin-immunostaining results in the caudal region. Scale bar, 100 μm . (d) Quantification of relative fluorescence intensity of DCX immunofluorescence (Rel. DCX IF) along the rostro-caudal axis of the hippocampus. Data are represented as means \pm SEM. Student's t-test, * $p<0.05$, ** $p<0.01$, ns; non-significant. Abbreviations: SGZ, subgranular zone; GCL, granule cell layer; IML, inner molecular layer.

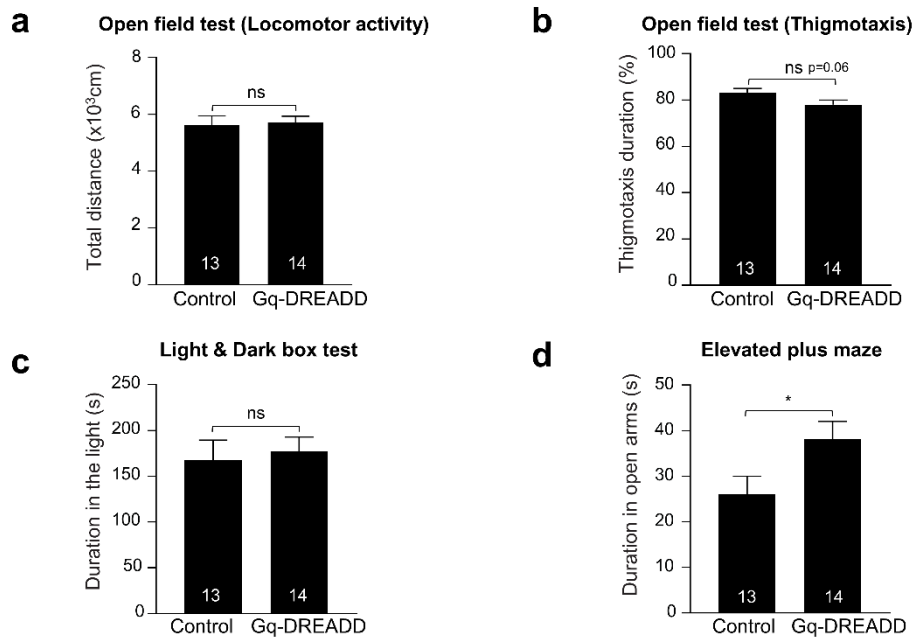


Figure 26. Effect of acute chemogenetic stimulation of mossy cells on the basal locomotion or anxiety-related behaviors.

(a) Basal locomotor activity of control and Gq-DREADD mice in the open field test. (b) Thigmotaxis in the open field test. (c) Light/Dark Box test. (d) Elevated plus maze test. Data are represented as means \pm SEM. Student's t-test, * $p < 0.05$, ns; non-significant.

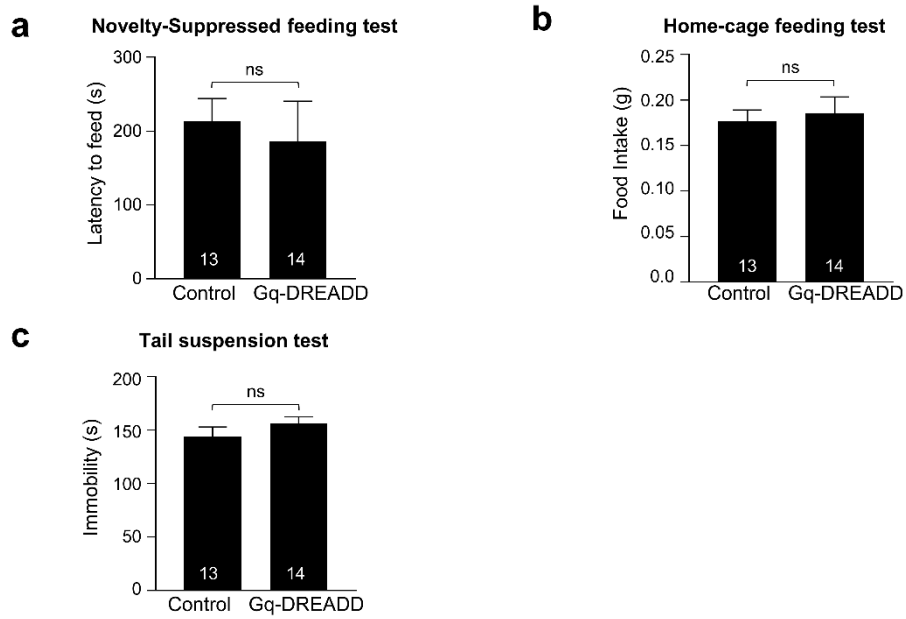


Figure 27. Effect of acute chemogenetic stimulation of mossy cells on depression-related behaviors.

(a) Novelty-suppressed feeding test. (b) Home-cage feeding test. (c) Tail suspension test. Data are represented as means \pm SEM. Student's t-test, ns; non-significant.

3.2.2 Effect of selective inhibition of dentate mossy cells on antidepressant actions in the hippocampus.

Next I examined whether inhibition of the mossy cells influences neurogenic and behavioral effects of chronic antidepressant treatment. With cre-dependent AAV injections, control mCherry (Control) and hM4D-Gi-mCherry (Gi-DREADD) were specifically expressed in the mossy cells along the dorso-ventral axis of the dentate gyrus (Figures 28a – 28d). By using electrophysiological recordings, I verified that the activity of mossy cells was silenced by CNO only in mossy cells expressing Gi-DREADD (Figures 29a – 29d).

Using the Gi-DREADD system, I examined the role of mossy cells on chronic fluoxetine-induced neurogenesis and behavioral changes (Figure 28a). I measured adult neurogenesis activities in control and Gi-DREADD mice. Chronic treatment with SSRI significantly increased the number of BrdU⁺ proliferating cells in the SGZ of the dentate gyrus of control mice, but the fluoxetine effect was significantly reduced in the Gi-DREADD mice (Figures 30a – 30d). I next analyzed the expression level of doublecortin (DCX), a marker for postmitotic immature neurons. DCX immunostaining intensity was increased by chronic

fluoxetine treatment in control mice, but to a much lower extent in Gi-DREADD mice (Figures 31a – 31d). Chronic fluoxetine administration promotes the newborn neural progenitors to survive and differentiate into mature neurons [73]. Inhibition of mossy cell activity results in significant reduction in survival and/or differentiation of post-mitotic newborn cells (Figures 31a and 31b). These results indicate that mossy cells may modulate chronic fluoxetine-induced proliferation of neural progenitors, differentiation and maturation into newborn granule cells. This phenotype is similar to that observed with genetic KO or inhibition of the p11/AnxA2/SMARCA3 complex in mossy cells. I additionally verified neurogenic effects by silencing mossy cells activity using membrane tethered toxin which technique has been reliably used to block synaptic transmission [74-76] (Figure 32a - 32c). Inhibition of neurotransmission in mossy cells abolished SSRI-induced neurogenesis (Figure 33a – 33c).

I further investigated the functional significance of mossy cell activity by profiling general locomotor activity and affective behaviors. Control and Gi-DREADD mice did not display a baseline difference in locomotor activity (open field test [OF], Figure 34a), anxiety-related behaviors (thigmotaxis, Figure 34b; light/dark box test [LDB], Figure 34c; elevated plus maze test [EPM], Figure 34d). The novelty-suppressed feeding [NSF] test is based on

depressive-like and anxiety behavior and has been widely used to assess the chronic effect of fluoxetine [77]. I examined the possible effect of mossy cell inhibition on behavioral changes after chronic antidepressant treatment, using the NSF test and the tail suspension test [TST], a classical depression test. I found that behavioral responses to chronic fluoxetine treatment were affected by CNO-induced silencing of mossy cell activity. In the NSF test, the reduced latency to feed after chronic fluoxetine treatment was abolished in the Gi-DREADD mice (Figure 35a). In contrast, the home cage feeding level was unaffected, which suggests that this behavioral change is unlikely due to different hunger levels between comparison groups (Figure 35b). In the TST, the effect of fluoxetine on immobility was significantly reduced in control mice, but not in Gi-DREADD mice (Figure 35c). Collectively, these results demonstrate that modulation of mossy cell activity in the dentate gyrus is critical for both neurogenic and behavioral responses to chronic fluoxetine administration.

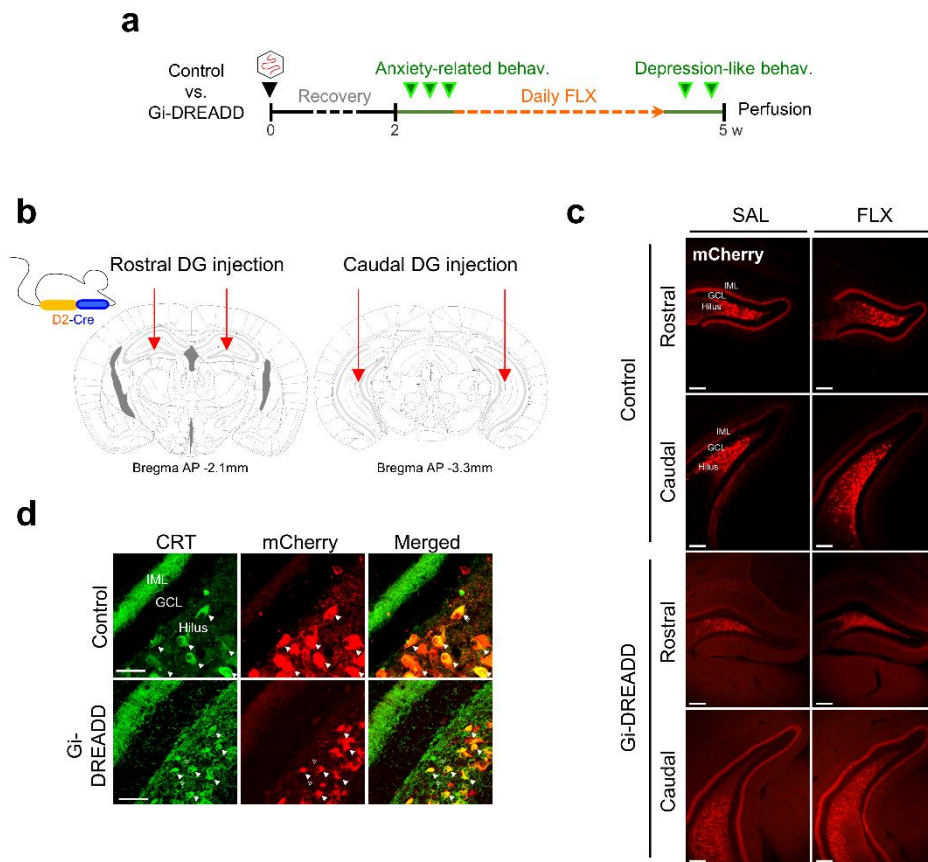


Figure 28. Mossy cell-specific expression of control or Gi-DREADD construct along the rostro-caudal axis of the hippocampus.

(a) Schematic of experimental design. Control and Gi-DREADD mice were administrated saline (SAL) or fluoxetine (FLX) for 3 weeks and labeled with BrdU for the last 3 hours prior to perfusion. (b) Schematic illustration for stereotaxic injection of Cre-dependent AAVs expressing either control or Gi-DREADD along the rostro-caudal axis of the hippocampus. Stereotaxic coordinate for either rostral or caudal injection of AAV (Rostral : AP -2.1 mm, ML \pm 1.4 mm, DV -1.95 mm. Caudal : AP -3.3 mm, ML \pm 2.7 mm, DV -3.6 mm). (c) Representative images showing longitudinal expression of control or Gi-DREADD in the rostral and the caudal subregion of the hippocampus of D2-Cre mice. Scale bar, 100 μ m. (d) Representative images for mossy cell-specific delivery of Gi-DREADD system. Hippocampal sections from AAV-injected mice were co-labeled with a mossy cell marker, CRT. Scale bar, 50 μ m.

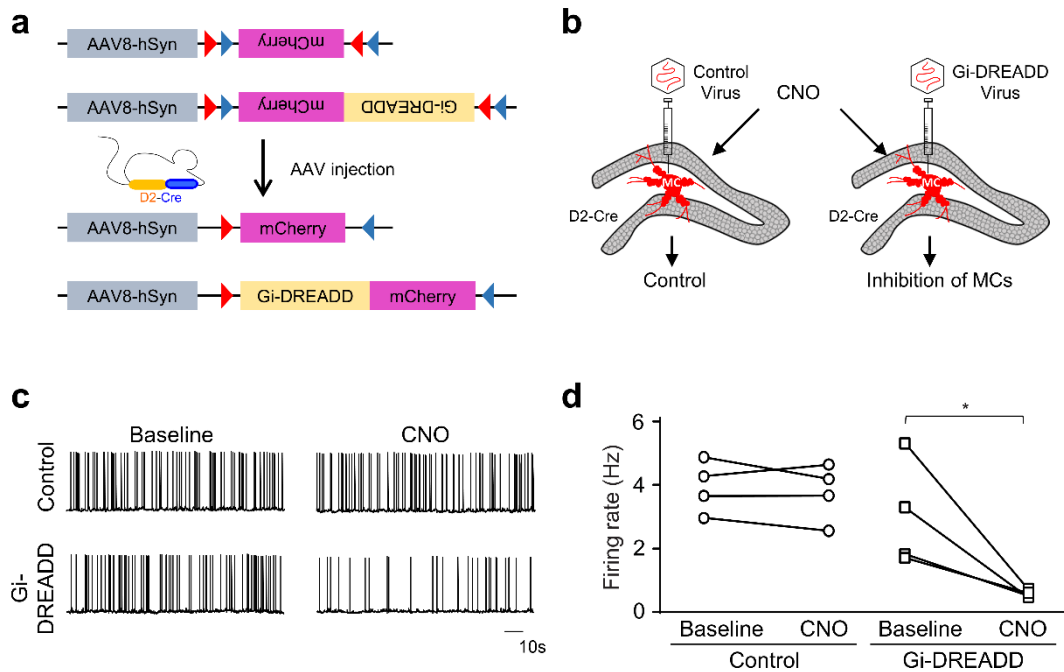


Figure 29. Mossy cell-specific expression of Gi-DREADD construct silences the mossy cell activity by CNO administration.

(a) Schematic illustration of the double-floxed Cre-dependent AAV vector expressing control and Gi-DREADD constructs under control of human Synapsin I (hSyn) promoter. (b) Schematic illustration of chemo-genetic silencing of mossy cells with Gi-DREADD system. (c and d) Representative traces (c) and dot plot (d) showing the spontaneous firing of mossy cells expressing either control mCherry (Control) or Gi-DREADD-mCherry (Gi-DREADD) before and after bath application of CNO (1 mM). $n = 4$ cells per group. Scale bar: 10 s, 50 mV. Two-way ANOVA with repeated measurement, [AAV x CNO interaction $F(1,6)=7.261$; $P=0.0395$, CNO factor $F(1,6)=6.473$; $P=0.0438$, CNO factor $F(1,6)=9.709$; $P=0.0321$], followed by the Sidak's multiple comparison post hoc test. Control (CNO effect); $P=0.9355$, Gi-DREADD (CNO effect); $*P=0.0343$. Data are represented as means \pm SEM. Pair-wise comparison; $* p < 0.5$, ns, non-significant. Abbreviations: CNO, clozapine-N-oxide.

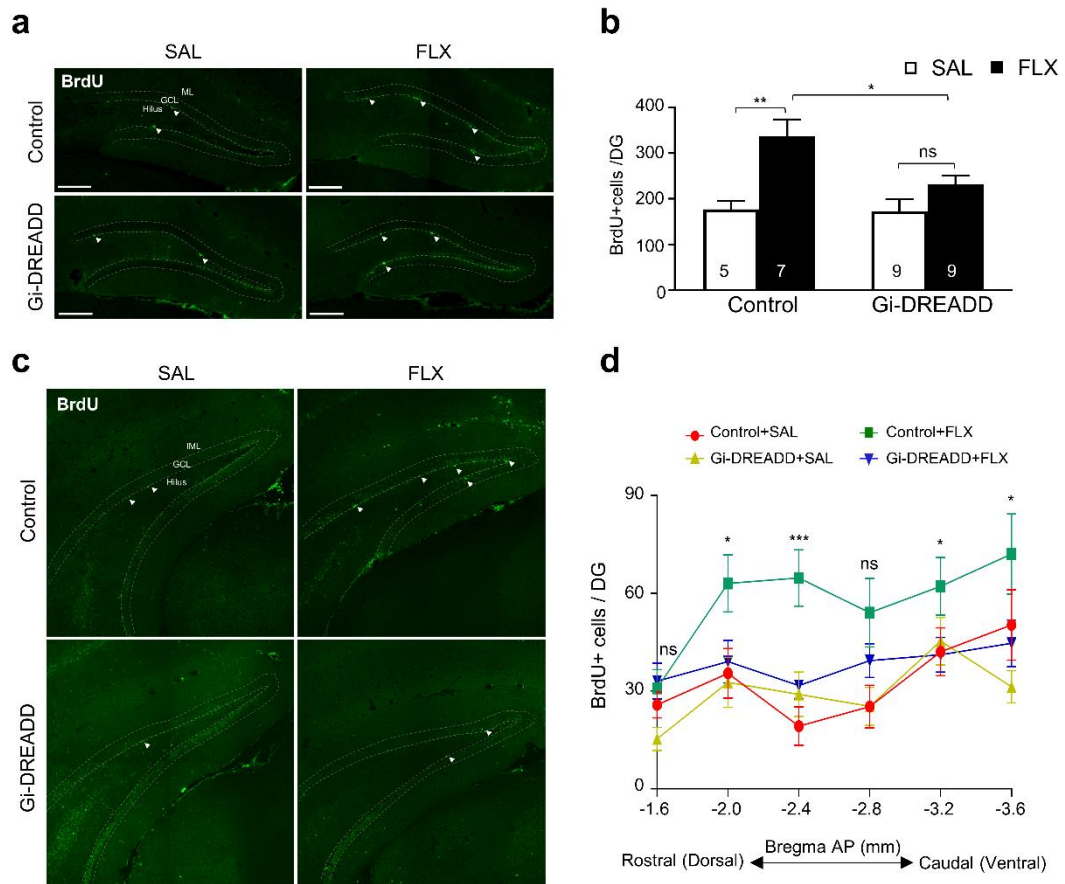


Figure 30. Effects of chemogenetic silencing of mossy cells on proliferation of newborn cells in response to chronic SSRI administration.

(a) Representative images to visualize proliferating neural stem cells with α -BrdU immunostaining (BrdU, Green, filled arrowheads). (b) BrdU+ cells were quantified along the subgranular zone. Two-way ANOVA, [AAV x drug interaction $F(1,28)=3.548$; $P=0.0700$, AAV $F(1,28)=1.707$; $P=0.2020$, drug $F(1,28)=13.55$; $P=0.001$], followed by the Turkey's post hoc test. (c) Representative images of BrdU immunostaining results. BrdU+ cells were indicated with solid arrowheads in the caudal hippocampal regions of the control or Gi-DREADD mice. Scale bar, 100 μ m. (d) Quantitation of BrdU-positive cell number along the dorso-ventral axis of the hippocampus. Data are represented as means \pm SEM. Student's t-test, * $p<0.05$, ** $p<0.01$, *** $p<0.001$, ns; non-significant. Abbreviations: GCL, Granule cell layer; IML, innermolecular layer; SAL, saline; FLX, Fluoxetine.

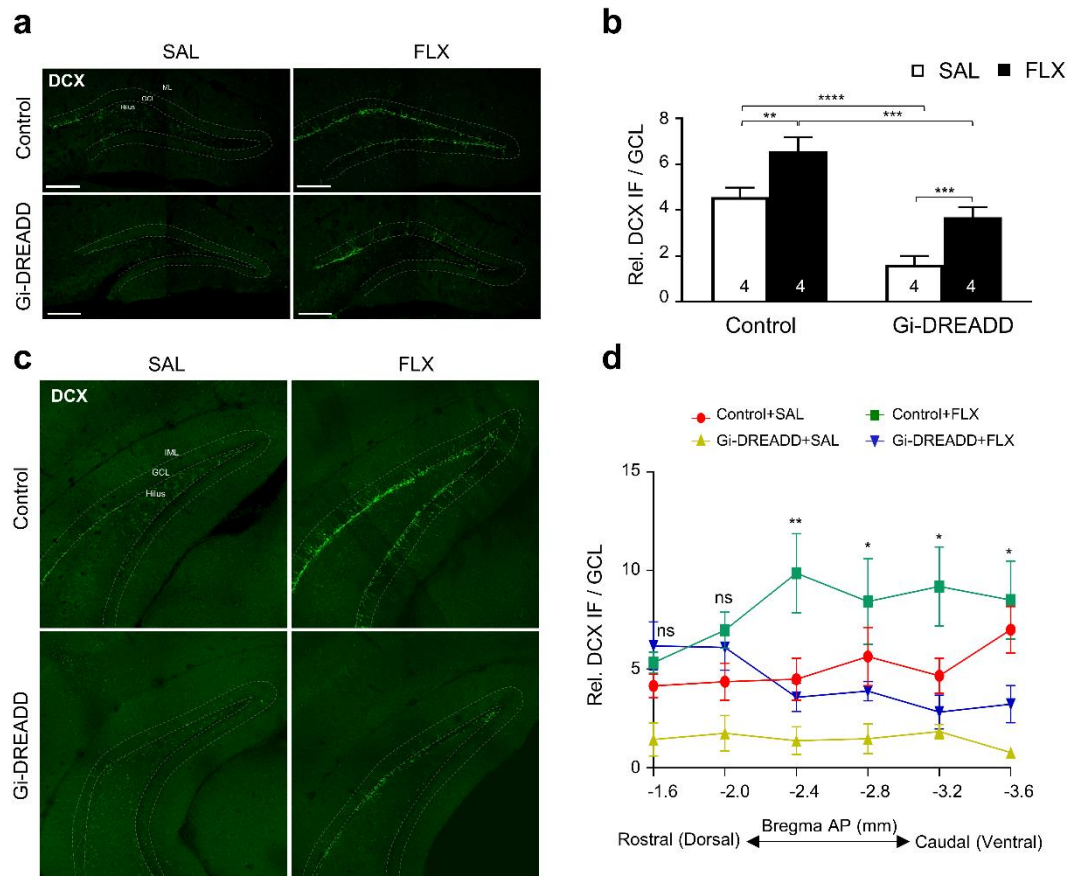


Figure 31. Effects of chemogenetic silencing of mossy cells on differentiation of newborn cells in response to chronic SSRI administration.

(a) Postmitotic immature neurons were immunostained with α -doublecortin antibody (DCX, green). Scale bar, 100 μ m. (b) Quantification of relative DCX immunofluorescence intensity (Rel. DCX IF) were quantified in the sub-granular and granular zone using Image J software. Pair-wise comparison with two-tailed, unpaired T-test. (c) Representative images of doublecortin immunostaining results (DCX, green) in the caudal hippocampal regions of the control or Gi-DREADD mice. (d) Quantitation of the relative fluorescence intensity of DCX immunofluorescence (Rel. DCX IF) along the rostro-caudal axis of the hippocampus. Data are represented as means \pm SEM. Student' s t-test, * p <0.05, ** p <0.01, *** p <0.001, ns; non-significant. Abbreviations: GCL, Granule cell layer; IML, innermolecular layer; SAL, saline; FLX, Fluoxetine.

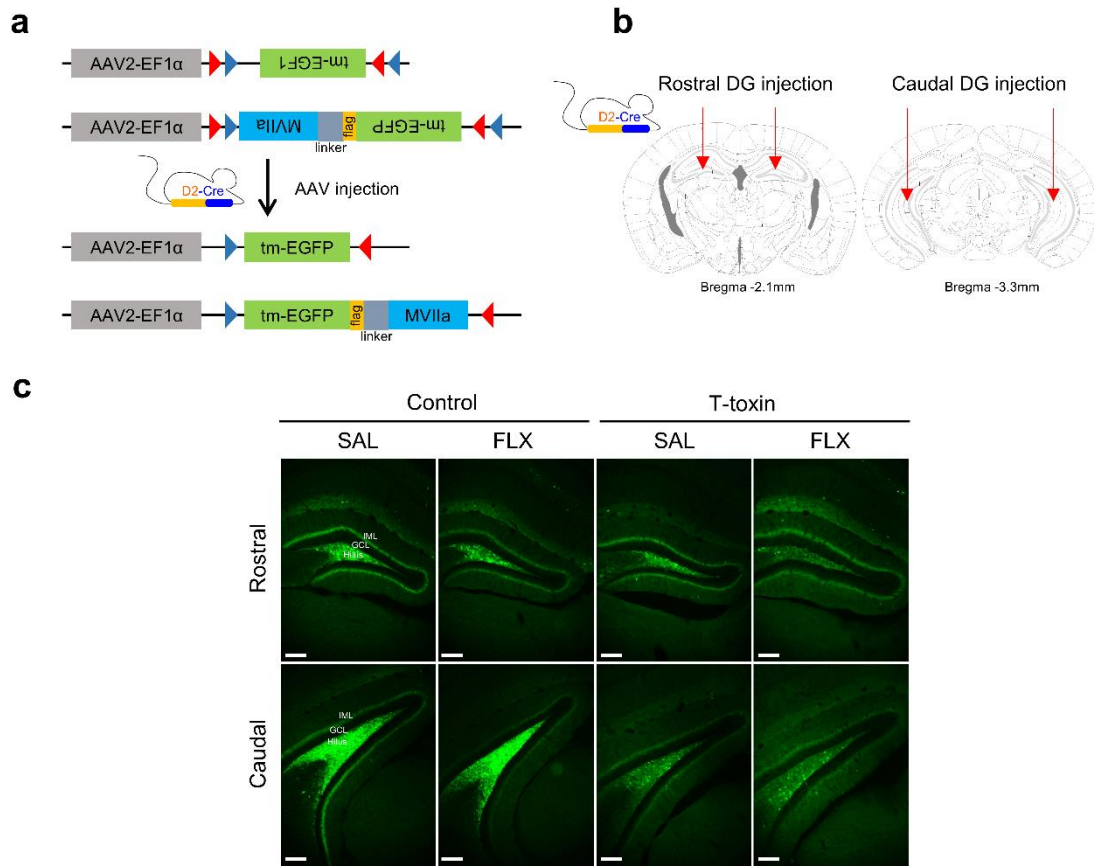


Figure 32. Mossy cell-specific expression of control or Tethered-toxin construct along the rostro-caudal axis of the hippocampus.

(a) Schematic illustration of the double-floxed Cre-dependent AAV vector expressing control and tethered-toxin constructs under control of EF-1 α promoter. (b) Schematic illustration for stereotaxic injection of Cre-dependent AAVs expressing either control or Tethered-toxin along the rostro-caudal axis of the hippocampus. Stereotaxic coordinate for either rostral or caudal injection of AAV (Rostral : AP -2.1 mm, ML \pm 1.4 mm, DV -1.95 mm. Caudal : AP -3.3 mm, ML \pm 2.7 mm, DV -3.6 mm). (c) Representative images showing longitudinal expression of control or Tethered-toxin in the rostral and the caudal subregion of the hippocampus of D2-Cre mice. Scale bar, 100 μ m.

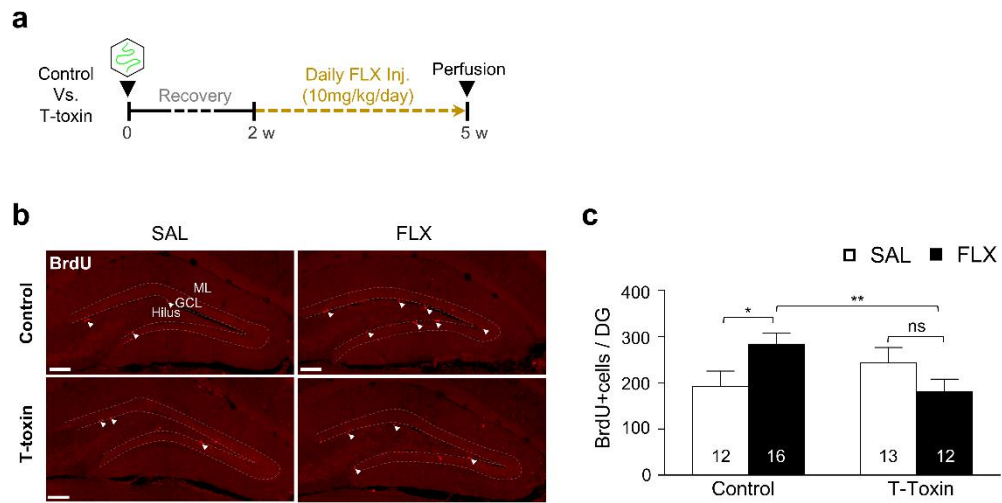


Figure 33. Effects of toxin-induced silencing of mossy cells on neurogenic responses to chronic SSRI administration.

(a) Schematic of experimental design. Control and T-toxin mice were administrated saline (SAL) or fluoxetine (FLX) for 3 weeks and labeled with BrdU for the last 3 hours prior to perfusion. (a) Representative images of BrdU immunostaining results. BrdU+ cells were indicated with solid arrowheads in the caudal hippocampal regions of the control or T-toxin mice. Scale bar, 100 μ m. (c) BrdU+ cells were quantified along the subgranular zone. Data are represented as means \pm SEM. Student's t-test. * $p < 0.05$, ** $p < 0.01$, ns; non-significant.

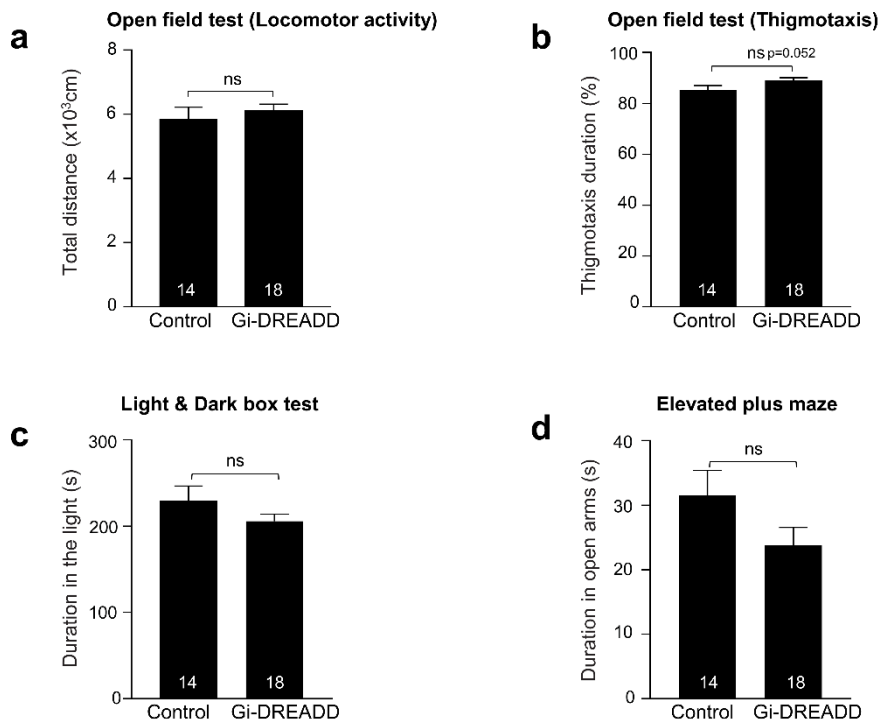


Figure 34. Effect of chemogenetic silencing of mossy cells on the basal locomotion or anxiety-related behaviors.

(a) Basal locomotor activity of control mCherry and Gi-DREADD mCherry mice in the open field [OF] test. (b) Thigmotaxis in the open field [OF] test. (c) Light/Dark Box [LDB] test. (d) Elevated plus maze [EPM] test. Data are represented as means \pm SEM. Paired Student's t-test, * $p < 0.05$, ns; non-significant.

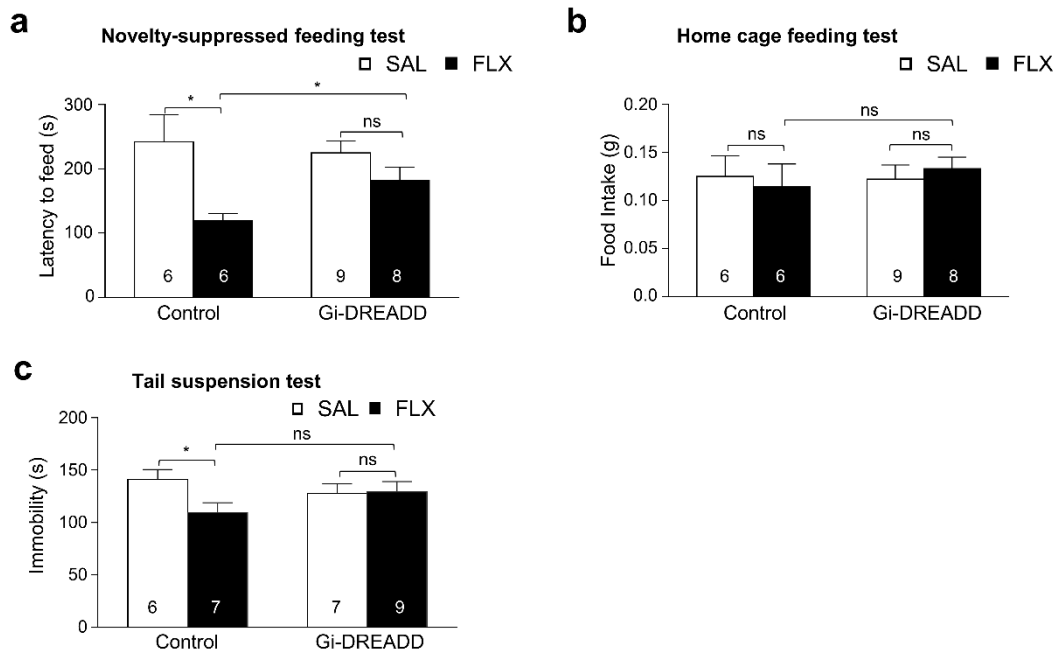


Figure 35. Effect of chemogenetic silencing of mossy cells on the depression-related behaviors in response to chronic SSRI treatment.

(a) Effect of Gi-DREADD-dependent inhibition of mossy cells on the novelty-suppressed feeding test after chronic fluoxetine treatment. Two-way ANOVA, [AAV x drug interaction $F(1,28)=4.212$; $P=0.0496$, AAV factor $F(1,28)=1.39$; $P=0.2484$, drug factor $F(1,28)=15.11$; $P=0.0006$], followed by the Turkey's post hoc test. (b) Home cage feeding test. (c) Tail suspension test [TST] after chronic treatment of SAL or FLX. Data are represented as means \pm SEM. Pair-wise comparison; * $p < 0.5$, ns, non-significant. Abbreviations: SAL, saline; FLX, fluoxetine.

3.3 Effects of modulation of mossy cells on micro-circuit in dentate gyrus.

According to previous studies, the net effects of mossy cells input on the granule cells is inhibitory, even it is unclear yet [37, 78]. For these reason, I investigated the immunostaining with excitability marker, c-Fos to evaluate the generally accepted net effect of the mossy cells after chemogenetic inhibition and counted c-Fos positive cells in the granule cells layer. The c-Fos positive cell population of granule cells was increased in the Gi-DREADD induced mice (Figure 36a - 36c). These results suggested that mossy cell activity silencing cause the hyper-excitability of granule cells. These effects can be presumed to be the result of blocking the indirect pathway via PV-positive basket cells from mossy cells to granule cells.

Furthermore, to examine the effects of mossy cells activity inhibition on GCs activity by blocking P11/AnxA2/Smarca3 complex using PASIP constructs. Before sacrificed them, I give the foot shock to maximize the activity of GCs by aversive stimuli (Figure 36d). Similar to Gi-DREADD effects, PASIP-AcGFP1 induced mice show the increased granule cells activity (Figure 36e and 36f).

Next, to examine the modulation effects of mossy cell activity to Parvalbumin (PV)-positive basket cells as a part of indirect pathway to GCs, I investigated the immunostaining

with PV antibody (Figure 37a). According to the previous studies, PV expression pattern is correlated with the activity of PV-positive cells [79, 80]. The PV-positive cell number in DG was not altered by p11/AnxA2/Smarca3 complex in the mossy cells. However, the PV-positive cell number in PASIP-induced mice was significantly reduced by chronic antidepressant administration (Figure 37b and 37c). This result suggested that mossy cell inhibition induce the dysregulation of PV-positive basket cells. In addition, Relative PV expression intensity was significantly reduced by p11/AnxA2/Smarca3 complex inhibition in the mossy cells. (Figure 37d and 37e). These results demonstrate that MCs activity inhibition cause the down-regulated activity of PV-positive basket cells, and thus, it eventually causes hyperexcitability in GCs. From these results, it is highly probable that the expression of certain gene that regulated by antidepressant treatment in mossy cells is likely to mediate regulation of micro-circuits in dentate gyrus.

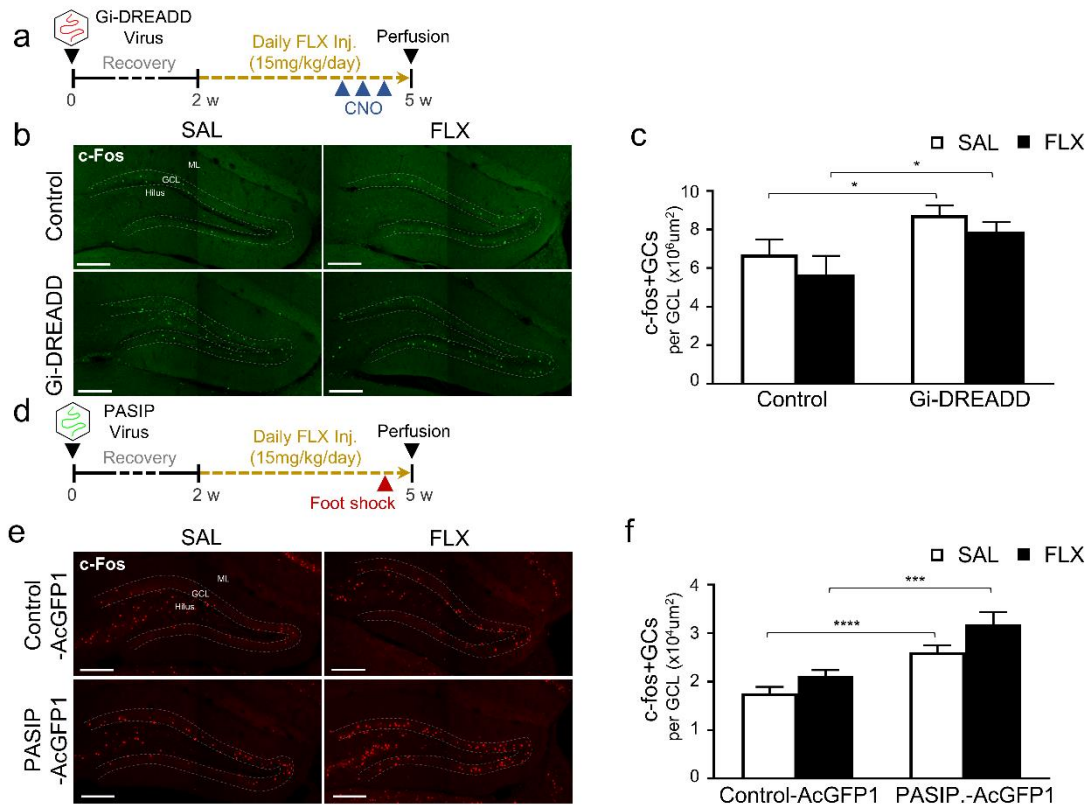


Figure 36. Effects of mossy cell suppression on dentate granule cells activity.

(a) Schematic illustration of chemogenetic inhibition of mossy cells with Gi-DREADD system. (b) Representative images of c-Fos positive cells (Green) in the dentate gyrus of control and Gi-DREADD mice. Scale bar, 200 μm . (c) Quantification of c-Fos positive cell number in the granule cell layers of the control or Gi-DREADD mice. Two-way ANOVA, [AAV x drug interaction $F(1,54)=0.0166$; $P=0.8977$, AAV $F(1,54)=9.421$; $P=0.0034$, drug $F(1,54)=1.793$; $P=0.1862$], followed by the Turkey's post hoc test. (d) Experimental design for MC-specific inhibition of P11/Anx2/Smarca3 complex, drug administration, and acute stress. All the mice were perfused at 90 min post a foot shock. (e) Representative images of c-Fos positive (Red) in the dentate gyrus of control-AcGFP1- and PASIP-AcGFP1-injected mice. Scale bar, 200 μm . (f) Quantitative graph of c-Fos positive cell number in granule cell layers of the Control-AcGFP1 or PASIP-AcGFP1 injected-mice. Two-way ANOVA, [AAV x drug interaction $F(1,101)=0.3439$; $P=0.5589$, AAV $F(1,101)=28.37$; $P<0.0001$, drug $F(1,101)=6.781$; $P=0.0106$], followed by the Turkey's post hoc test. Data are represented as means \pm SEM. Pairwise comparison, * $p<0.05$, *** $p<0.001$, **** $p<0.0001$. Abbreviations: GC, Granule cells; GCL, Granule cell layer; IML, innermolecular layer; SAL, saline; FLX, Fluoxetine.

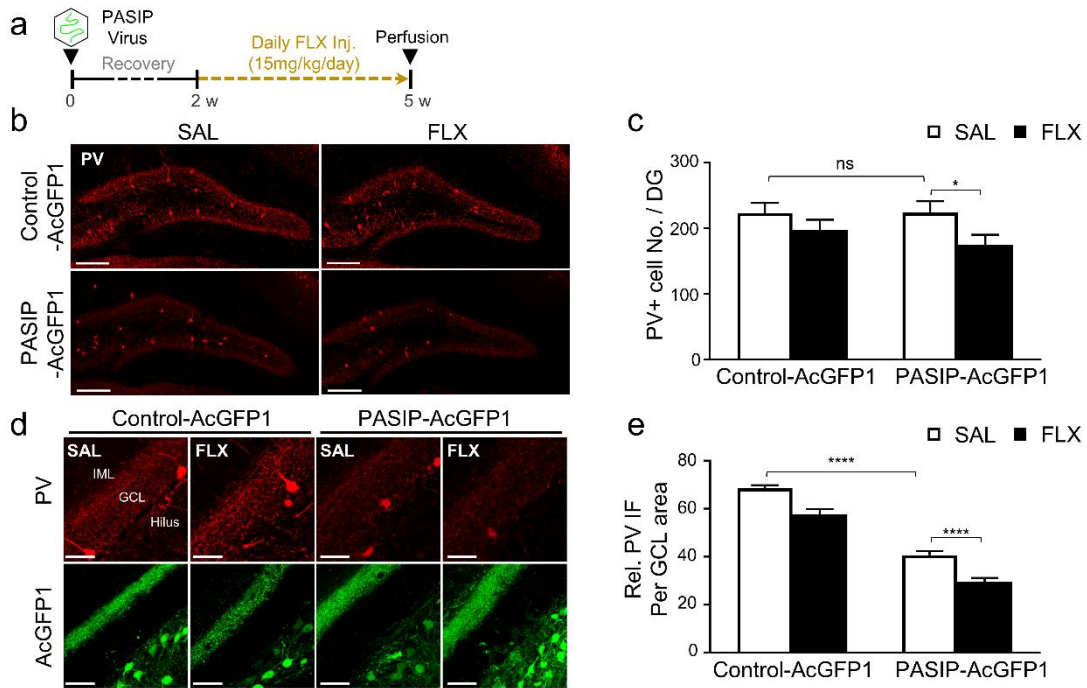


Figure 37. Effects of mossy cell-specific disruption of the p11/AxnA2/SMARCA3 complex on PV-positive basket cells in dentate gyrus.

(a) Experimental design. Control AcGFP1- or PASIP-AcGFP1-injected mice were administered saline (SAL) or fluoxetine (FLX) for 3 weeks. (b) Representative immunofluorescence images to show PV expression in PV+basket cells (Red) in the dentate gyrus of Control AcGFP1- or PASIP-AcGFP1 mice. Scale bar, 200 μ m. (c) Quantification of PV+basket cells number in the dentate gyrus. Two-way ANOVA, [AAV x drug interaction $F(1,101)=0.3439$; $P=0.5589$, AAV $F(1,101)=28.37$; $P<0.0001$, drug $F(1,101)=6.781$; $P=0.0106$], followed by the Turkey's post hoc test. Two-way ANOVA, [AAV x drug interaction $F(1,244)=0.5482$; $P=0.4597$, AAV $F(1,244)=0.4691$; $P=0.4941$, drug $F(1,244)=5.366$; $P=0.0214$], followed by the Turkey's post hoc test. (d) Representative high-resolution images for anti-PV immunostaining of the dentate gyrus of Control AcGFP1 and PASIP-AcGFP1-injected mice. Scale bar, 50 μ m. (e) Quantification of relative intensity of PV immunofluorescence (Rel. PV IF). Two-way ANOVA, [AAV x drug interaction $F(1,86)=0.0065$; $P=0.9358$, AAV $F(1,86)=286.7$; $P<0.0001$, drug $F(1,86)=43.41$; $P<0.0001$], followed by the Turkey's post hoc test. Data are represented as means \pm SEM. Pair-wise comparison; unpaired T-test, * $p<0.05$, *** $p<0.001$, **** $p<0.0001$, ns; non-significant. Abbreviations: PV, parvalbumin; GCL, Granule cell layer; IML, innermolecular layer; Rel. PV IF, relative parvalbumin immune-fluorescence; SAL, saline; FLX, Fluoxetine.

4. DISCUSSION

Despite wide clinical use, current antidepressants including SSRIs still remain with insufficient responsiveness, and even worse with significant delay in their therapeutic onset. Still our understanding about beneficial effects of SSRIs is yet far beyond rapid elevation of serotonin in the brain. It is now believed that their therapeutic onset may require through slow adaptive changes in the neural circuitry over long-term treatment. In the present study, I have demonstrated a role for hippocampal mossy cells in mediating the responses to chronic antidepressant treatment, using electrophysiological, histological and behavioral approaches. Modulation of mossy cell activity by using the DREADD system regulates chronic antidepressant responses in behaviors and adult neurogenesis. Furthermore, I have shown that p11 and SMARCA3 play a crucial role in modulating mossy cell activity. Blockage of the p11/AnxA2/SMARCA3 complex in mossy cells attenuated chronic antidepressant responses, consistently with reduced neuronal activity of mossy cells. The current study shows that chronic SSRI medication regulates mossy cells, which involves in the behavioral and neurogenic response to the drug (Figure 38).

Role of mossy cells in the behavioral response to chronic SSRI medication

In addition to established roles in cognitive processes, the hippocampus has been associated with emotional control by taking prominent position in the limbic circuitry. There is the well-established link between the hippocampal dysfunction and the pathogenesis of mood and anxiety-related disorders. In addition, antidepressive medication has been shown to enhance neuronal plasticity in the hippocampus [81-83]. It thus has been regarded as an important target area for development of advanced antidepressive therapeutics [84, 85].

Different from other hippocampal subregions, the dentate gyrus contains an additional glutamatergic neuron, hilar mossy cells other than the primary glutamatergic principal neurons, granule cells in the granule cell layer. A characteristic feature of mossy cells is their extensive associational/commissural projections connecting multiple lamellae along the septotemporal axis and both dentate gyri in the hippocampal formation [86]. Mossy cells are very active reflected by spontaneous action potentials and high-frequency spontaneous excitatory postsynaptic currents (EPSCs) [26, 87]. Here, I found that chronic exposure to unpredictable stress suppresses mossy cell activity as measured by c-fos expression, a neuronal

excitation marker, which is reversed by chronic SSRI administration. In addition, my electrophysiological recordings showed that the tonic firing rate of mossy cells is enhanced by chronic, but not acute, treatment with a SSRI, fluoxetine, which is consistent with the induction pattern of p11 and its ternary complex, p11/AnxA2/SMARCA3 in the hippocampus [46]. In contrast, mossy cell-specific knockout of *p11* or of *Smarca3* or disruption of the p11/AnxA2/SMARCA3 complex reduces the tonic firing and c-fos expression of mossy cells, suggesting the significant role of the ternary complex in regulating the neuronal activity of mossy cells. This finding, to our best of our knowledge, the first to demonstrate that mossy cell activity are regulated by pharmacological treatment or genetic KOs. These results suggest that mossy cells are labile neurons that undergo considerable neuroplastic changes in response to external stress or chronic antidepressant administration.

P11 has been shown to interact with various classes of cellular proteins in multiple subcellular location including the plasma membrane, the cytosol and the nucleus [88]. Our previous study demonstrated that p11/AnxA2 complex in mossy cells interact with a chromatin remodeling factor, SMARCA3 which is mainly localized inside the nucleus of mossy cells [46]. There is growing evidence that epigenetic regulation of the neural circuit is a key

mechanism underlying depression and antidepressant actions. The gradually developing but persistent therapeutic effects of antidepressant medications may be achieved in part via epigenetic mechanisms [89]. Interestingly, I observed that nucleus-specific inhibition of the p11/AnxA2/SMARCA3 complex displays inhibitory effects of mossy cell activity, just like whole-cell inhibition of the ternary complex. Our previous study showed that p11 protein, upon induction by chronic SSRI treatment, forms the ternary active complex with SMARCA3, which may facilitate the DNA binding affinity of SMARCA3 [46]. Just like most chromatin-remodelers, the active SMARCA3 complex may initiate ATP-dependent chromatin remodeling of the target genes, which may provide substantial mechanism underlying altered mossy cell activity in response to SSRI treatment over long-term. It is therefore important to investigate a subset of genes to regulate the ion channels and synaptic transmission of mossy cells, possibly through the cell type-specific transcriptional profiling approach.

Another feature of mossy cells is that they are vulnerable to insults or injury, such as ischemia, traumatic brain injury and neurotoxic insults [25, 67, 90, 91]. Despite potential involvement of mossy cells in the neurological and neuropsychiatry disorder, our understanding of their functions and pathological implications remained have remained unclear. To date,

few studies have been performed to examine animal behaviors by manipulating mossy cells. A previous study deleted mossy cells by using a cytotoxic toxin expression and found transient elevation of anxiety and impaired pattern separation in rodents [37]. A recent study adopted an optogenetic approach and showed that mossy cells control spontaneous convulsive seizures and spatial memory [92]. Here I demonstrated that behavioral effects of chronic fluoxetine treatment are significantly diminished when mossy cell activity is suppressed with blockage of the p11/AnxA2/SMARCA3 complex. Furthermore, chemogenetic inhibition of mossy cells activity impairs the SSRI-induced changes in affective behaviors. Collectively, my findings provide strong evidence that mossy cells play a significant role in antidepressant actions, in addition to their reported role in cognitive behaviors. However, acute chemogenetic stimulation of mossy cells is unlikely to be sufficient to achieve full behavioral improvement as seen by chronic SSRI administration. Behavioral benefit after chronic SSRI administration may require cooperative neuroplastic changes in micro-circuits in dentate gyrus that include hippocampal mossy cells.

Previous studies showed that conventional p11-KO mice exhibited depression-like phenotypes [38, 93]. p11 protein is widely expressed in the multiple brain areas but displays cell

type specific expression patterns. Moreover, deletion of p11 from specific cell types in different brain regions shows different phenotypes [37, 40, 94, 95]. P11-dependent regulation of cholinergic interneurons is sufficient to induce a depression-like behaviors, but not reduce the effect of SSRIs [40, 50]. In contrast, p11 induction in the cortex and the hippocampus is required for SSRI antidepressant responses, but not influence on the depression-like behavior [46, 49, 93, 96]. Consistent with our previous reports, the p11/AnxA2/SMARCA3 complex in mossy cells is required to mediate behavioral changes by chronic SSRI administrations, but does not influence on basal affective behaviors in naive animals. These results are consistent with behavioral outcomes from chemogenetic manipulation of mossy cells, suggesting the specific involvement of mossy cells in antidepressant actions. I speculate that simple inhibition of mossy cell activity in the absence of drug treatment, appears insufficient to influence on basal depressive-like and anxiety behaviors. However, the previous reports regarding the role of mossy cells in affective behaviors seems rather inconsistent. Previous report using toxin-induced degeneration of mossy cells showed the transient elevation of anxiety behavior [37], whereas the latest study reported that optogenetic inhibition of mossy cells does not

alter anxiety behavior [92], which is consistent with my result. Presumably, apparent discrepancy across studies might be due to significant differences in strength and/or duration of mossy cell manipulation in each experimental approach.

According to previous studies, antidepressants exert similar pharmacological effects in depressed and non-depressed model [97-99], but mood generalization is only induced in the depressed models [100]. In this study, although I gave sub-threshold stressful condition during the experiments with normal mice models, such as I.P injection or handling, and even they showed improved mood states compare to saline-treated group, it is hard to assume that this is depression-induced models. Therefore, the present results are closer to research that reveal the pharmacological mechanisms of SSRIs. In addition, to verify the therapeutic effects of SSRIs by modulating specific cell populations, it seems to require further investigation with depression-induced model.

Collectively, my findings revealed selective involvement of mossy cells in the actions of chronic SSRI treatment, which may further provide strong evidence that the neural circuitry underlying the pharmacological effects of antidepressant actions could be distinct from

the neural circuitry governing basal depression-like and anxiety behaviors in naïve animals.

Role of mossy cells in the neurogenic response to chronic SSRI medication.

It has been unknown whether mossy cells are involved in adult neurogenesis, although a previous study suggests that mossy cells provide the first excitatory input to adult-born granule cells [101]. The current study is the first to show that mossy cells influence SSRI-induced neurogenesis. I report here that mossy cells, regulated by the p11/AnxA2/SMARCA3 complex, mediate the neurogenic responses to chronic antidepressant administration. Consistent with our previous reports using *p11* or *Smarca3* conventional KO mice [46, 93], disruption of the p11/AnxA2/SMARCA3 complex in mossy cells impairs adult neurogenesis in response to chronic fluoxetine treatment. Consistently, chemogenetic inhibition of mossy cells result in decrease in SSRI-induced adult neurogenesis in the hippocampus. Furthermore, acute chemogenetic stimulation of mossy cells is able to trigger early neurogenic activities including the proliferation of neural stem cells, survival and differentiation into new-born granule cells. Thus, these results suggest crucial roles of mossy cells in multiple stages of SSRI-induced neurogenesis in the hippocampus.

Despite extensive studies performed over the past 20 years, the molecular mechanisms underlying SSRI-induced neurogenesis still remain unclear. Previous studies indicate that the modulation of neurogenesis may be associated with an antidepressant response rather than with induction of depressive-like behaviors [102, 103]. However, involvement of hippocampal neurogenesis in antidepressant actions is still controversial [65, 104, 105]. Several genetic and pharmacological approaches demonstrated that 5-HT_{1A} and 5-HT₄ receptors, enriched in dentate granule cells, are crucial for SSRI-induced neurogenesis [106-108]. In contrast, the basal maintenance level of hippocampal neurogenesis is not altered in either 5-HT_{1A} receptor- or 5-HT₄ receptor-deficient mice, which indicate the specific involvement of these serotonin pathways in SSRI-induced neurogenesis. Here I observed that the p11/AnxA2/SMARCA3 complex in mossy cells regulates SSRI-induced neurogenesis, but not in the basal maintenance level, as does 5-HT_{1A} or 5-HT₄ receptors in granule cells. Given that mossy cells and granule cells make extensive reciprocal connections to construct the neural circuit of the dentate gyrus, it is plausible that serotonergic regulation of both granule cells and mossy cells may cooperate to induce neurogenesis and further behavioral response to chronic SSRI administration.

During the past decade, adult neurogenesis has been implicated in the beneficial effects of antidepressant drugs and other antidepressive therapeutics, including physical exercise, and electroconvulsive shock (ECS) treatment [9, 103, 109]. In numerous animal models, both loss- and gain-of-function approaches suggest that adult neurogenesis in the dentate gyrus may regulate cognitive and affective behaviors [102, 110-112]. Nonetheless, neurogenesis is still controversial as to whether it actually participates in the behavioral actions of antidepressants [77, 113, 114]. In spite of the ongoing controversy about the causal relationship between neurogenesis and behavioral change in response to chronic antidepressant treatment, the concomitant regulation of both events by mossy cells in our animal models is quite interesting. In this regard, future studies are warranted to determine further whether adult neurogenesis is possibly uncoupled from SSRI-induced behavioral changes or not, by using animal models in which mossy cell activity is manipulated. It is plausible that neurogenesis-dependent or –independent pathways might work together to mediate mossy cell-dependent behavioral responses to chronic SSRI administration.

Role of mossy cells on regulation of micro-circuits in dentate gyrus.

SSRI-induced alteration of mossy cell activity may further propagate to its postsynaptic targets within the local circuit of the dentate gyrus. Mossy cells excite or inhibit dentate granule cells through direct glutamatergic input or indirect GABAergic input respectively [26, 27, 115, 116], although the net effects of mossy cell input on granule cells are still inconsistent between previous reports [26, 28, 117]. Monosynaptic tracing study shows functional synapse formation from mossy cells to granule cells [29] and new-born granule cells receive the first glutamatergic inputs from mossy cells [101]. In contrast, toxin-induced degeneration of mossy cells results in transient disinhibition of granule cells, indicating the dominant inhibitory control from mossy cells [37]. Another optogenetic approach shows that the inhibitory effects of mossy cells on granule cells are dominant compared to the excitatory effects [115]. Importantly, excitation-inhibition microcircuits involving glutamatergic granule cells and GABAergic interneurons play essential roles in the network oscillation and synchrony of the dentate gyrus [118, 119]. Dysregulations of the dentate gyrus microcircuit have been causally associated with various cognitive and affective disorders [120-123]. In this

regard, altered mossy cells activity may influence on excitation-inhibition balance of the dentate gyrus, which may contribute to chronic antidepressant responses and proper regulation of micro-circuits is important for antidepressant responses.

In conclusion, the present data establish that mossy cells play a crucial role in mediating the behavioral and neurogenic effects of chronic antidepressant medication. The neuronal activity of mossy cells is altered in response to chronic SSRI administration, possibly through gene regulation of the p11/AnxA2/SMARCA3 complex, which in turn provides neural mechanisms underlying slow adaptive changes in the mossy cells for behavioral and neurogenic responses to SSRIs. I identified a novel role of mossy cells in affective behaviors and antidepressant actions, in addition to their established role for cognitive behaviors. This study may contribute to better understanding the neural mechanism mediating beneficial effects of SSRI medication and eventually to developing novel therapeutics to specifically target the neural cell type in the mood-regulatory circuits.

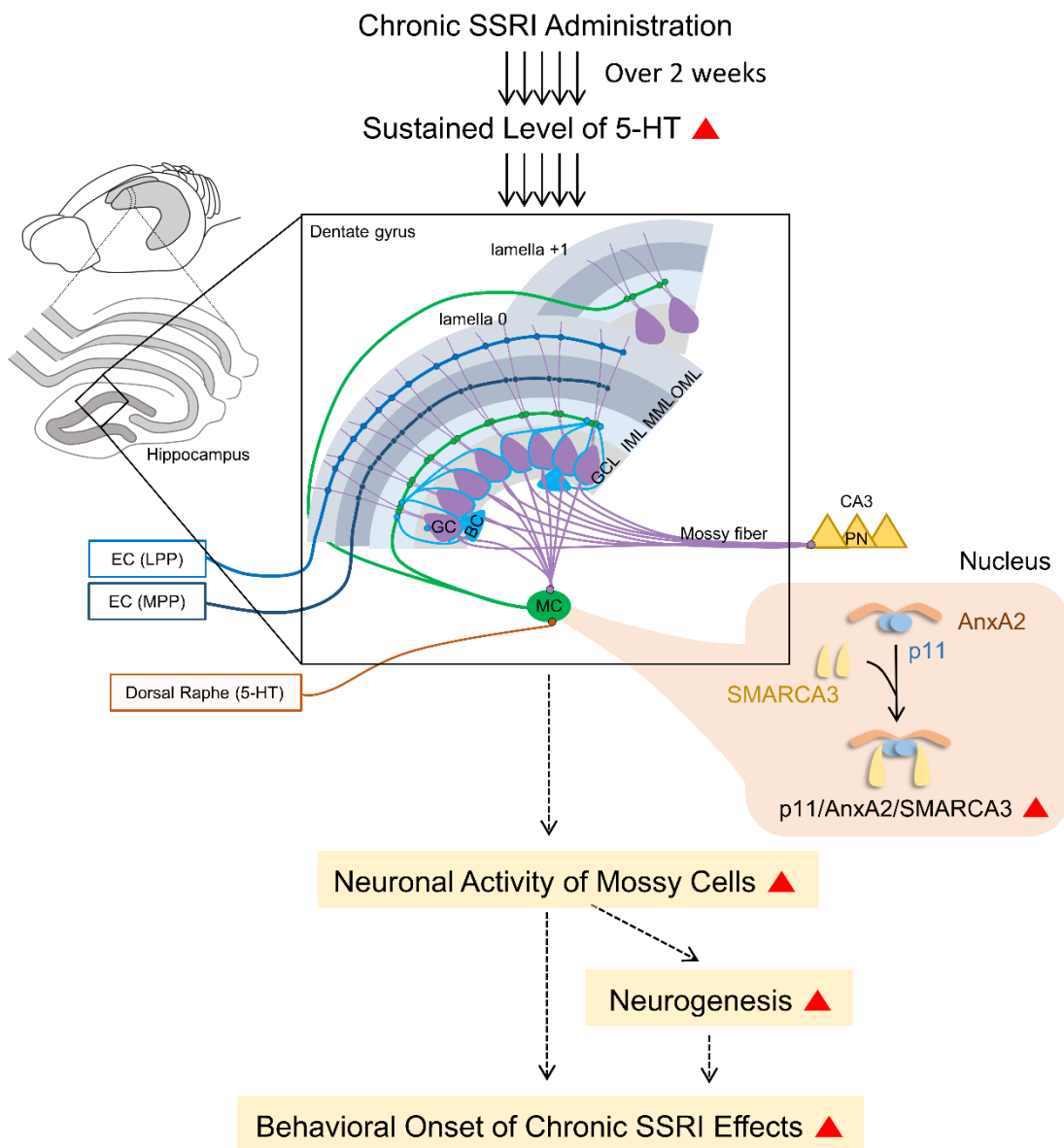


Figure 38. Graphical Summary: Significant role of hilar mossy cells in neurogenic and behavioral responses to chronic SSRI administration.

Chronic SSRI administration induces a sustained elevation of the 5-HT level in the hippocampus, which results in slow adaptive changes in mossy cells and their neural circuits. The mossy cell activity is regulated by p11/AnxA2/SMARCA3, an SSRI-inducible protein complex. The altered neuronal activity of mossy cells is crucial for the behavioral onset of chronic antidepressant effects via either neurogenesis-dependent or –independent pathway. Abbreviation: SSRI, selective serotonin reuptake inhibitor; 5-HT, 5-hydroxytryptamin; MC, mossy cell; BC, basket cell; GC, granule cell; GCL, granule cell layer; IML, inner molecular layer; MML, medial molecular layer; OML, outer molecular layer; EC, entorhinal cortex; LPP, lateral perforant pathway; MPP, medial perforant pathway.

REFERENCES

1. Friedrich, M.J., *Depression Is the Leading Cause of Disability Around the World*. JAMA, 2017. **317**(15): p. 1517-1517.
2. Bromet, E., et al., *Cross-national epidemiology of DSM-IV major depressive episode*. BMC Medicine, 2011. **9**(1): p. 90.
3. Moussavi, S., et al., *Depression, chronic diseases, and decrements in health: results from the World Health Surveys*. Lancet, 2007. **370**(9590): p. 851-8.
4. Whooley, M.A. and J.M. Wong, *Depression and cardiovascular disorders*. Annu Rev Clin Psychol, 2013. **9**: p. 327-54.
5. Risch, N., et al., *Interaction between the serotonin transporter gene (5-HTTLPR), stressful life events, and risk of depression: a meta-analysis*. Jama, 2009. **301**(23): p. 2462-71.
6. Barden, N., *Implication of the hypothalamic-pituitary-adrenal axis in the pathophysiology of depression*. Journal of psychiatry & neuroscience : JPN, 2004. **29**(3): p. 185-193.
7. Pittenger, C. and R.S. Duman, *Stress, depression, and neuroplasticity: a convergence of mechanisms*. Neuropsychopharmacology, 2008. **33**(1): p. 88-109.
8. Campbell, S., et al., *Lower hippocampal volume in patients suffering from depression: a meta-analysis*. Am J Psychiatry, 2004. **161**(4): p. 598-607.
9. Sahay, A. and R. Hen, *Adult hippocampal neurogenesis in depression*. Nat Neurosci, 2007. **10**(9): p. 1110-5.
10. Banasr, M., J.M. Dwyer, and R.S. Duman, *Cell atrophy and loss in depression: reversal by antidepressant treatment*. Curr Opin Cell Biol, 2011. **23**(6): p. 730-7.
11. Magarinos, A.M. and B.S. McEwen, *Stress-induced atrophy of apical dendrites of hippocampal CA3c neurons: comparison of stressors*. Neuroscience, 1995. **69**(1): p. 83-8.
12. Delgado, P.L., *Depression: the case for a monoamine deficiency*. J Clin Psychiatry, 2000. **61 Suppl 6**: p. 7-11.
13. Muller, J.C., et al., *Depression and anxiety occurring during Rauwolfia therapy*. J Am Med Assoc, 1955. **159**(9): p. 836-9.
14. Kucukbrahimoglu, E., et al., *The change in plasma GABA, glutamine and glutamate levels in fluoxetine- or S-citalopram-treated female patients with major depression*. Eur J Clin Pharmacol, 2009. **65**(6): p.

- 571-7.
15. Altamura, C.A., et al., *Plasma and platelet excitatory amino acids in psychiatric disorders*. Am J Psychiatry, 1993. **150**(11): p. 1731-3.
 16. Duman, R.S. and G.K. Aghajanian, *Synaptic dysfunction in depression: potential therapeutic targets*. Science, 2012. **338**(6103): p. 68-72.
 17. Nestler, E.J., et al., *Neurobiology of depression*. Neuron, 2002. **34**(1): p. 13-25.
 18. Berton, O. and E.J. Nestler, *New approaches to antidepressant drug discovery: beyond monoamines*. Nat Rev Neurosci, 2006. **7**(2): p. 137-151.
 19. Holtzheimer, P.E. and H.S. Mayberg, *Stuck in a rut: rethinking depression and its treatment*. Trends Neurosci, 2011. **34**(1): p. 1-9.
 20. Covington, H.E., 3rd, V. Vialou, and E.J. Nestler, *From synapse to nucleus: novel targets for treating depression*. Neuropharmacology, 2010. **58**(4-5): p. 683-93.
 21. Duman, R.S., et al., *Synaptic plasticity and depression: new insights from stress and rapid-acting antidepressants*. Nat Med, 2016. **22**(3): p. 238-49.
 22. Krishnan, V. and E.J. Nestler, *Linking molecules to mood: new insight into the biology of depression*. The American journal of psychiatry, 2010. **167**(11): p. 1305-20.
 23. Rush, A.J., et al., *Acute and longer-term outcomes in depressed outpatients requiring one or several treatment steps: a STAR*D report*. Am J Psychiatry, 2006. **163**(11): p. 1905-17.
 24. Amaral, D.G., *A Golgi study of cell types in the hilar region of the hippocampus in the rat*. J Comp Neurol, 1978. **182**(4 Pt 2): p. 851-914.
 25. Henze, D.A. and G. Buzsaki, *Hilar mossy cells: functional identification and activity in vivo*. Prog Brain Res, 2007. **163**: p. 199-216.
 26. Scharfman, H.E., *Electrophysiological evidence that dentate hilar mossy cells are excitatory and innervate both granule cells and interneurons*. J Neurophysiol, 1995. **74**(1): p. 179-94.
 27. Scharfman, H.E., *The enigmatic mossy cell of the dentate gyrus*. Nat Rev Neurosci, 2016. **17**(9): p. 562-75.
 28. Jinde, S., V. Zsiros, and K. Nakazawa, *Hilar mossy cell circuitry controlling dentate granule cell excitability*. Front Neural Circuits, 2013. **7**: p. 14.
 29. Sun, Y., et al., *Local and Long-Range Circuit Connections to Hilar Mossy Cells in the Dentate Gyrus*. eNeuro, 2017. **4**(2).
 30. Gage, F.H. and R.G. Thompson, *Differential distribution of norepinephrine and serotonin along the dorsal-ventral axis of the hippocampal formation*. Brain Res Bull, 1980. **5**(6): p. 771-3.

31. Lisman, J.E. and A.A. Grace, *The hippocampal-VTA loop: controlling the entry of information into long-term memory*. Neuron, 2005. **46**(5): p. 703-13.
32. Patel, A. and K. Bulloch, *Type II glucocorticoid receptor immunoreactivity in the mossy cells of the rat and the mouse hippocampus*. Hippocampus, 2003. **13**(1): p. 59-66.
33. Danielson, N.B., et al., *In Vivo Imaging of Dentate Gyrus Mossy Cells in Behaving Mice*. Neuron, 2017.
34. GoodSmith, D., et al., *Spatial Representations of Granule Cells and Mossy Cells of the Dentate Gyrus*. Neuron, 2017.
35. Senzai, Y. and G. Buzsaki, *Physiological Properties and Behavioral Correlates of Hippocampal Granule Cells and Mossy Cells*. Neuron, 2017.
36. Nakazawa, K., *Dentate Mossy Cell and Pattern Separation*. Neuron, 2017. **93**(3): p. 465-467.
37. Jinde, S., et al., *Hilar mossy cell degeneration causes transient dentate granule cell hyperexcitability and impaired pattern separation*. Neuron, 2012. **76**(6): p. 1189-200.
38. Svenningsson, P., et al., *Alterations in 5-HT1B receptor function by p11 in depression-like states*. Science, 2006. **311**(5757): p. 77-80.
39. Svenningsson, P., et al., *p11 and its role in depression and therapeutic responses to antidepressants*. Nat Rev Neurosci, 2013. **14**(10): p. 673-80.
40. Alexander, B., et al., *Reversal of depressed behaviors in mice by p11 gene therapy in the nucleus accumbens*. Sci Transl Med, 2010. **2**(54): p. 54ra76.
41. Anisman, H., et al., *Serotonin receptor subtype and p11 mRNA expression in stress-relevant brain regions of suicide and control subjects*. J Psychiatry Neurosci, 2008. **33**(2): p. 131-41.
42. Egeland, M., et al., *Neurogenic effects of fluoxetine are attenuated in p11 (S100A10) knockout mice*. Biol Psychiatry, 2010. **67**(11): p. 1048-56.
43. Eriksson, T.M., et al., *Bidirectional regulation of emotional memory by 5-HT1B receptors involves hippocampal p11*. Mol Psychiatry, 2013. **18**(10): p. 1096-105.
44. Lee, K.W., et al., *Alteration by p11 of mGluR5 localization regulates depression-like behaviors*. Mol Psychiatry, 2015. **20**(12): p. 1546-56.
45. Milosevic, A., et al., *Cell- and region-specific expression of depression-related protein p11 (S100a10) in the brain*. J Comp Neurol, 2017. **525**(4): p. 955-975.
46. Oh, Y.S., et al., *SMARCA3, a chromatin-remodeling factor, is required for p11-dependent antidepressant action*. Cell, 2013. **152**(4): p. 831-43.
47. Schmidt, E.F., et al., *Identification of the cortical neurons that mediate antidepressant responses*. Cell, 2012. **149**(5): p. 1152-63.

48. Seo, J.S., et al., *Elevation of p11 in lateral habenula mediates depression-like behavior*. Mol Psychiatry, 2017.
49. Warner-Schmidt, J.L., et al., *A role for p11 in the antidepressant action of brain-derived neurotrophic factor*. Biol Psychiatry, 2010. **68**(6): p. 528-35.
50. Warner-Schmidt, J.L., et al., *Cholinergic interneurons in the nucleus accumbens regulate depression-like behavior*. Proceedings of the National Academy of Sciences, 2012. **109**(28): p. 11360-11365.
51. Gerke, V., C.E. Creutz, and S.E. Moss, *Annexins: linking Ca²⁺ signalling to membrane dynamics*. Nat Rev Mol Cell Biol, 2005. **6**(6): p. 449-61.
52. Gurskaya, N.G., et al., *A colourless green fluorescent protein homologue from the non-fluorescent hydromedusa Aequorea coerulescens and its fluorescent mutants*. Biochem J, 2003. **373**(Pt 2): p. 403-8.
53. Kalderon, D., et al., *A short amino acid sequence able to specify nuclear location*. Cell, 1984. **39**(3 Pt 2): p. 499-509.
54. Lanford, R.E., P. Kanda, and R.C. Kennedy, *Induction of nuclear transport with a synthetic peptide homologous to the SV40 T antigen transport signal*. Cell, 1986. **46**(4): p. 575-82.
55. Lister, R.G., *The use of a plus-maze to measure anxiety in the mouse*. Psychopharmacology (Berl), 1987. **92**(2): p. 180-5.
56. Samuels, B.A. and R. Hen, *Novelty-Suppressed Feeding in the Mouse*. Mood and Anxiety Related Phenotypes in Mice : Characterization Using Behavioral Tests, Volume II, 2011. **Volume: 63**: p. 107-121.
57. Can, A., et al., *The tail suspension test*. JoVE (Journal of Visualized Experiments), 2012(59): p. e3769-e3769.
58. Mineur, Y.S., C. Belzung, and W.E. Crusio, *Effects of unpredictable chronic mild stress on anxiety and depression-like behavior in mice*. Behav Brain Res, 2006. **175**(1): p. 43-50.
59. Wojtowicz, J.M. and N. Kee, *BrdU assay for neurogenesis in rodents*. Nat Protoc, 2006. **1**(3): p. 1399-405.
60. Medrihan, L., et al., *Initiation of Behavioral Response to Antidepressants by Cholecystinin Neurons of the Dentate Gyrus*. Neuron, 2017. **95**(3): p. 564-576 e4.
61. Gangarossa, G., et al., *Characterization of dopamine D1 and D2 receptor-expressing neurons in the mouse hippocampus*. Hippocampus, 2012. **22**(12): p. 2199-207.
62. Puighermanal, E., et al., *drd2-cre:ribotag mouse line unravels the possible diversity of dopamine d2 receptor-expressing cells of the dorsal mouse hippocampus*. Hippocampus, 2015. **25**(7): p. 858-75.
63. Duman, R.S., et al., *Neuronal plasticity and survival in mood disorders*. Biol Psychiatry, 2000. **48**(8): p.

- 732-9.
64. Lucassen, P.J., et al., *Regulation of adult neurogenesis by stress, sleep disruption, exercise and inflammation: Implications for depression and antidepressant action*. Eur Neuropsychopharmacol, 2010. **20**(1): p. 1-17.
 65. Santarelli, L., et al., *Requirement of hippocampal neurogenesis for the behavioral effects of antidepressants*. Science, 2003. **301**(5634): p. 805-9.
 66. Couillard-Despres, S., et al., *Doublecortin expression levels in adult brain reflect neurogenesis*. Eur J Neurosci, 2005. **21**(1): p. 1-14.
 67. Scharfman, H.E. and C.E. Myers, *Hilar mossy cells of the dentate gyrus: a historical perspective*. Front Neural Circuits, 2012. **6**: p. 106.
 68. Moretto, J.N., A.M. Duffy, and H.E. Scharfman, *Acute restraint stress decreases c-fos immunoreactivity in hilar mossy cells of the adult dentate gyrus*. Brain Struct Funct, 2017. **222**(5): p. 2405-2419.
 69. Willner, P., *Chronic mild stress (CMS) revisited: consistency and behavioural-neurobiological concordance in the effects of CMS*. Neuropsychobiology, 2005. **52**(2): p. 90-110.
 70. Dragunow, M. and H.A. Robertson, *Kindling stimulation induces c-fos protein(s) in granule cells of the rat dentate gyrus*. Nature, 1987. **329**(6138): p. 441-2.
 71. Das, S., et al., *Signal Transducer and Activator of Transcription 6 (STAT6) Is a Novel Interactor of Annexin A2 in Prostate Cancer Cells*. Biochemistry, 2010. **49**(10): p. 2216-2226.
 72. Liu, J. and J.K. Vishwanatha, *Regulation of nucleo-cytoplasmic shuttling of human annexin A2: a proposed mechanism*. Mol Cell Biochem, 2007. **303**(1-2): p. 211-20.
 73. Wang, J.W., et al., *Chronic fluoxetine stimulates maturation and synaptic plasticity of adult-born hippocampal granule cells*. J Neurosci, 2008. **28**(6): p. 1374-84.
 74. Auer, S., et al., *Silencing neurotransmission with membrane-tethered toxins*. Nat Methods, 2010. **7**(3): p. 229-36.
 75. Christoffel, D.J., et al., *Excitatory transmission at thalamo-striatal synapses mediates susceptibility to social stress*. Nat Neurosci, 2015. **18**(7): p. 962-4.
 76. Neumann, P.A., et al., *Cocaine-Induced Synaptic Alterations in Thalamus to Nucleus Accumbens Projection*. Neuropsychopharmacology, 2016. **41**(9): p. 2399-410.
 77. David, D.J., et al., *Neurogenesis-dependent and -independent effects of fluoxetine in an animal model of anxiety/depression*. Neuron, 2009. **62**(4): p. 479-93.
 78. Zappone, C.A. and R.S. Sloviter, *Translamellar disinhibition in the rat hippocampal dentate gyrus after seizure-induced degeneration of vulnerable hilar neurons*. J Neurosci, 2004. **24**(4): p. 853-64.

79. Megahed, T., et al., *Parvalbumin and neuropeptide Y expressing hippocampal GABA-ergic inhibitory interneuron numbers decline in a model of Gulf War illness*. Front Cell Neurosci, 2014. **8**: p. 447.
80. Donato, F., S.B. Rompani, and P. Caroni, *Parvalbumin-expressing basket-cell network plasticity induced by experience regulates adult learning*. Nature, 2013. **504**(7479): p. 272-276.
81. Karpova, N.N., et al., *Fear erasure in mice requires synergy between antidepressant drugs and extinction training*. Science, 2011. **334**(6063): p. 1731-4.
82. Castrén, E., *Is mood chemistry?* Nature Reviews Neuroscience, 2005. **6**: p. 241.
83. Shuto, T., et al., *Obligatory roles of dopamine D1 receptors in the dentate gyrus in antidepressant actions of a selective serotonin reuptake inhibitor, fluoxetine*. Molecular Psychiatry, 2018.
84. Krishnan, V. and E.J. Nestler, *The molecular neurobiology of depression*. Nature, 2008. **455**(7215): p. 894-902.
85. Berton, O. and E.J. Nestler, *New approaches to antidepressant drug discovery: beyond monoamines*. Nature reviews. Neuroscience, 2006. **7**(2): p. 137-51.
86. Buckmaster, P.S., et al., *Axon arbors and synaptic connections of hippocampal mossy cells in the rat in vivo*. Journal of Comparative Neurology, 1996. **366**(2): p. 270-292.
87. Scharfman, H.E. and P.A. Schwartzkroin, *Electrophysiology of morphologically identified mossy cells of the dentate hilus recorded in guinea pig hippocampal slices*. J Neurosci, 1988. **8**(10): p. 3812-21.
88. Rescher, U. and V. Gerke, *SI00A10/p11: family, friends and functions*. Pflugers Arch, 2008. **455**(4): p. 575-82.
89. Vialou, V., et al., *Epigenetic mechanisms of depression and antidepressant action*. Annu Rev Pharmacol Toxicol, 2013. **53**: p. 59-87.
90. Ratzliff, A., et al., *Mossy cells in epilepsy: rigor mortis or vigor mortis?* Trends in neurosciences, 2002. **25**(3): p. 140-4.
91. Sloviter, R.S., et al., *"Dormant basket cell" hypothesis revisited: relative vulnerabilities of dentate gyrus mossy cells and inhibitory interneurons after hippocampal status epilepticus in the rat*. J Comp Neurol, 2003. **459**(1): p. 44-76.
92. Bui, A.D., et al., *Dentate gyrus mossy cells control spontaneous convulsive seizures and spatial memory*. Science, 2018. **359**(6377): p. 787-790.
93. Egeland, M., et al., *Neurogenic Effects of Fluoxetine Are Attenuated in p11 (SI00A10) Knockout Mice*. Biological psychiatry, 2010. **67**(11): p. 1048-1056.
94. Jinde, S., V. Zsiros, and K. Nakazawa, *Hilar mossy cell circuitry controlling dentate granule cell excitability*. Frontiers in neural circuits, 2013. **7**: p. 14.

95. Sun, H.L., et al., *Role of hippocampal p11 in the sustained antidepressant effect of ketamine in the chronic unpredictable mild stress model*. *Transl Psychiatry*, 2016. **6**: p. e741.
96. Schmidt, E.F., et al., *Identification of the Cortical Neurons that Mediate Antidepressant Responses*. *Cell*, 2012. **149**(5): p. 1152-1163.
97. Lerer, B., et al., *5-HT1A receptor function in normal subjects on clinical doses of fluoxetine: blunted temperature and hormone responses to ipsapirone challenge*. *Neuropsychopharmacology*, 1999. **20**(6): p. 628-39.
98. Porter, R.J., R.H. McAllister-Williams, and A.H. Young, *Acute effects of venlafaxine and paroxetine on serotonergic transmission in human volunteers*. *Psychopharmacology (Berl)*, 1999. **146**(2): p. 194-8.
99. Blier, P. and N.M. Ward, *Is there a role for 5-HT1A agonists in the treatment of depression?* *Biol Psychiatry*, 2003. **53**(3): p. 193-203.
100. Salomon, R.M., et al., *Lack of behavioral effects of monoamine depletion in healthy subjects*. *Biol Psychiatry*, 1997. **41**(1): p. 58-64.
101. Chancey, J.H., et al., *Hilar mossy cells provide the first glutamatergic synapses to adult-born dentate granule cells*. *J Neurosci*, 2014. **34**(6): p. 2349-54.
102. Snyder, J.S., et al., *Adult hippocampal neurogenesis buffers stress responses and depressive behaviour*. *Nature*, 2011. **476**(7361): p. 458-61.
103. Malberg, J.E., et al., *Chronic antidepressant treatment increases neurogenesis in adult rat hippocampus*. *J Neurosci*, 2000. **20**(24): p. 9104-10.
104. Feldmann, R.E., Jr., A. Sawa, and G.H. Seidler, *Causality of stem cell based neurogenesis and depression--to be or not to be, is that the question?* *J Psychiatr Res*, 2007. **41**(9): p. 713-23.
105. Hill, A.S., A. Sahay, and R. Hen, *Increasing Adult Hippocampal Neurogenesis is Sufficient to Reduce Anxiety and Depression-Like Behaviors*. *Neuropsychopharmacology*, 2015. **40**(10): p. 2368-78.
106. Imoto, Y., et al., *Role of the 5-HT4 receptor in chronic fluoxetine treatment-induced neurogenic activity and granule cell dematuration in the dentate gyrus*. *Mol Brain*, 2015. **8**: p. 29.
107. Samuels, B.A., et al., *5-HT1A receptors on mature dentate gyrus granule cells are critical for the antidepressant response*. *Nat Neurosci*, 2015. **18**(11): p. 1606-16.
108. Segi-Nishida, E., *The Effect of Serotonin-Targeting Antidepressants on Neurogenesis and Neuronal Maturation of the Hippocampus Mediated via 5-HT1A and 5-HT4 Receptors*. *Front Cell Neurosci*, 2017. **11**: p. 142.
109. Santarelli, L., et al., *Requirement of hippocampal neurogenesis for the behavioral effects of antidepressants*. *Science*, 2003. **301**(5634): p. 805-809.

110. Denny, C.A., et al., *Hippocampal memory traces are differentially modulated by experience, time, and adult neurogenesis*. *Neuron*, 2014. **83**(1): p. 189-201.
111. Frankland, P.W. and S.A. Josselyn, *Hippocampal Neurogenesis and Memory Clearance*. *Neuropsychopharmacology*, 2016. **41**(1): p. 382-3.
112. Akers, K.G., et al., *Hippocampal neurogenesis regulates forgetting during adulthood and infancy*. *Science*, 2014. **344**(6184): p. 598-602.
113. Navailles, S., P.R. Hof, and C. Schmauss, *Antidepressant drug-induced stimulation of mouse hippocampal neurogenesis is age-dependent and altered by early life stress*. *J Comp Neurol*, 2008. **509**(4): p. 372-81.
114. Schauwecker, P.E., *Genetic influence on neurogenesis in the dentate gyrus of two strains of adult mice*. *Brain Res*, 2006. **1120**(1): p. 83-92.
115. Hsu, T.T., et al., *Differential Recruitment of Dentate Gyrus Interneuron Types by Commissural Versus Perforant Pathways*. *Cereb Cortex*, 2016. **26**(6): p. 2715-27.
116. Larimer, P. and B.W. Strowbridge, *Nonrandom local circuits in the dentate gyrus*. *J Neurosci*, 2008. **28**(47): p. 12212-23.
117. Jackson, M.B. and H.E. Scharfman, *Positive feedback from hilar mossy cells to granule cells in the dentate gyrus revealed by voltage-sensitive dye and microelectrode recording*. *J Neurophysiol*, 1996. **76**(1): p. 601-16.
118. Hu, H., J. Gan, and P. Jonas, *Interneurons. Fast-spiking, parvalbumin(+) GABAergic interneurons: from cellular design to microcircuit function*. *Science*, 2014. **345**(6196): p. 1255-263.
119. Buzsaki, G., *Hippocampal GABAergic interneurons: a physiological perspective*. *Neurochem Res*, 2001. **26**(8-9): p. 899-905.
120. Kheirbek, M.A., et al., *Differential control of learning and anxiety along the dorsoventral axis of the dentate gyrus*. *Neuron*, 2013. **77**(5): p. 955-68.
121. Zou, D., et al., *DREADD in parvalbumin interneurons of the dentate gyrus modulates anxiety, social interaction and memory extinction*. *Curr Mol Med*, 2016. **16**(1): p. 91-102.
122. Boldrini, M., et al., *Hippocampal granule neuron number and dentate gyrus volume in antidepressant-treated and untreated major depression*. *Neuropsychopharmacology*, 2013. **38**(6): p. 1068-77.
123. Marin, O., *Interneuron dysfunction in psychiatric disorders*. *Nat Rev Neurosci*, 2012. **13**(2): p. 107-20.

요 약 문

항우울 약물 기전에서의 해마 모시 세포의 역할

Selective serotonin reuptake inhibitors(SSRI)를 포함한 대부분의 항우울제는 약물 복용 즉시 체내 세로토닌의 양이 증가하게 된다. 반면, 항우울 약물 복용으로 인한 치료 효과가 나타나기까지는 수주 동안의 시간이 필요하다. 이러한 치료 지연 현상은 약물 복용 이후 신경세포에서 장기간에 걸쳐 일어나는 유전자 발현 및 신경회로의 변화가 동반되어 나타나는 결과라고 할 수 있다. 모시세포는 치아이랑의 hilus 구역에 존재하는 흥분성 뉴런으로, 치아이랑의 활성화 및 기능을 조절하는 역할을 한다고 알려져 있다. 본 연구에서는 해마 모시세포가 항우울제 단기 복용이 아닌, 장기복용에 의해서 활성이 강화 된다는 것을 보였다. 또한, SSRI, fluoxetine 장기 복용에 따른 행동학적 그리고 신경발생학적 효과가 모시세포에 한해서 p11 또는 Smarca3 단백질을 억제하거나 혹은 p11/AnxA2/Smarca3 복합체를 억제하였을 경우 사라졌음을 보였다. 더불어, Gq-DREADD 시스템을 이용한 모시세포의 활성화 강화는 신경 줄기 세포의 증식과 생존을 증진시키기에 충분함을 보였다. 반대로, Gi-DREADD 시스템을 이용한 모시세포의 활성화 억제는 항우울 약물 장기 복용에 의해 나타나는 행동학적 그리고 신경발생학적 효과를 손상시킴을 보였다. 모시세포의 활성화 변화는 치아이랑 내부의 흥분성 / 억제성 신호의 조화에 영향을 끼치는 것 또한 확인할 수 있었다. 따라서 본연구에서는 항우울 약물 반응을 매개하는데 있어서

모시세포가 중요한 역할을 한다는 것을 입증하였다. 해당 연구 결과는 해마 내 모시세포가 새로운 항우울 약물 개발에 중요 후보군이 될 것임을 보여준다.

핵심어: 해마, 모시세포, 항우울제, p11/AnxA2/Smad3 복합체.